63-32

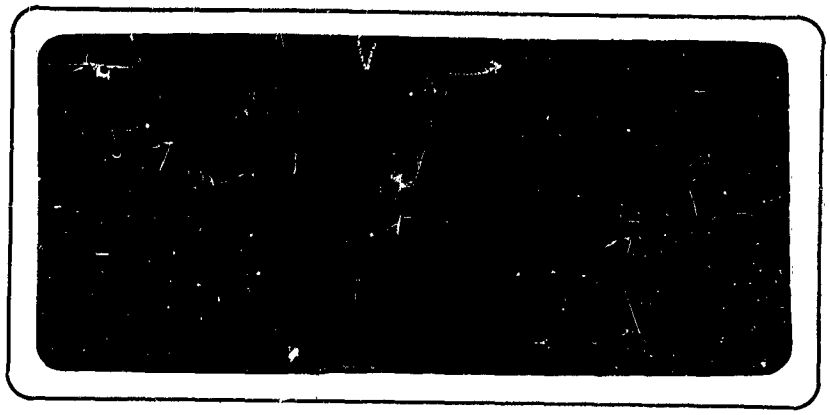

Beech Aircraft Corporation
BOULDER, COLORADO
U. S. A.

AFFTC TR 60-43
VOLUME III

ESTABLISHING TANK DESIGN CRITERIA FOR LIQUID HYDROGEN ROCKETS

VOLUME III - Materials for Liquid Hydrogen Boost Tanks

FINAL REPORT
PERIOD ENDING 15 SEPTEMBER 1961

J. E. BELL
H. E. SUTTON

BEECHCRAFT RESEARCH AND DEVELOPMENT, INC.
BOULDER, COLORADO

BEECHCRAFT ENGINEERING REPORT NO. 8768

CONTRACT AF33(616)-5154
SUPPLEMENT S3(59-207)
PROJECT No. 3084
TASK NO. 30304

MAY 1962

AIR FORCE FLIGHT TEST CENTER
AIR RESEARCH AND DEVELOPMENT COMMAND
UNITED STATES AIR FORCE
EDWARDS AIR FORCE BASE, CALIFORNIA

FOREWARD

This contract was initiated by the Propulsion Laboratory, Wright-Patterson Air Force Base, Ohio, and has been monitored by the Rocket Propulsion Laboratory at the Air Force Flight Test Center, Edwards Air Force Base, California. The work upon which this report is based was accomplished by Beechcraft Research and Development, Inc., Boulder, Colorado, under Air Force Contract AF33(616)5154, Supplement S3(59-207). Mr. J. Branigan at the Rocket Propulsion Laboratory is the Air Force Project Engineer in charge of the work done under this contract.

This is Volume III of the final report submitted per Item IV, Part I of the S3(59-207) Supplement to the contract. This report covers all work accomplished from December 1958 to September 1961.

LIST OF SYMBOLS

N85-100	Nuclear powered ICBM vehicle with range of 8500 nautical miles and payload of 100,000 lbs.
C85-100	Chemical powered ICBM vehicle with range of 8500 nautical miles and payload of 100,000 lbs.
K	Thermal conductivity
C_p	Specific heat at constant pressure
LBI	Load-bearing insulation
LOX	Liquid oxygen
RP	Rocket propellant

NOTICES

When Government drawings, specifications, or other data are used for any purpose other than in connection with a definitely related Government procurement operation, the United States Government thereby incurs no responsibility nor any obligation whatsoever; and the fact that the Government may have formulated, furnished, or in any way supplied the said drawings, specifications, or other data, is not to be regarded by implication or otherwise as in any manner licensing the holder or any other person or corporation, or conveying any rights or permission to manufacture, use, or sell any patented invention that may in any way be related thereto.

Copies of AFFTC Technical Reports should not be returned to Air Force Flight Test Center unless return is required by security considerations, contractual obligations, or notice on a specific document.

TABLE OF CONTENTS

TABLE OF CONTENTS

(Continued)

LIST OF FIGURES

LIST OF FIGURES
(Continued)

LIST OF FIGURES

(Continued)

LIST OF TABLES

INTRODUCTION

This is Volume III of the final report on work performed under Contract AF33(616)-5154, Supplement 53(59-207), involving research of materials for liquid-hydrogen boost tanks. The extremely low temperature of liquid hydrogen presents some unique problems in selecting materials for tanks. Insulated tanks are a necessity to prevent high boiloff losses during standby and flight. These insulations must withstand large thermal differences between the exterior surface and the interior surface. To qualify for rocket vehicle tankage, the insulation must also withstand the vibrations from the engine, dynamic pressure during flight through the atmosphere, and the aerodynamic heating associated with flight through the atmosphere. The vibration and dynamic pressure effects are beyond the scope of this study, but the requirements for materials capable of withstanding aerodynamic heating are considered in detail. For cryogenic application, many insulations that can be evacuated make a very good insulation provided an exterior encapsulating material can be placed over the insulation for vacuum sealing.

This volume considers structural material for liquid hydrogen tanks, insulation for the side walls and the ends, and encapsulation materials. The materials chosen are primarily for the 7,000-gallon test tank which was tested in the thermal test facility, but the materials for the most part are applicable to actual rocket vehicle tanks containing cryogenic liquids.

1.0 PRIMARY STRUCTURAL MATERIALS

1.1 Tank Structural Material Selection

There is only one combination of tank structural material and tank sidewall insulation that will produce the lowest overall system weight for a given rocket (whether it be a ballistic missile, an orbital vehicle or a space probe) to accomplish a definite mission. The lowest overall system weight must include not only material weight; but, also, the weight of the unusable, vented or residual fuel. In the analysis of these various combinations, it is possible to determine the temperature limits that the material will have to endure. The determination of this optimum system weight is quite complicated and involves a rather long period of time using an electronic computer. See Section 4.0 of Volume I of this report for the details of this type of analysis.

In order to expedite the material selection for the 7,000-gallon test tanks, it was decided to use -423°F to 1000°F as the range of operating temperature. It was felt that this range would embrace the majority of temperatures resulting from optimum system weight studies.

Using these temperature limits, the preliminary selection was based on the strength-to-weight ratios of various high-strength materials. Known values of the ratios are shown in Figure 1.

In addition to possessing a high strength-to-weight ratio over the temperature range, the tank material should also have the following characteristics:

(1) A practical heat treatment for the large structure or no heat treatment.

(2) Retain ductile behavior at liquid hydrogen temperature, good fracture toughness or low sharp-notch sensitivity.

(3) Good weldability, preferably coupled with high efficiency.

(4) Low thermal coefficient of expansion to minimize thermal stresses.

(5) Available in large sheets of thin gages with minimum thickness tolerances.

(6) Ease of fabrication and repair.

The final selection of the tank material should be based on a combination of these considerations that will yield an optimum tank design. By consideration of the strength-to-weight ratio, the list of considered materials was reduced to the following metals:

FIGURE 1
STRENGTH-TO-WEIGHT RATIO VERSUS TEMPERATURE
OF SOME STRUCTURAL MATERIALS

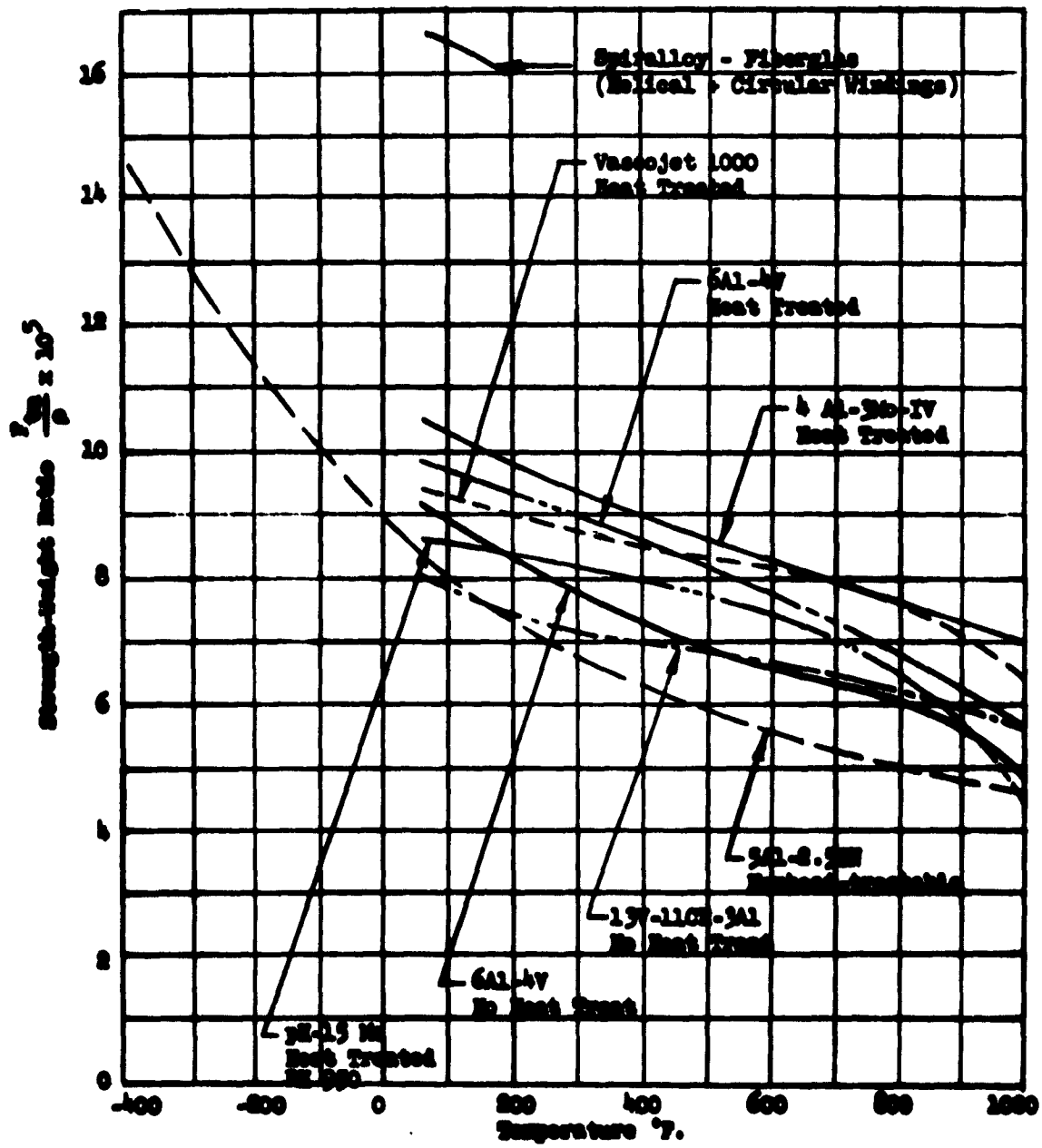

(1) Ultra-high-strength chromium steels such as Vascojet 1000 (Vanadium-Alloys Steel Company).

(2) Precipitation hardened stainless steels such as pH-15-7-Mo or 17-7pH (Armco Steel Corporation).

(3) Titanium alloys as follows:

(a) 13V-11Cr-3Al (B-120VCA Crucible Steel Company).
(b) 4Al-3Mo-1V (Ti-4Al-3Mo-1V, Titanium Metals Corporation).
(c) 5Al-2.5Sn (Ti-5Al-2.5Sn, Titanium Metals Corporation or A-110-AT, Crucible Steel Company).
(d) 6Al-4V (Ti-6Al-4V Titanium Metals Corporation).

The aluminum and magnesium alloys, as well as the reinforced plastic, were eliminated because their strengths are too low at 1000°F.

1.1.1 Ultra-High-Strength Chromium Steels

According to the literature purblished by the manufacturer, Vascojet 1000 (with a Rockwell hardness of 50) has an ultimate tensile strength of 180,000 psi and a strength-to-weight ratio of 643,000 inches. These high allowables look attractive at first glance; however, in order to obtain these strengths, the metal must be processed through an elaborate heat treatment.

The heat treating of very large tanks after welding presents a major problem. It is very doubtful that facilities exist, or would exist, to handle such large envelopes. Several methods of simplifying the mechanical problems of the heat treat process have been suggested, although none of them appear too feasible at this time. One such method would utilize the tank itself for the heating furnace. This would require a vast amount of high-temperature insulation if it were to be done effectively or economically. Another method would use heat-treated sheets, and only the welded area would be reheat-treated.

Vascojet 1000 in the annealed condition offers no strength-to-weight ratio advantage due to its low strength in that condition. Another disadvantage is the fact that it is available only in .025-inch minimum thicknesses and 24 inches maximum width. This would, of course, require additional welded joints and reduce the overall reliability of the tank.

One definite advantage of this alloy is that it possesses a low thermal contraction rate which is very close to that of titanium. This alloy could find utilization in fittings and parts that are subsequently bolted to titanium flanges. The equal contraction rates would help to minimize sealing problems that are generally encountered at these joints.

1.1.2 Precipitation Hardened Stainless Steels

These alloys are similar to the previously mentioned alloys in that they possess high strength-to-weight ratios at elevated temperatures. Again, however, this is brought about by sacrificing ductility and impact strength and subjecting the alloy to a complex heat treatment that does not lend itself to the large objects under study.

Very little low temperature data was available on these alloys; however, a General Electric Report (Reference 9) indicated that the elongation of 17-7pH at LH_2 temperatures is only 6/10 of 1% while the ultimate tensile stress approaches 280,000 psi.

Because of this low elongation property and because of low welded joint efficiencies at high temperatures, the precipitation hardened stainless steels are not recommended for the intended tankage application.

1.1.3 13V-11Cr-3Al Titanium Alloy

This all beta alloy, in the aged condition, possess high-strength levels, and the simple aging process makes this high-strength level easily obtainable in a fabricated article. The high strength-weight ratio makes the alloy one of the most efficient structural materials available. Maximum operating temperature is limited to +600°F for prolonged periods of time. Temperatures above 600°F can be tolerated for only short time periods due to the transformation of the beta form to the alpha form.

When thermally controlled, the alloy has excellent formability, weldability and adaptability to hydrospinning. These characteristics make the alloy particularly suitable for lightweight pressure vessels. Due to loss of ductility (attributed to the 11% chromium content), the lower temperature limit for pressure vessel use is -65°F. This limitation precludes the use of this alloy for tanks containing liquid hydrogen or liquid oxygen. The use of this material should be limited to storable propellant tanks.

1.1.4 4Al-3Mo-1V Titanium Alloy

This is a relatively new alloy produced by Titanium Metals Corporation that has high strength properties at elevated temperatures combined with excellent formability, ductility and creep resistance. The solution treatment and aging process are similar to that of the previous titanium alloy discussed although the temperatures are slightly higher.

The elongation of the aged material is only 5% at room temperature, and it would be expected to be even lower at LH_2 temperature. The manufacturer indicates that the alloy can be readily welded, although the ductility of the welded metal is even lower than the parent metal.

This alloy was not recommended because of low ductility; also, because of limited availability in the desired gages and sizes.

1.1.5 5Al-2.5Sn Titanium Alloy

This alloy is a medium strength all-alpha titanium alloy designed primarily for use in sheet and strip form. It is readily weldable and adaptable to all kinds of sheet metal forming. This alloy shows amazing ductility even at -423°F, which makes it highly desirable for cryogenic applications.

Since the alloy is nonheat-treatable, the problems associated with this operation are eliminated. Because of this characteristic, the strength allowables, hence the strength-to-weight ratio, is lower than some of the other alloys.

The primary reason for its rejection at this time is that it is a difficult alloy to roll and, therefore, cannot be supplied in thicknesses less than .040". On some of the larger tanks under study where the skin gages will be over this thickness, the use of this alloy appears quite attractive.

1.1.6 6Al-4Zr-1V Titanium Alloy

Titanium Metals Corporation of America is presently developing a new titanium alloy, Ti-6Al-4Zr-1V, which appears particularly favorable for a near future pressure vessel application.

Advantages of this new alloy are:

(1) Provides higher strengths than 6Al-4V.

(2) Welding characteristics are equal to 5Al-2.5Sn, which is presently the best of the weldable titanium alloys.

(3) It is easy to roll, thus will provide sheet sizes of .025" x 36" x 120" probable and .025" x 48" x 120" possible.

1.1.7 6Al-4V Titanium Alloy

The 6Al-4V alloy has received wide acceptance by the airframe and missile industry. It is a heat-treatable alpha-beta alloy, available in sheet and strip stock, as well as in a variety of other mill forms.

This alloy is not considered as weldable as the all-alpha alloys although satisfactory weldments have been made with joint strengths equal to or greater than the parent metal. The welding process must include not only an inert gas shielded electrode but, also, an inert gas back-up shield. In addition, the welding head must have an inert gas trailing shield that will isolate the welded area until it has time to cool down to approximately 900°F. It is suggested that all welds be stress relieved, although it may not be necessary with the thin gages that are to be used.

The ultimate tensile strength (at 1000°F) of this alloy in the mill-annealed condition is 78,000 psi. The alloy can, however, be heat-treated to strengths upwards to 94,000 psi (at 1000°F) through the use of a solution treatment and aging process.

The ductility of this alloy is not as great as 4Al-2.5Sn, although it is better than most of the other titanium alloys. This ductility is said to be nondirectional and applies to both the nonfiller-type weld and parent metal.

This alloy is relatively easy to roll and is available in large sheets (36" x 96") in thicknesses as low as .016".

The alloy has been used successfully in other cryogenic applications; and, therefore, some low-temperature property data was available.

This titanium alloy possesses the right combination of the desired characteristics as outlined earlier and was recommended for the proposed test tank. Utilization in the mill-annealed condition eliminated the problem of heat treatment.

The overall differences between the 5Al-2.5Sn and the 6Al-4V in the mill-annealed state are quite small. The 5Al-2.5Sn has the greater ductility at cryogenic temperatures and better weldability. On the other hand, the 6Al-4V has higher strength at elevated temperatures and can be rolled into thinner, more uniform gages. For the 7,000-gallon test tank, the thinner 6Al-4V sheets were desirable to effect minimum tank weight. Properties of mill-annealed 6Al-4V are presented in Figures 2 through 7. These plots were obtained from data available at the time. Extrapolation was necessary in some cases.

1.1.8 Material Tolerances

The selection of tolerances for the sheet material required a study of cost versus weight saving. The allowable thickness tolerance on the titanium sheet was reduced from the recommended mill practice at a cost premium. The increase in price was worthwile when compared to weight savings as shown by the following analysis.

Using the N85-100 configuration as reported in Reference 8, the ratio of wet weight to dry weight is:

$$536{,}460 \text{ lb} / 145{,}040 \text{ lb} = 3.70$$

The total tank skin area of that configuration is 13,430 ft^2. Based on a 0.001" thickness reduction over the entire skin area, the reduction in weight would be

$$(0.001)(13{,}430)(144)(0.161) = 311 \text{ lbs}$$

FIGURE 2
AVERAGE TENSILE STRENGTH OF 6Al-4V ANNEALED TITANIUM ALLOY

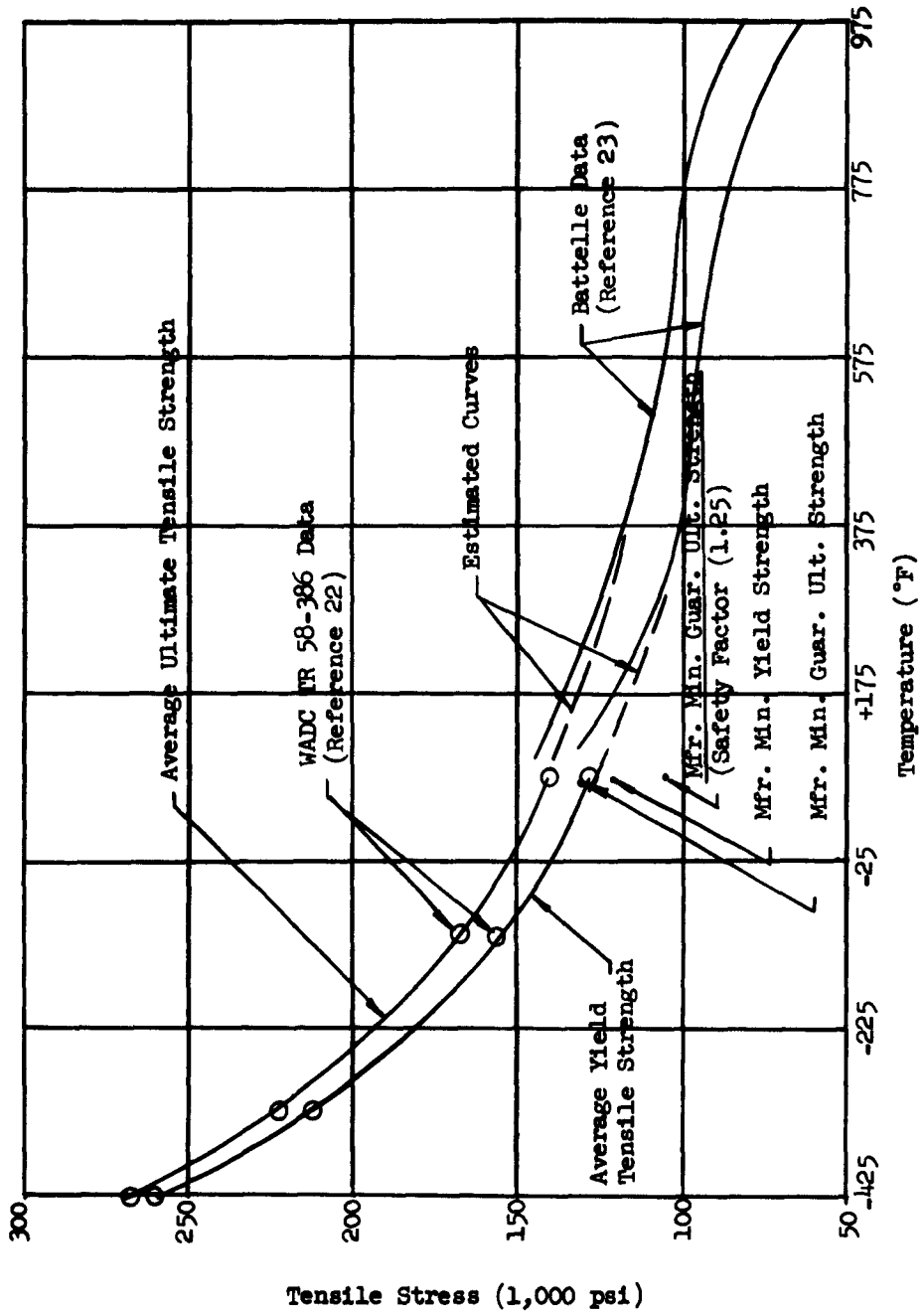

FIGURE 3
AVERAGE ELONGATION AND REDUCTION IN AREA
OF 6Al-4V ANNEALED TITANIUM ALLOY

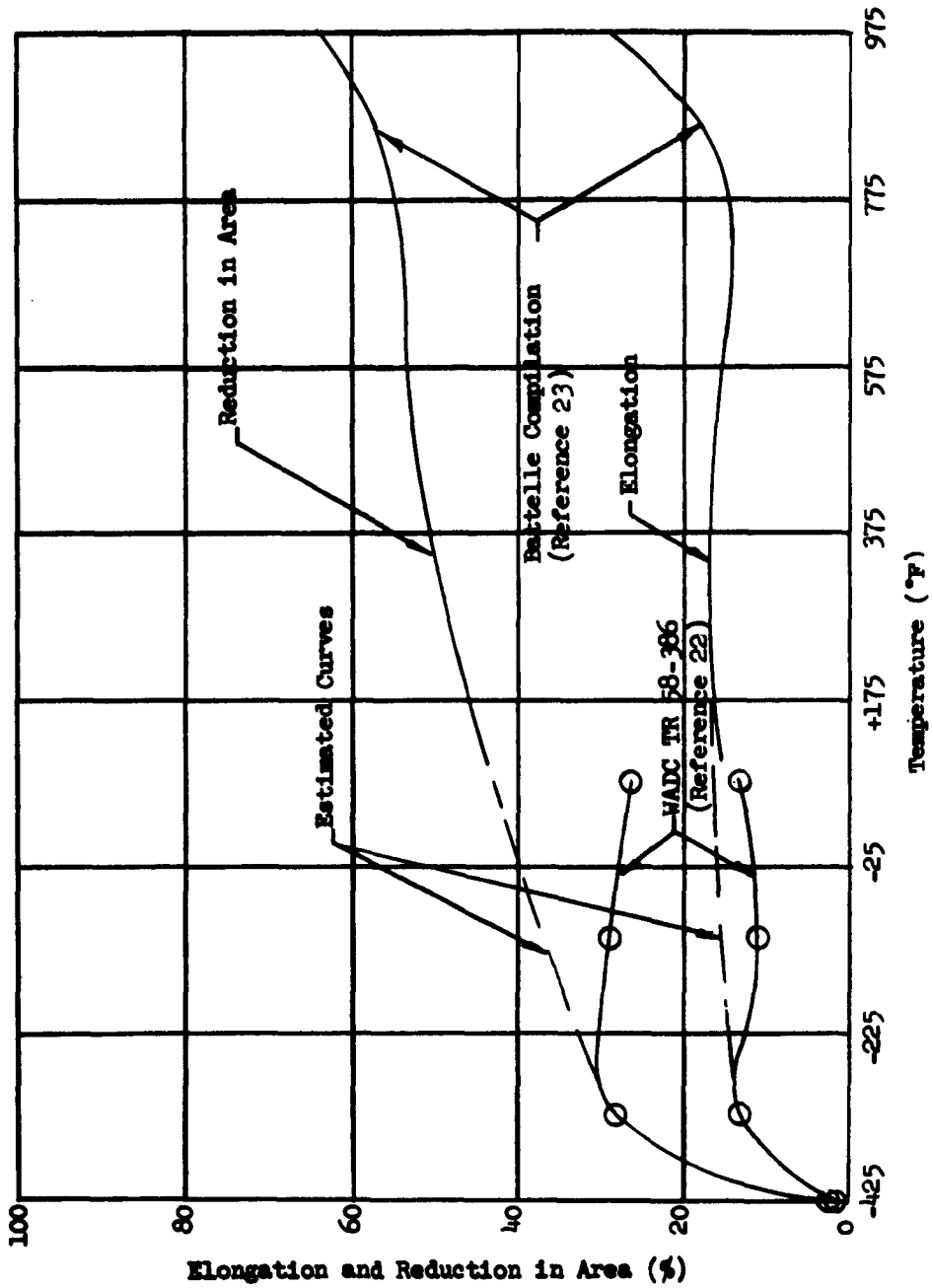

FIGURE 4
YOUNG'S MODULUS OF 6Al-4V TITANIUM ALLOY

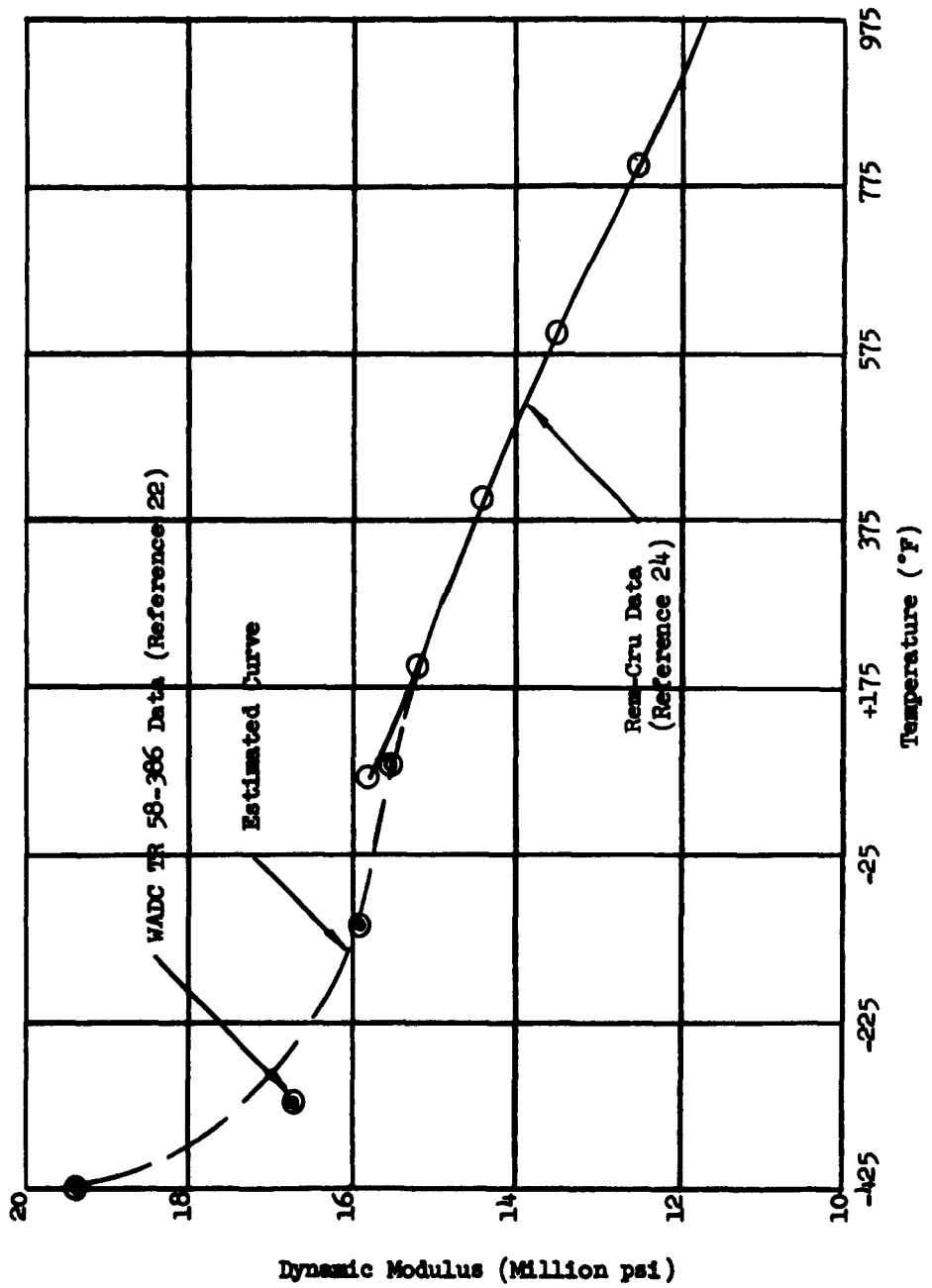

FIGURE 5
THERMAL EXPANSION OF TITANIUM

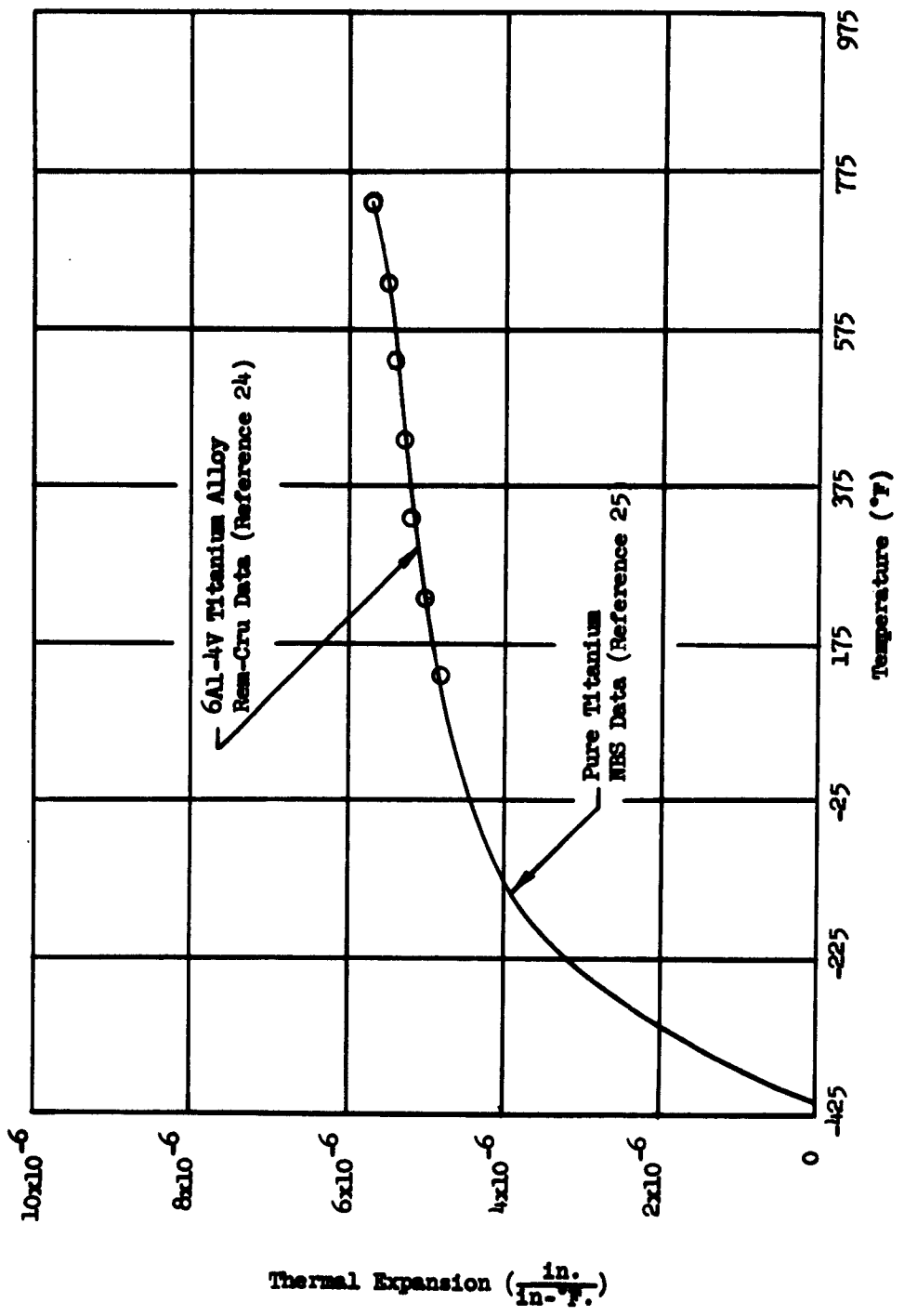

FIGURE 6
THERMAL CONDUCTIVITY OF TITANIUM

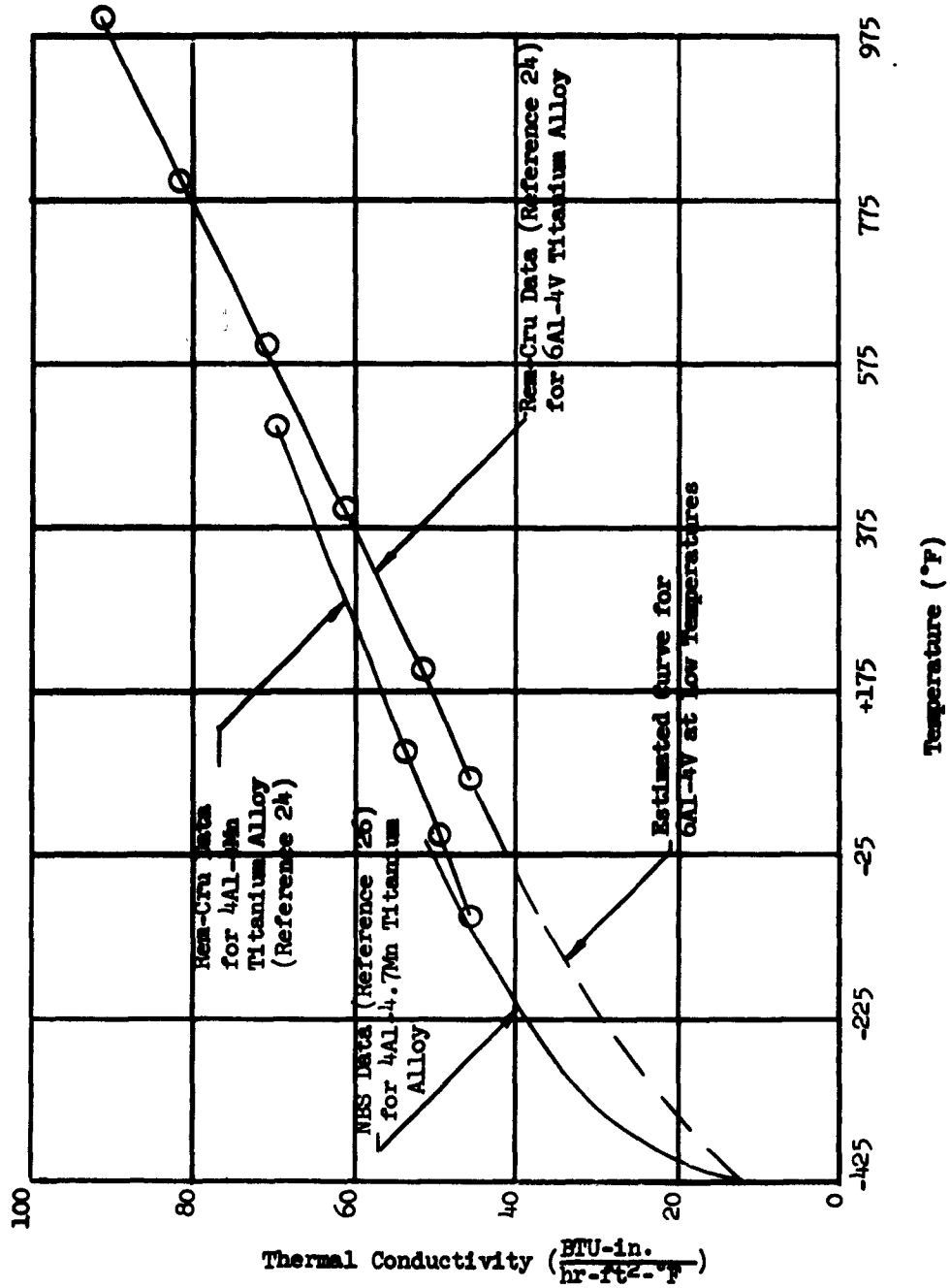

FIGURE 7
SPECIFIC HEAT OF TITANIUM

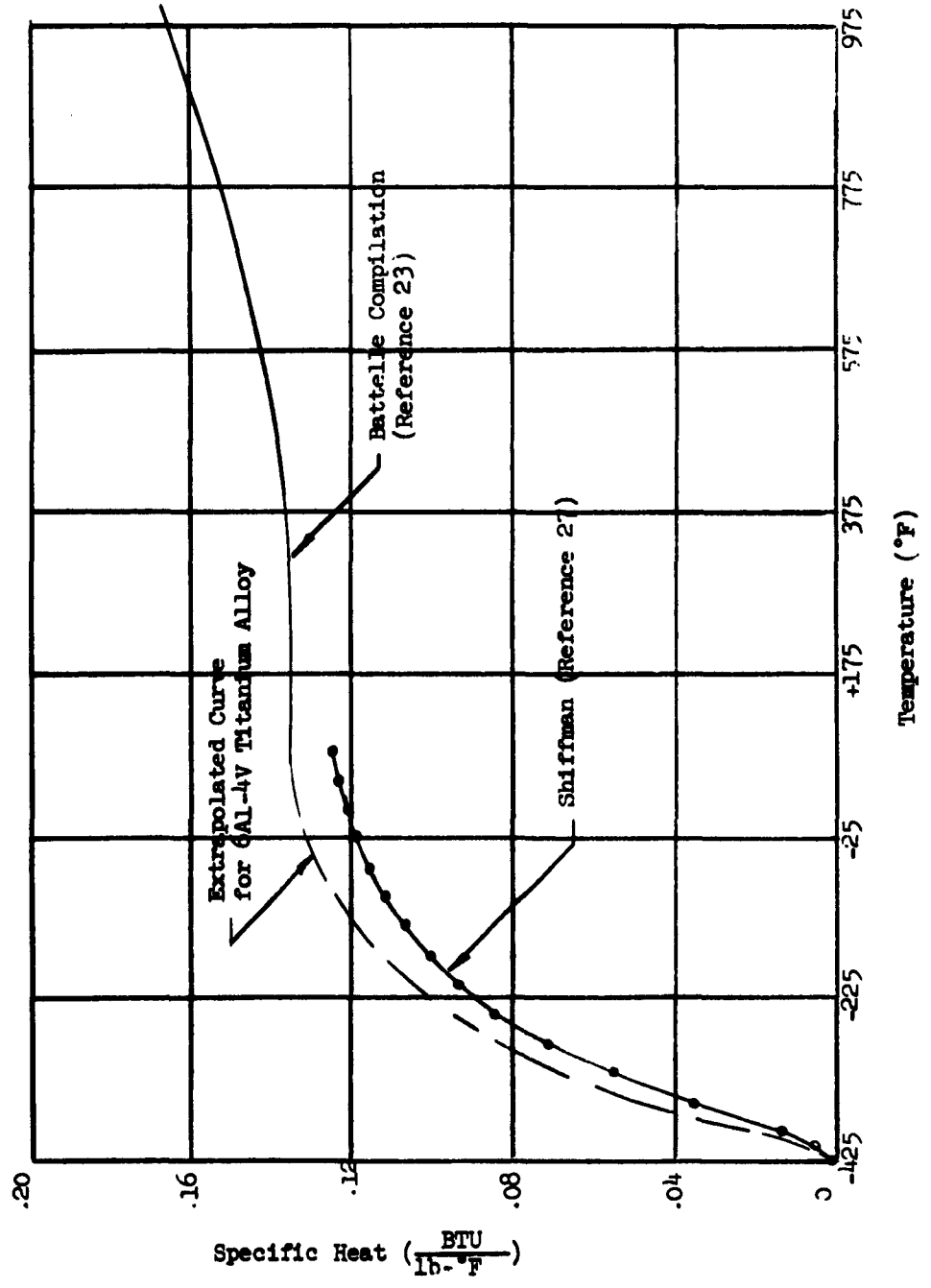

To save the 0.001" in skin thickness, the manufacturer will charge a tolerance premium for special mill roll. A conservative estimate of this premium was made at $1.75/lb. The actual premium was closer to $1.00/lb. The total weight of a titanium tank for the N85-100 configuration is 8,450 lbs (based on room temperature tensile allowables) with a resulting tolerance premium of ($1.75/lb)8,450) = $14,800.

The ratio of wet weight (launch weight) to dry weight (burnout weight) being 3.70, the theoretical weight saved at launch is (3.70)(311) = 1,150 lbs.

Assuming that the cost of fuel will be $0.50/lb, that structural cost is $50/lb, and that 73% of the total launch weight is fuel, the gross dollar savings of the 1,150-lb reduced launch weight is:

Fuel	(1,150)(0.73)($0.50)	= $ 420
Structure	(1,150)(0.27)($50)	= 15,500
	Gross Dollar Savings	= $15,920

Thus, at an expense of $14,800 for tolerance, a net savings of $15,920 - $14,800 = $1,120 per launched vehicle is effected. The actual premium for closer tolerance of $1.00/lb would have increased this savings to $7,470. It should be noted that such dollar savings are gained by only a 0.001" savings in tolerances.

Another important point to be considered is the maximum wall temperature of the tank. As the maximum operating temperature decreases, the design allowables increase, thereby decreasing skin thickness. As the skin thickness decreases, a .001" saving through thickness tolerance represents a larger percentage of vehicle cost. This is illustrated, using the N85-100 configuration with fuel cost at $0.50/lb and fuel weight at 73% of total tank wet weight, in Figure 8 where net savings versus operating temperatures for various structural unit costs is shown.

As a result of this study, certain reductions in sheet tolerance for the test tank material were required of the titanium supplier. The 0.018" thick sheet had a standard tolerance of $\pm$ .003 in. A tolerance of $\pm$ .002" was specified on this sheet effecting a $\bar{0}$.001" weight savings and a $\bar{0}$.001" design allowable increase. The 0.025" thick sheet had a standard tolerance of $\pm$ .003". A tolerance of plus .002" minus .001" was specified providing a $\bar{0}$.001" weight saving and a .002" design allowable increase. The reason for including this design parameter for the test tank was to determine true weights and cost of actual cryogenic flight tanks.

1.2 Material Testing

The selection of mill-annealed 6Al-4V titanium as the tank structural material necessitated some material testing. The reasons for this test are given below.

FIGURE 8
NET DOLLAR SAVINGS DUE TO REDUCED SKIN TOLERANCES
VERSUS TANK SKIN MAXIMUM OPERATING TEMPERATURE

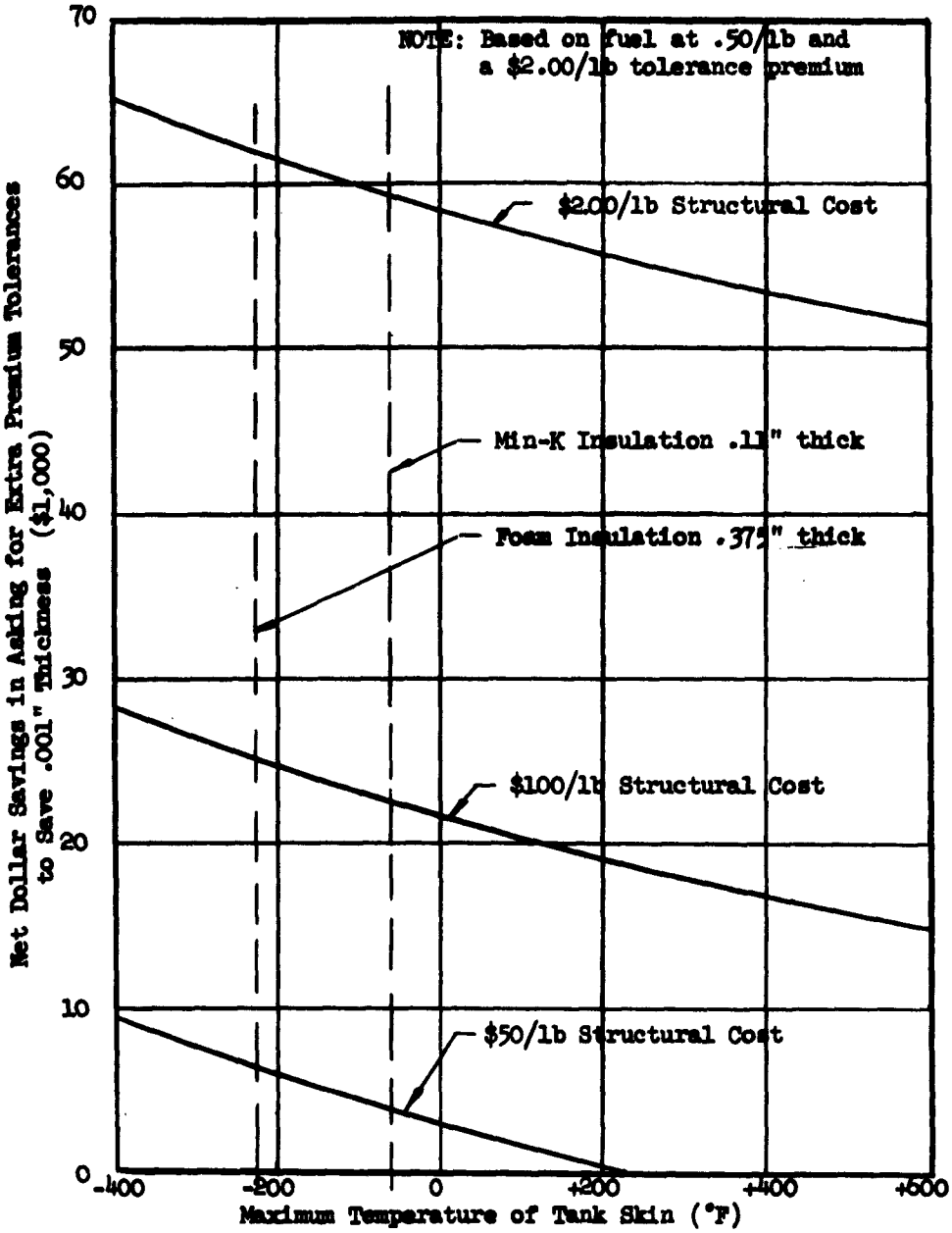

(a) The material was relatively new, thus material properties at cryogenic and elevated temperatures were limited particularly for the welded specimens.

(b) Fabrication methods such as fusion welding of thin sheet and requirement for stress relief must be verified prior to actual tank construction.

Before the welded test specimens could be prepared, it was necessary for the fabrication personnel to develop suitable methods of welding that would guarantee good welds. Using the titanium manufacturer's welding recommendations as a guide, a series of welding techniques were employed in an effort to determine the optimum settings for the welding speed and the argon gas feed. Table 1 presents a record of this welding test work. The settings that were used in Sheets No. 9 through 17 produced welds of good quality, and all tensile and bend specimens were prepared from these sheets. The sheets were vapor degreased and burrs were removed by filing and all of the sheets were welded with the following equipment:

Welder	Miller direct current welder, Model SR-200
Torch	Linde Heli-Arc Torch, Model H.W.18, No. 7 ceramic cup
Electrode	Tungsten 2% thoria finish centerless ground, .040 diameter ground to a point
Back-up bar	1020 steel, groove 1/8" wide, .020" deep, 3/64" diameter orifices, staggered 1-1/2" apart along edge of groove.

1.2.1 Tensile Testing

Specimens were prepared in accordance with Beechcraft Specification 6157 which is presented in the Appendix of this volume. Prior to shearing the specimens from the welded sheets, X-ray pictures were taken. In addition, the welds were leak checked with a mass spectrometer assuring that the welds were leaktight.

1.2.1.1 Room Temperature Tests

The twelve (12) specimens were sheared to a constant one-half-inch width as an economy measure instead of the conventional dumbbell shape.

Figures 9 and 10 show the pulled specimens with their respective parent metal grain direction. Each specimen is identified with its ultimate tensile strength and per cent elongation in two (2) inches. Specimens G_{1c}, G_{2c}, G_{3c}, and G_{4c} were notched .032" on each edge of the weld.

TABLE I
6Al-4V TITANIUM ALLOY WELD TEST STRIPS
(PER BEECH SPECIFICATION 6157)

SHEET NO.	WELD PREPARATION	WELDING	BEND TEST	X-RAY TEST
1	Weld area cleaned and wiped with lint-free cloth	Amperes: 30 Argon gas: 15 ft^3/hr @ torch 3 ft^3/hr @ back-up Weld Speed: 16 I.P.M.	Failed	Showed some gas porosity and gas holes
2	Same as No. 1	Amperes: 32 Argon gas: 15 ft^3/hr @ torch 5 ft^3/hr @ back-up Weld Speed: 18 I.P.M.	Failed	Showed trace of gas
3	Same as No. 1	Amperes: 33 Argon gas: 15 ft^3/hr @ torch 5 ft^3/hr @ back-up Weld Speed: 21.5 I.P.M.	Specimens stress relieved @ 1000° for 15 minutes. Transverse ok. Longitudinal failed at edge of weld.	Showed trace of gas
4	Same as No. 1	Amperes: 29 Argon gas: 16 ft^3/hr @ torch 5 ft^3/hr @ back-up	Failed	Showed trace of gas
5	Same as No. 1	Amperes: 31 Argon gas: 15 ft^3/hr @ torch 5 ft^3/hr @ back-up Weld Speed: 18 I.P.M.	Failed	Showed Good Quality

TABLE I (continued)
6Al-4V TITANIUM ALLOY WELD TEST STRIPS
(PER BEECH SPECIFICATION 6157)

SHEET NO.	WELD PREPARATION	WELDING	BEND TEST	X-RAY TEST
6	Weld area was cleaned by scrubbing with Ajax and wiped with lint-free alcohol cloth	Amperes: 30 Argon gas: 15 ft^3/hr @ torch 5 ft^3/hr @ back-up No gas in trailing shield	Failed	Specimen was not x-rayed
7	Same as No. 6	Amperes: 30 Argon gas: 15 ft^3/hr @ torch 3 ft^3/hr @ shield Weld Speed: 15.5 I.P.M.	Failed	Showed excessive porosity
8	Same as No. 6	Amperes: 31 Argon gas: 15 ft^3/hr @ torch 5 ft^3/hr @ back-up 15 ft^3/hr @ shield	Small Fractures	Specimen was not x-rayed
9	Weld area was cleaned with steel wool to remove oxides and wiped w/ lint-free cloth	Amperes: 31 Argon gas: 15 ft^3/hr @ torch 5 ft^3/hr @ back-up 20 ft^3/hr @ shield Weld Speed: 15 I.P.M.	Transverse to weld, 4.5t root ok 4.5t face ok Parallel with weld, 4.5t root ok 4.5t face ok with aluminum back-up strip	Good Quality
10 thru 17	Same as No. 9	Same as No. 9	ok	Good Quality

FIGURE 9
ROOM TEMPERATURE TENSILE TESTS
6Al-4V ANNEALED TITANIUM ALLOY

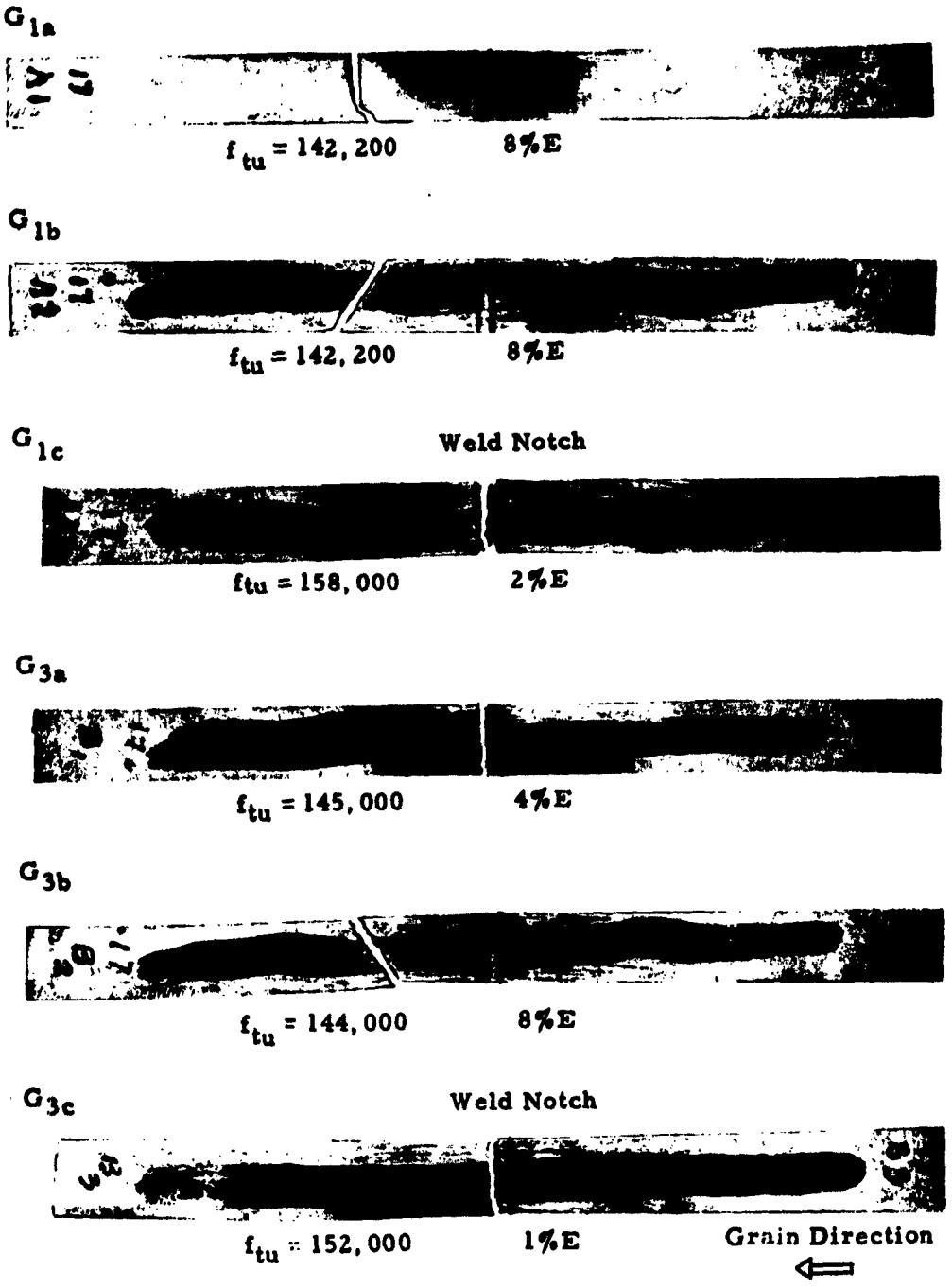

FIGURE 10
ROOM TEMPERATURE TENSILE TESTS
6Al-4V ANNEALED TITANIUM ALLOY

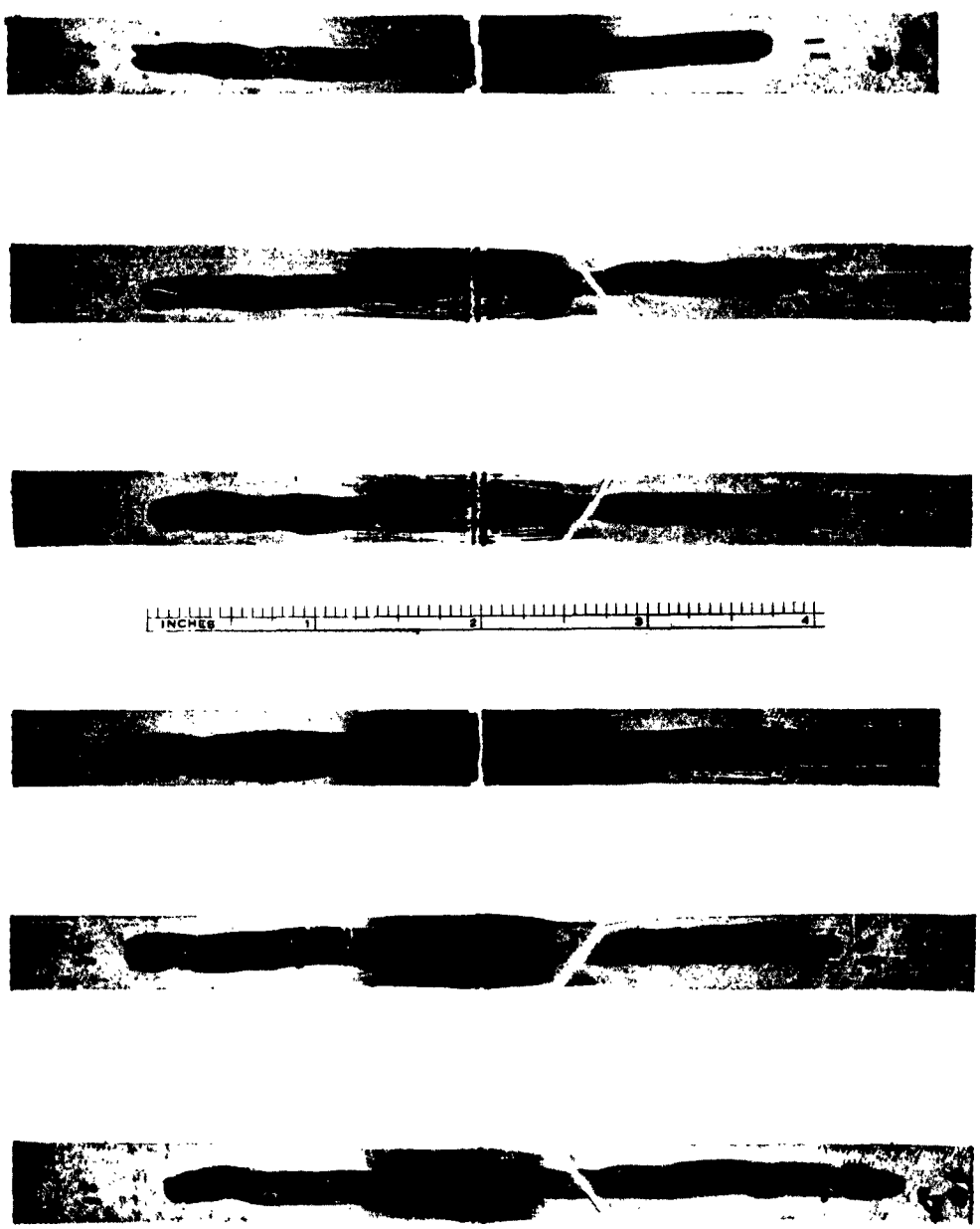

This was done to insure failure in the weld material and no attempt was made to duplicate ASTM notched tensile specimens. The test areas were liquid honed to remove any burrs.

All of the specimens failed in the parent metal area or the notched weld area, except Specimen No. G_{3a}, which failed in the unnotched weld area. Examination of the X-ray of this specimen showed a dark area approximately .06 inches in length at the edge of the weld. This porosity was caused by the difficulty of starting a weld at the edge of the original sheet and undoubtedly accounted for the irrational weld fracture. The average ultimate tensile stress for the parent metal was 143,000 psi with 8% elongation in 2 inches (transverse grain) and 139,000 psi with 10% elongation in 2 inches (longitudinal grain). These values compared favorably with the manufacturer's guaranteed minimum values of 130,000 psi with 8% elongation in 2 inches.

1.2.1.2 1000°F Testing

Fourteen (14) tensile specimens were tested at 1000°F by Titanium Metals Corporation of America at Toronto, Ohio. The specimens were welded by Beech, but milled to final size by T.M.C.A. The test furnace temperature was stabilized at 1000°F and each specimen was held at this temperature for ten (10) minutes prior to applying the tensile load.

Figures 11 and 12 show the separated specimens with respective parent metal grain direction. Each specimen in these figures is identified with its yield and ultimate tensile stress plus the per cent elongation in two (2) inches. Specimens B_3 and B_4 were notched .032" on each edge of the weld to produce failure in the weld material.

The average ultimate tensile stress for the parent metal was 85,300 psi with 12.3% average elongation in 2" (transverse grain) and 78,600 psi with 15.3% average elongation in 2" (longitudinal grain). The average ultimate tensile stress for the weld metal was 83,800 psi with 6% average elongation in 2" (transverse grain) and 80,200 psi with 8.5% average elongation in 2" (longitudinal grain).

These values compare favorably with Battelle published data of 78,000 psi ultimate stress and 60,000 psi yield stress.

Specimens C_1, C_2, C_3, and C_4 which were pulled 45° to the grain direction showed an ultimate tensile strength consistently 20% less in value than the transverse and longitudinal grain specimens.

1.2.1.3 Weld Gap and Mismatch Testing

With poor joint fitup it is difficult to properly weld thin-gage titanium sheets. Poor fitup enables the molten metal to fall through instead of fusing to form a welded joint and increases the possibility of contamination

FIGURE 11
1000°F TEMPERATURE TENSILE TESTS
6A1-4V ANNEALED TITANIUM ALLOY

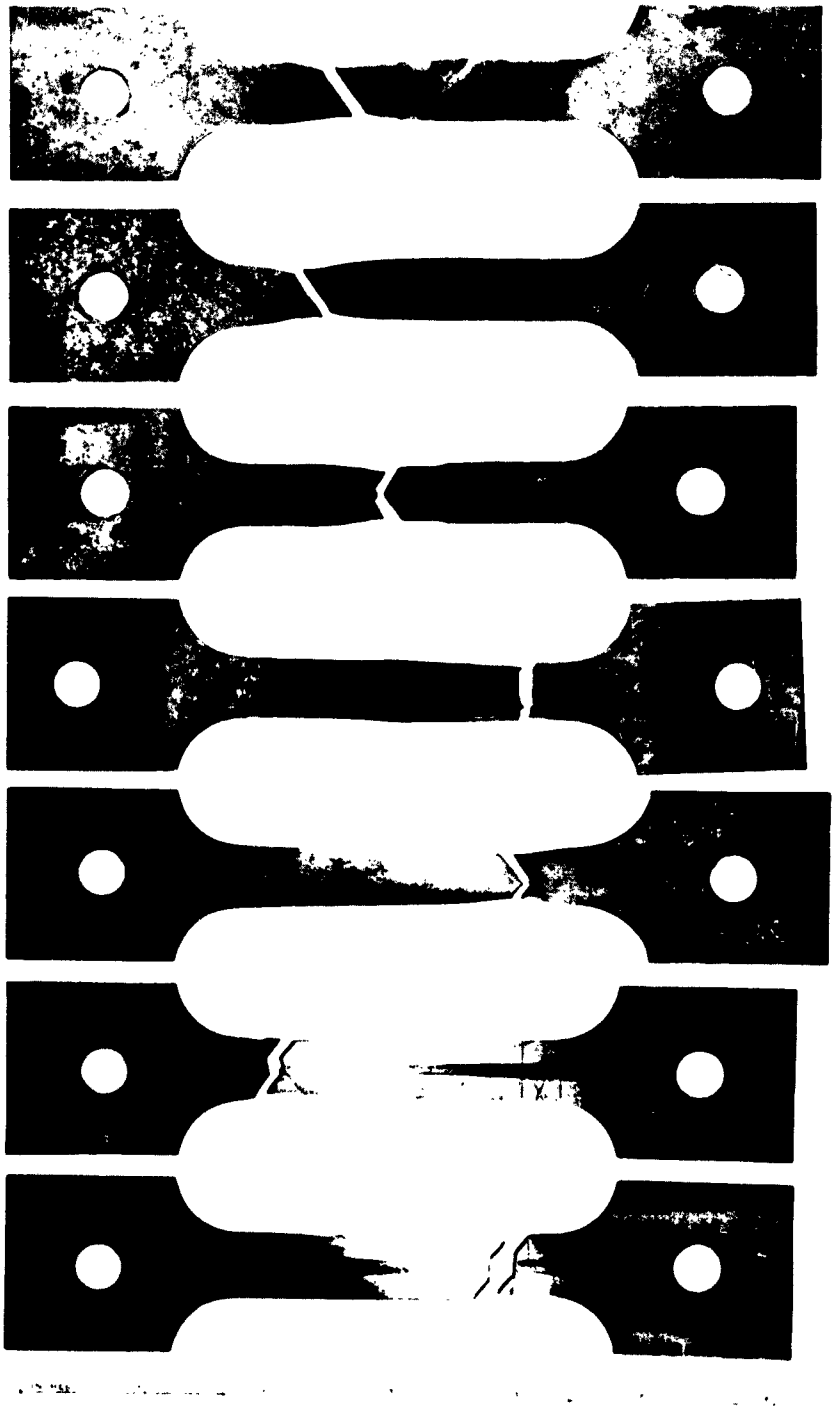

FIGURE 12
1000°F TEMPERATURE TENSILE TESTS
6Al-4V ANNEALED TITANIUM ALLOY

from air trapped in the joint. A series of tests were performed to determine the effect of the gap and mismatch on the strength of the weld.

The titanium manufacturer recommended a maximum root opening (gap) of 0.002 inch for thin sheets. During fabrication shearing and trimming, the maximum root opening could be exceeded; consequently, a series of tensile tests were conducted to determine the strength of various welded gaps. Figure 13 shows the tested specimens with their respective grain direction.

The specimens were welded together after the gap was carefully measured with a feeler gage. Specimens with gaps larger than .007 inch could not be effectively fusion-welded together. All of the specimens failed in the parent metal except the .007" gap specimen which failed in the weld. Even though the specimens with .006" gap proved to have sufficient weld strength, welding of long seams with this much gap was erratic. Table 2 lists the various gapped specimens and the resulting ultimate tensile strengths.

The next series of tensile tests included specimens with combined mismatch and gap. This combination of joint fitup actually occurred. The specimens were prepared in a weld fixture using a shim to produce the desired mismatch. The specimens are listed in Table 3 showing gap and mismatch combinations tested plus their respective strengths. Figure 14 shows the failed specimens with the grain direction noted.

It was concluded that the maximum welding gap be maintained at the manufacturer's recommendation of 0.002 inch in combination with a maximum mismatch of 0.003 inch. In cases where no mismatch would exist, the maximum gap was extended to 0.005 inch.

From the limited number of specimens tested, it was concluded that the weld material properties as compared to the parent metal were 18% higher in yield strength, 28% higher in ultimate tensile strength, and 29% lower in per cent elongation.

1.2.2 Bend Testing

Bend test specimens were prepared in accordance with Beechcraft Specification 6157 and discussed in the following sections.

1.2.2.1 Room Temperature Testing

Series L and M specimens were tested with various bend radii. Figure 15 shows the result of the tests. All of the specimens showed acceptable ductility except M_1, M_2, M_3, and M_4. The weld areas of specimens M_1 and M_2 fractured abruptly with a 4.5t-bend radius. The weld areas of specimens M_3 and M_4 fractured with an 8t-bend radius. Additional tests with

FIGURE 13
PHOTOGRAPH OF GAP WELDED TENSILE SPECIMENS
(.016t, 6Al-4V ANNEALED TITANIUM, ROOM TEMPERATURE TEST)

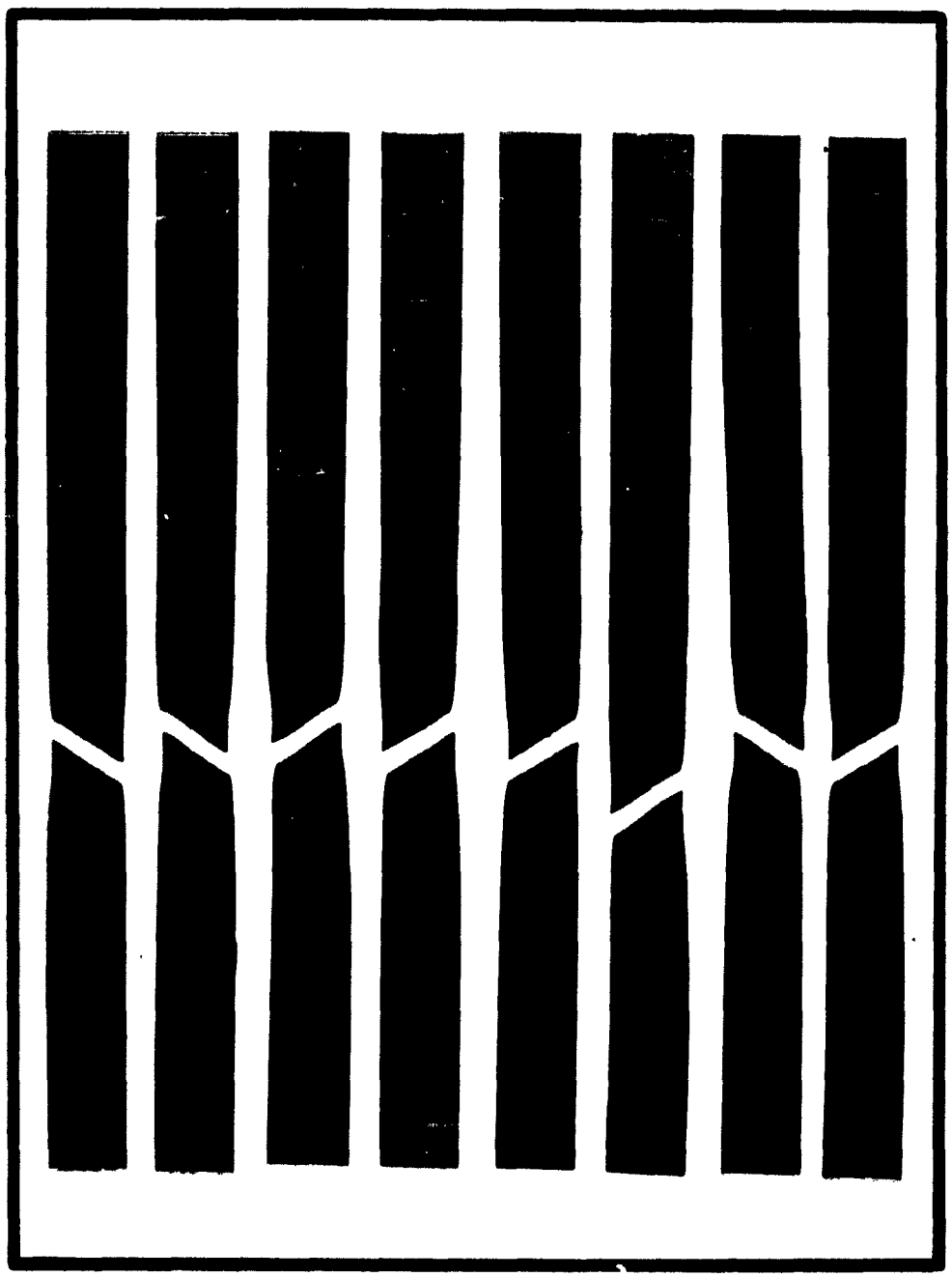

FIGURE 13 (continued)
PHOTOGRAPH OF GAP WELDED TENSILE SPECIMENS
(6016t, 6Al-4V ANNEALED TITANIUM, ROOM TEMPERATURE TEST)

TABLE 2
GAP WELDED TENSILE SPECIMENS
(.016t, 6Al-4V ANNEALED TITANIUM, ROOM TEMPERATURE TEST)

Specimen Number	Gap inch	Mismatch inch	Yield psi	Ultimate psi	Elong. %2"	Fracture Location
A	.000	.000		145,600		Parent Metal
A_1	.000	.000		143,800		"
B	.0025	.000		146,400		"
B_1	.0025	.000		144,800		"
C	.003	.000		142,400		"
C_1	.003	.000		143,300		"
D	.004	.000	Not Recorded	135,700	Not Recorded	"
D_1	.004	.000		137,800		"
E	.005	.000		144,600		"
E_1	.005	.000		141,900		"
F	.006	.000		152,700		"
F_1	.006	.000		154,800		"
G	.007	.000		143,800		"
G_1	.007	.000		146,000		"

TABLE 3
GAP AND MISMATCH WELDED TENSILE SPECIMENS
(.016t, 6Al-4V ANNEALED TITANIUM, ROOM TEMPERATURE TEST)

Specimen Number	Gap	Mismatch	Yield	Ultimate	Elong.	Fracture Location
	inch	inch	psi	psi	%2"	
1A	.000	.003	127,500	135,700	5	Parent Metal
1B	.000	.003	128,700	135,200	7	"
1C	.000	.003	136,300	148,800	7.5	"
1D	.000	.003	137,100	148,700	8.5	"
2A	.002	.003	121,600	144,100	7	"
2B	.002	.003	126,200	149,300	8.5	"
2C	.002	.003	129,300	136,500	8.5	"
2D	.002	.003	130,200	136,600	4.5	"
3A	.002	.000	128,100	134,900	7.5	"
3B	.002	.000	128,000	135,500	8.5	"
3C	.002	.000	135,100	149,600	6	"
3D	.002	.000	138,600	149,600	6	"
4A	.000	.000	125,900	135,700	10	"
4B	.000	.000	128,400	136,200	10	"
4C	.000	.000	137,600	149,100	10	"
4D	.000	.000	139,000	148,900	9	"

TABLE 3 (continued)
GAP AND MISMATCH WELDED TENSILE SPECIMENS
(.016t, 6Al-4V ANNEALED TITANIUM, ROOM TEMPERATURE TEST)

Specimen Number	Gap	Mismatch	Weld	Ultimate	Elong.	Fracture Location
	inch	inch.	psi	psi	%2"	
5A	.002	.003	126,400	137,700	7	Parent Metal
5B	.002	.003	127,200	136,300	5.5	"
5C	.002	.003	131,000	144,300	4.5	"
5D	.002	.003	138,200	150,600	4	"
6A	.000	.003	127,000	135,300	8	"
6B	.000	.003	130,900	138,700	5.5	"
6C	.000	.003	129,700	144,900	5.5	"
6D	.000	.003	128,400	144,800	7	"
7A	.002	.000	138,700	150,000	8.5	"
7B	.002	.000	140,900	151,600	7	"
7C	.002	.000	118,700	131,400	5	"
7D	.002	.000	125,300	138,100	6	"
8A	.000	.000	129,800	135,900	8	"
8B	.000	.000	126,900	134,600	7	"
8C	.000	.000	135,900	148,700	4	"
8D	.000	.000	136,200	149,300	5.5	"

FIGURE 14
PHOTOGRAPH OF GAP AND MISMATCH WELDED TENSILE SPECIMENS
(.016t, 6Al-4V ANNEALED TITANIUM, ROOM TEMPERATURE TEST)

FIGURE 14 (continued)
PHOTOGRAPH OF GAP AND MISMATCH WELDED TENSILE SPECIMENS
(.016t, 6Al-4V ANNEALED TITANIUM, ROOM TEMPERATURE TEST)

FIGURE 14 (continued)
PHOTOGRAPH OF GAP AND MISMATCH WELDED TENSILE SPECIMENS
(.016t, 6Al-4V ANNEALED TITANIUM, ROOM TEMPERATURE TEST)

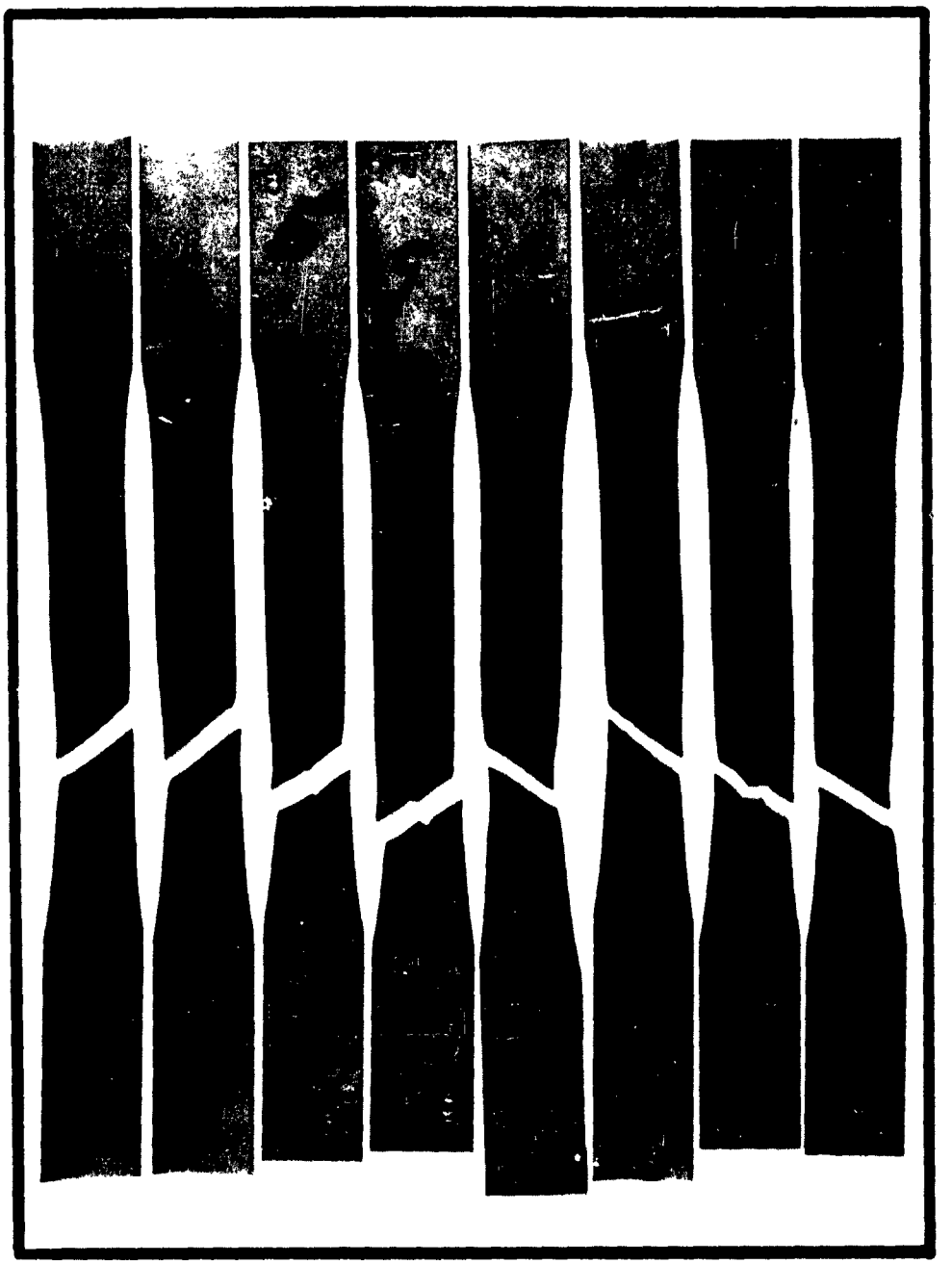

FIGURE 14 (continued)
PHOTOGRAPH OF GAP AND MISMATCH WELDED TENSILE SPECIMENS
(.016t, 6Al-4V ANNEALED TITANIUM, ROOM TEMPERATURE TEST)

FIGURE 15
ROOM TEMPERATURE BEND SPECIMENS
6Al-4V ANNEALED TITANIUM ALLOY

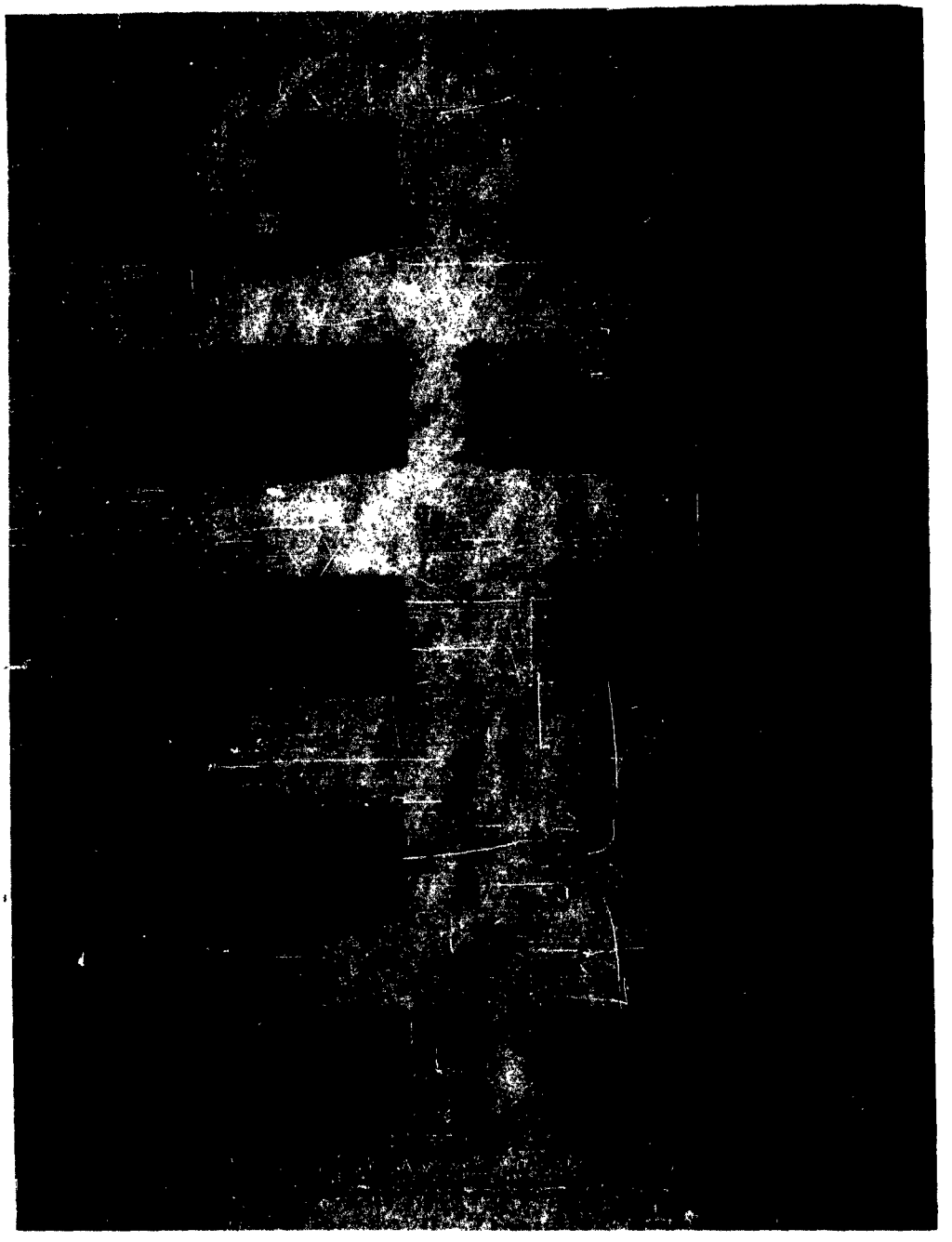

10t-bend radius were required to prove acceptable weld ductility.

1.2.2.2 -320°F Testing

Series N and P specimens were bend tested at liquid nitrogen temperature. The 105° vee block was placed in a small, foam-insulated container of LN_2 open to the atmosphere and the specimen allowed two minutes to reach equilibrium temperature. Figure 16 presents photographs of these specimens.

Transverse welded specimens P_1 and P_4 fractured abruptly at 10t-bend radius while specimens P_2 and P_3 with the same bend radius showed acceptable ductility. A bend radius of 10t appeared marginal at liquid nitrogen temperature for the transverse specimens.

Longitudinal welded specimen N_2 with 8t bend radius showed acceptable ductility. Specimen N_4 with 4.5t bend radius showed a slight weld fracture.

1.2.2.3 -423°F Testing

A thorough investigation of the equipment and time required to conduct small-scale pressure-vessel burst tests at liquid hydrogen temperatures was made. Such testing would permit evaluation of whether brittle or ductile fracture occurs and the correlation of uniaxial properties with actual biaxial stresses. It was concluded from this study that such a testing program was beyond the scope of the present contract.

It was felt desirable to make a token test by subjecting a test specimen to combined uniaxial loading plus bending at liquid hydrogen temperature. No implication was intended that such a test would provide correlation between the test tank strength and the theoretical analysis, but it provided an indication of the ability of the material to stretch and bend at -423°F.

The test equipment consisted of a titanium die block that had a machined contour matching the most severe calculated deflection curve as determined by the discontinuity stress analysis. The worse deflection was found at the skirt-hemisphere transition and was taken at 43 psi tank pressure.

The specimen was made from .025" thick, 6Al-4V sheet and bolted to the die block as shown in Figure 17. The distance between bolts was calculated for a stress range in the specimen of 44,600 psi to 100,000 psi with the specimen fully deflected. This range of stress was caused by the accumulation of tolerances. The analyses of stresses and the determination of die-block contour are found in Reference 5.

FIGURE 16
-321°F TEMPERATURE BEND SPECIMENS
6Al-4V ANNEALED TITANIUM ALLOY

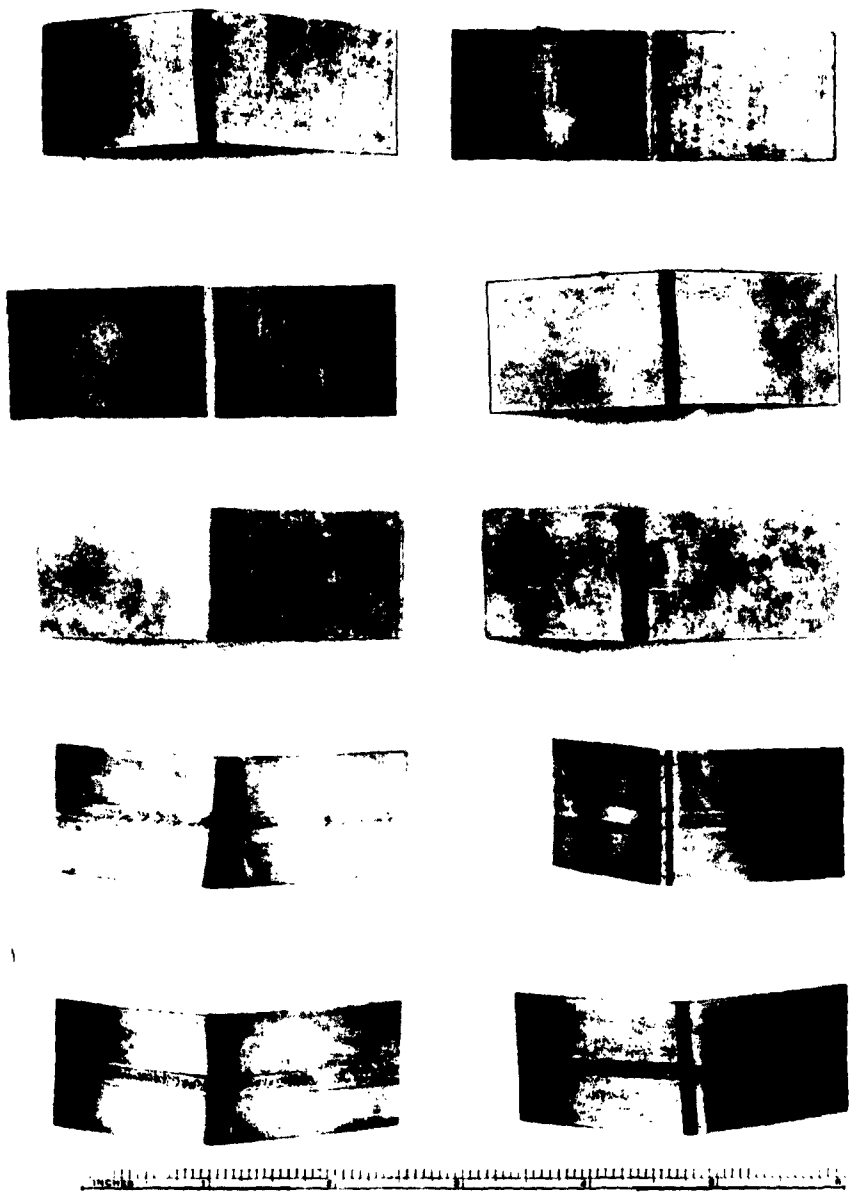

FIGURE 17
6Al-4V TITANIUM ALLOY SPECIMEN AND DIE BLOCK FOR
BEND TESTING AT -423°F

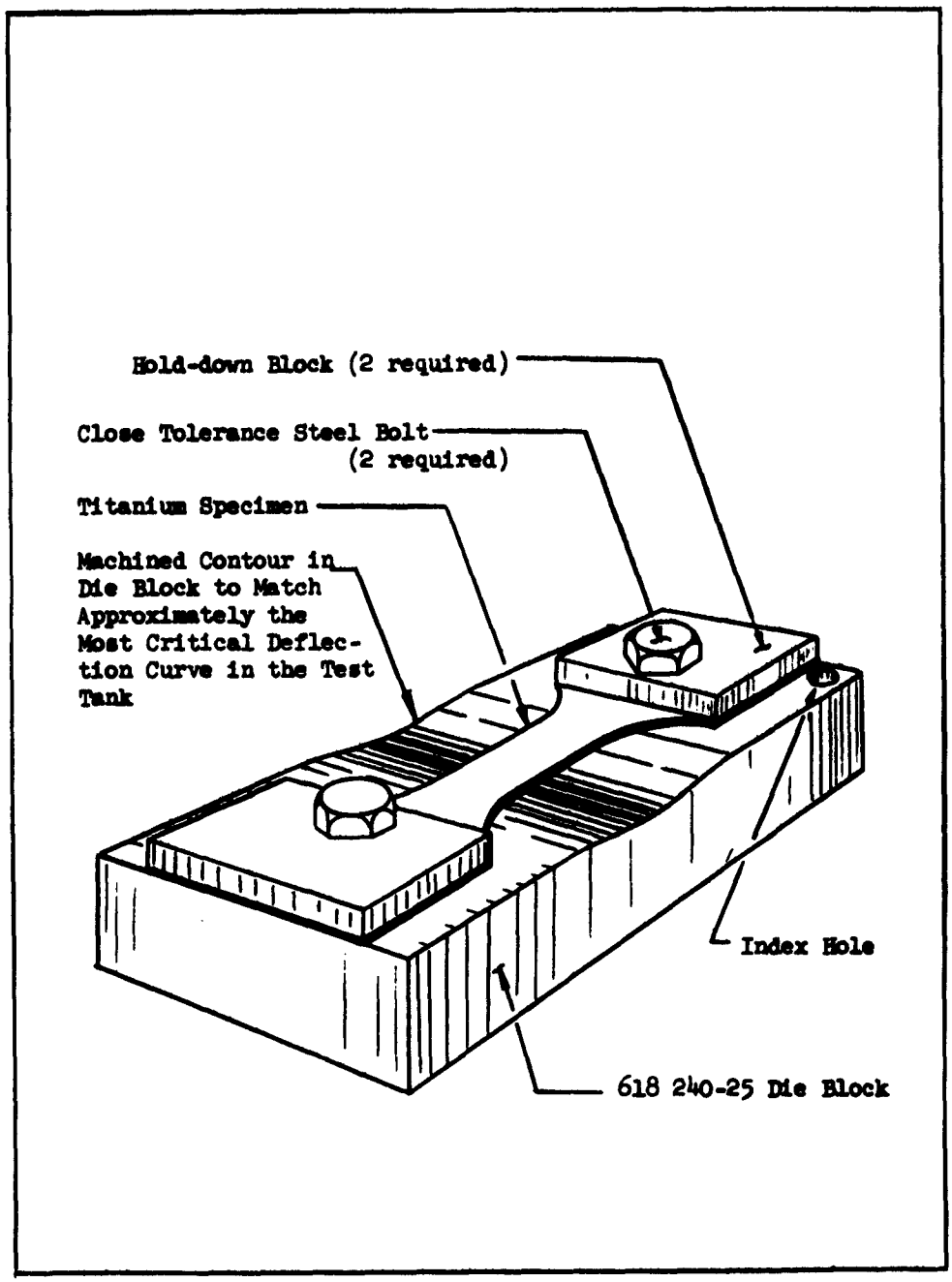

A total of nine (9) specimens were prepared as shown below.

(a) Three (3) specimens had longitudinal welds and a transverse grain direction.

(b) Three (3) specimens had longitudinal welds and longitudinal grain direction.

(c) Three (3) specimens had longitudinal and transverse welds and a longitudinal grain direction.

The test requirements for each specimen were:

(a) Acceptable weld under X-ray inspection.

(b) Place specimen on die block with transverse weld located within .030 inch of die block centerline. Tighten bolts to 18-20 in-lb of torque.

(c) Fill dewar with LH_2 and maintain liquid level approximately 6 inches above guide.

(d) Deflect specimen into die block by applying 300 $\pm$ 25 psi pressure within a 15-second time period and hold for 15 seconds.

(e) Repeat load cycle ten times.

(f) X-ray all specimens for cracks in parent heat-affected or weld zones.

Results of the tests showed that the test specimens retained sufficient ductility at -423°F.

The effect of combined axial tension and bending plus cryogenic temperature over a period of time on the ductility of 6Al-4V was tested as follows:

(a) The specimen was deflected ten (10) times as previously outlined.

(b) The specimen was then held in fully deflected position for twelve hours at liquid hydrogen temperature.

(c) The specimen was then deflected ten (10) more times.

(d) Steps (b) and (c) were repeated.

(e) The specimen was then subject to X-ray crack inspection.

No cracks were propagated in any of the specimens.

1.2.3 Hydrogen Effects on Tensile Specimens

The principal known source of hydrogen contamination in titanium alloys occurs in the sponge-to-alloy metal conversion and during scaling and acid pickling operations. All available reports indicated that contamination during service should not occur if certain temperature and pressure levels are not exceeded. Information from material manufacturers lead to the conclusion that there should be no significant hydrogen absorption with 100% H_2 environment if the metal temperature is below 300°F and the pressure is below several atmospheres.

To provide substantiation of this information, several specimens were exposed to a hydrogen gas atmosphere under approximately 18 psi pressure. The specimens were placed into test tubes, purged, and pressurized with 100% hydrogen gas at room temperature. The tests were conducted at room temperature and 200°F $\pm$ 25°F. Table 4 lists the respective test conditions for each specimen together with their respective strength level. Figure 18 identifies the failed specimens. Specimen Y18 was the only one of the 24 specimens that separated in the weld; the cause was not determined. X-ray inspection showed acceptable welding in all specimens.

The average strength of all specimens was 133,800 psi yield strength and 144,200 psi ultimate tensile strength. The average ductility was 7.7% elongation in 2 inches. These strength values are still 4.5% better than the manufacturer's published typical values. The low per cent elongation reflects weld ductility. No definite material property trends as a function of time exposure, temperature or pressure conditions were detected. It was concluded that the temperature, pressure and time element of liquid hydrogen in the test tank would not affect the structural material.

1.2.4 Single Versus Two-Pass Welds

The material supplier pointed out that some shops prefer several passes using a very low heat input each time to avoid excessive grain growth. The tests of single-pass welds had revealed sufficient strength and ductility; however, it was anticipated that multiple-pass welding might be necessary where difficulties were encountered on the first pass.

Initial tests on four specimens with a 0.200-inch-width necked section revealed slightly higher strength resulted from two-pass welding.

Additional testing of twenty more specimens was made to verify the weld strength characteristics. Tables 5 and 6 list the results of these tests. The double-pass welds again showed higher strength than the single-pass weld while showing no appreciable difference in per cent elongation. Some difficulty was experienced during these tests with failure occurring at the gripping holes attributed to poor specimen preparation. Figures 19 and 20 show the failed specimens along with their respective grain directions.

TABLE 4
WELDED TENSILE SPECIMENS EXPOSED TO GASEOUS HYDROGEN ENVIRONMENT
(.016t, 6Al-4V ANNEALED TITANIUM, ROOM TEMPERATURE TEST)

Specimen Number	Environmental Temp±25°	Pressure	Time Exposed to H_2	Yield	Ultimate	Elong.	Fracture Location
	°F	psi	hr	psi	psi	%2"	
Y_1	Comparative specimens not exposed to H_2.			130,000	136,800	8	Parent Metal
Y_2	" "			129,100	145,000	8	"
Y_3	200	17	1	128,400	144,300	7	"
Y_4	"	"	1	128,700	145,000	6	"
Y_5	"	"	2	131,900	146,000	6.5	"
Y_6	"	"	2	138,000	147,000	7	"
Y_7	"	"	4	137,400	141,800	9.5	"
Y_8	"	"	4	138,900	143,600	8.5	"
Y_9	"	"	8	137,800	144,200	9.5	"
Y_{10}	"	"	8	130,400	146,700	8.5	"
Y_{11}	"	Test tube fractured during test.					
through Y_{16}	"	Test tube fractured during test.					
Y_{17}	200	17	24	128,200	143,500	7	Parent metal
Y_{18}	"	17	24	137,700	142,200	4	Weld

TABLE 4 (continued)
WELDED TENSILE SPECIMENS EXPOSED TO GASEOUS HYDROGEN ENVIRONMENT
(.016t, 6Al-4V ANNEALED TITANIUM, ROOM TEMPERATURE TEST)

Specimen Number	Environmental Temp±25°	Pressure	Time Exposed to H_2	Yield	Ultimate	Elong.	Fracture Location
	°F	psi	hr	psi	psi	%2"	
Y_{21}	Comparative specimen			135,200	143,800	7	Parent Metal
Y_{22}	not exposed to H_2			137,700	144,200	8	"
Y_{23}	R.T.	18	48	135,300	145,200	7	"
Y_{24}	"	"	48	134,200	144,700	9	"
Y_{25}	Test tube fractured during test.						
Y_{26}	Test tube fractured during test.						
Y_{27}	R.T.	18	168	134,000	145,900	9	"
Y_{28}	"	"	168	132,600	144,700	8	"
Y_{29}	"	"	24	137,100	146,300	6	"
Y_{30}	"	"	24	134,500	143,700	9	"
Y_{31}	"	"	24	133,900	145,400	7	"
Y_{32}	"	"	24	137,700	146,700	7	"
Y_{33}	"	"	96	134,300	143,200	7	"
Y_{34}	"	"	96	130,000	144,500	8	"

FIGURE 18
PHOTOGRAPH OF WELDED TENSILE SPECIMENS
EXPOSED TO GASEOUS HYDROGEN ENVIRONMENT
(.016t, 6Al-4V ANNEALED TITANIUM, ROOM TEMPERATURE TEST)

FIGURE 18 (continued)
PHOTOGRAPH OF WELDED TENSILE SPECIMENS
EXPOSED TO GASEOUS HYDROGEN ENVIRONMENT
(.016, 6Al-4V ANNEALED TITANIUM, ROOM TEMPERATURE TEST)

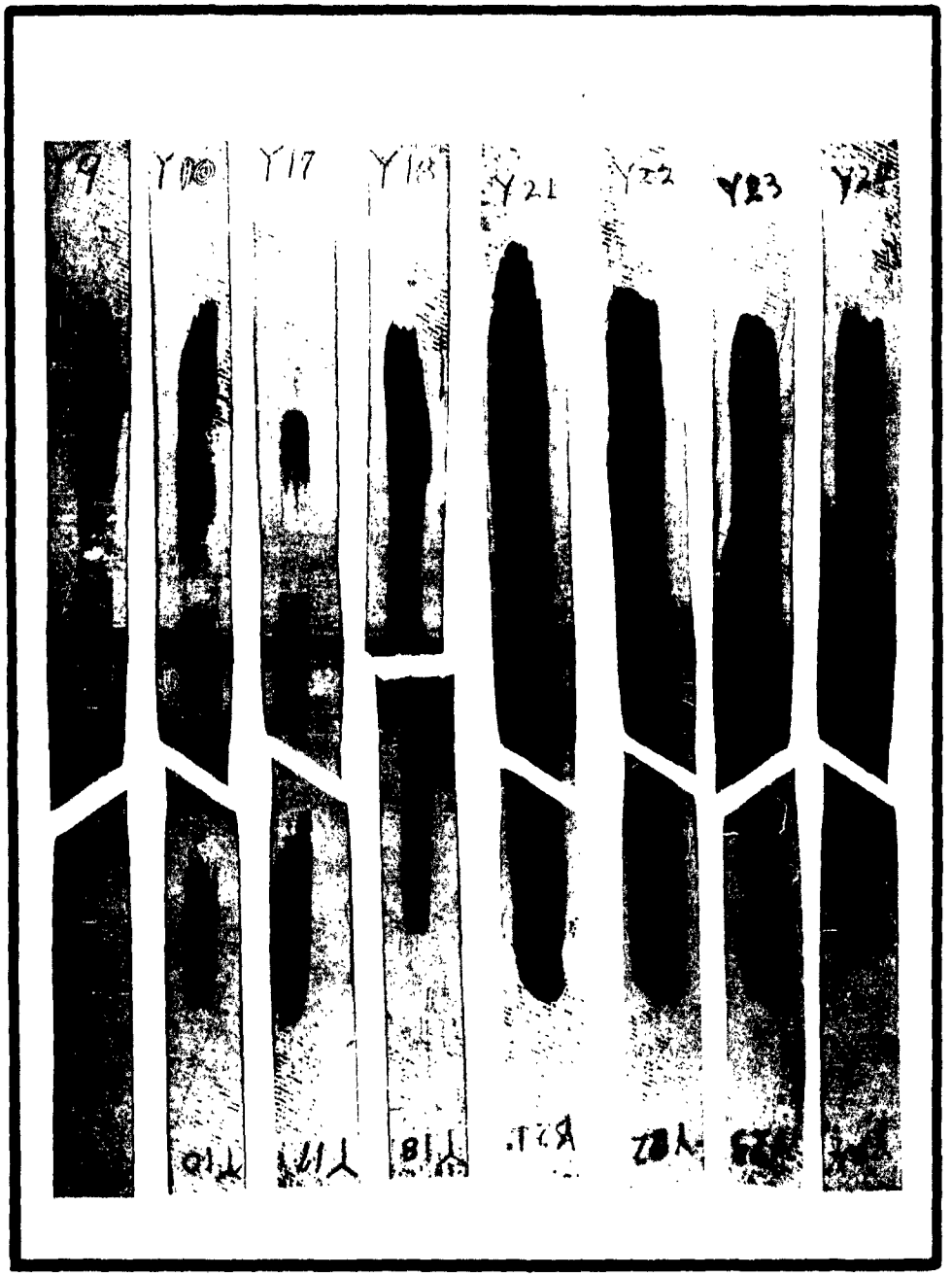

FIGURE 18 (continued)
PHOTOGRAPH OF WELDED TENSILE SPECIMENS
EXPOSED TO GASEOUS HYDROGEN ENVIRONMENT
(.016t, 6Al-4V ANNEALED TITANIUM, ROOM TEMPERATURE TEST)

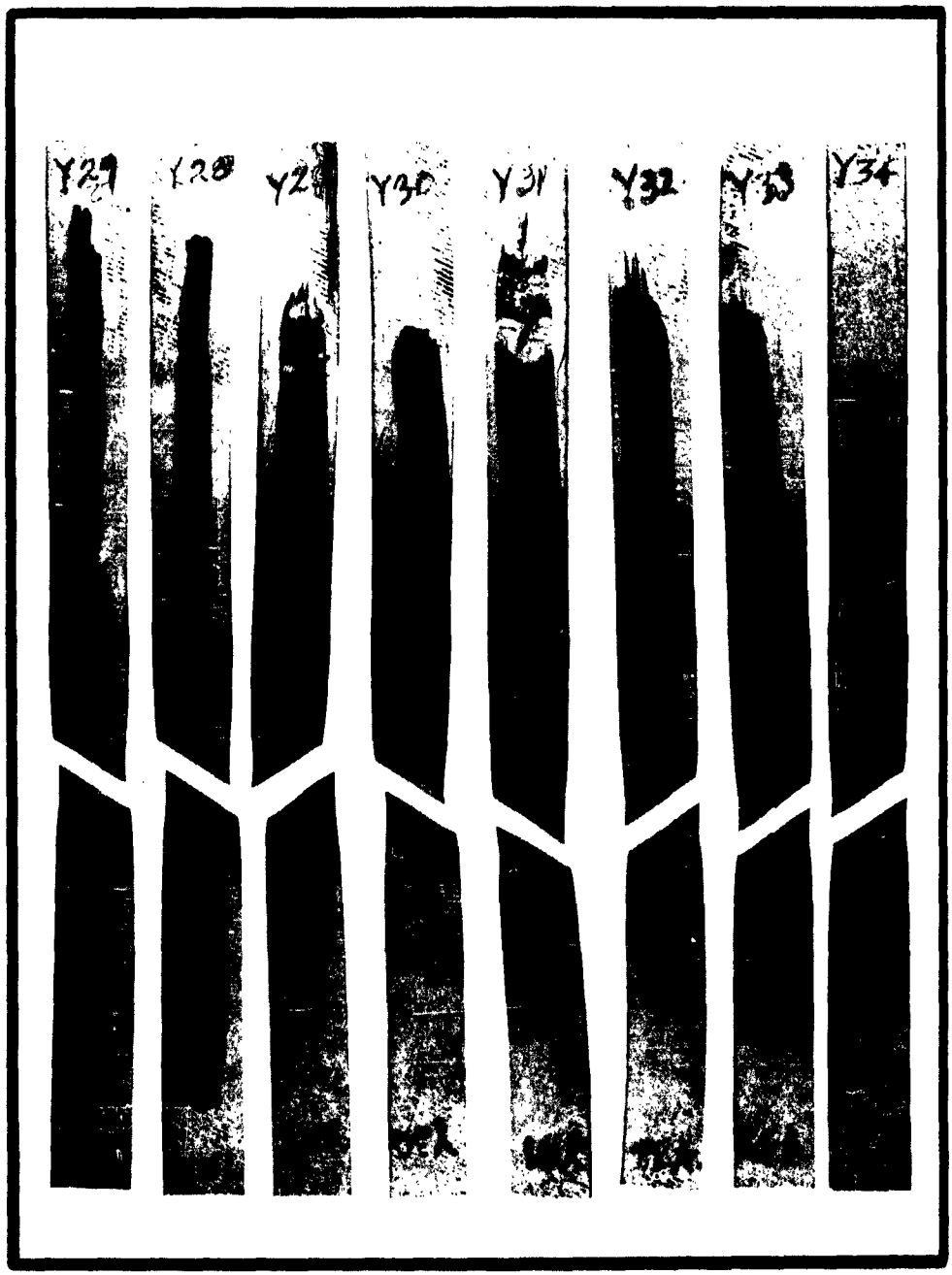

TABLE 5
SINGLE-PASS WELD TENSILE SPECIMENS
(.016t, 6Al-4V ANNEALED TITANIUM ROOM TEMPERATURE TEST)

Specimen Number	Test Area	Yield Stress	Ultimate Stress	Elongation	Fracture Location
	in^2	lb/in^2	lb/in^2	% 2"	
S_1	.00306	133,000	147,000	Fractured Outside of Marks	Weld
S_2	.00777	129,500	138,500	10	Parent Metal
S_3	.00759	132,000	140,500	9.5	"
S_4	.00758	131,000	139,400	7	"
S_5	.00762	131,000	140,000	8	"
S_6	.00321	137,000	155,000	4	Weld
S_7	.00759	132,000	144,000	9	Parent Metal
S_8	.00767	Fractured in Holes			"
S_9	.00762	131,000	142,000	10	"
-					
-					

TABLE 6
DOUBLE-PASS WELD TENSILE SPECIMENS
(.016t, 6Al-4V ANNEALED TITANIUM ROOM-TEMPERATURE TEST)

Specimen Number	Test Area	Yield Stress	Ultimate Stress	Elongation	Fracture Location
	in^2	lb/in^2	lb/in^2	% 2"	
D_1	.003	143,000	154,000	2.5	Weld
D_2	.00750	126,000	170,000	7	Parent Metal
D_3	.00762	128,700	141,800	9	"
D_4	.003	140,000	152,000	2	Weld
D_5	.00756	131,600	139,000	10	Parent Metal
D_6	.00753	130,000	137,000	10	"
D_7	.00752	131,000	142,000	6	"
D_8	.00768	130,000	137,000	11	"
D_9	.00767	Fractured in Holes			"
D_{10}	.00764	128,000	139,000	5	"
D_{11}	.00777	129,000	140,000	5.5	"

FIGURE 19
PHOTOGRAPH OF SINGLE-PASS WELD TENSILE SPECIMENS
(.016 t, 6Al-4V Annealed Titanium Room Temperature Test)

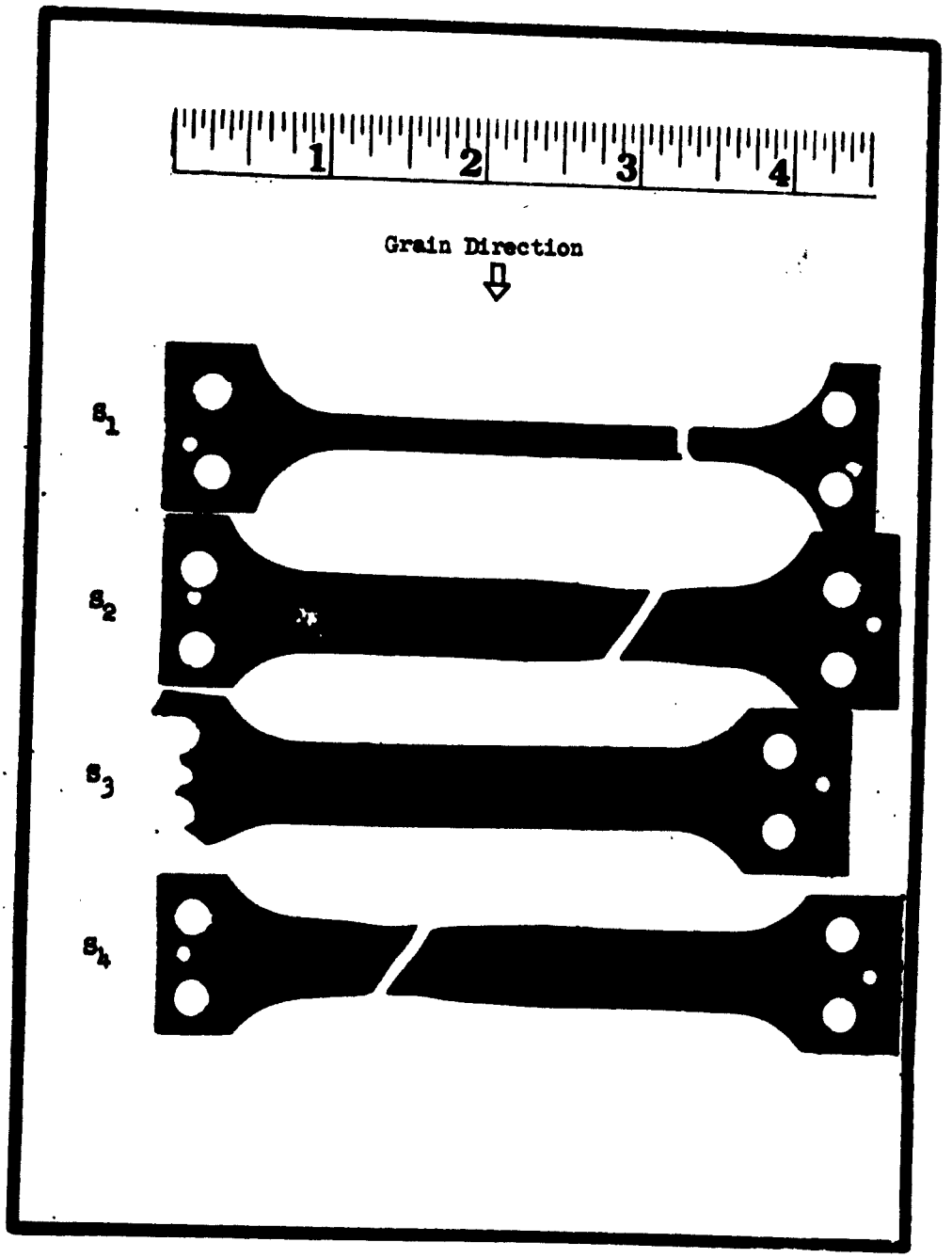

FIGURE 19 (continued)
PHOTOGRAPH OF SINGLE-PASS WELD TENSILE SPECIMENS
(.016t, 6Al-4V ANNEALED TITANIUM ROOM-TEMPERATURE TEST)

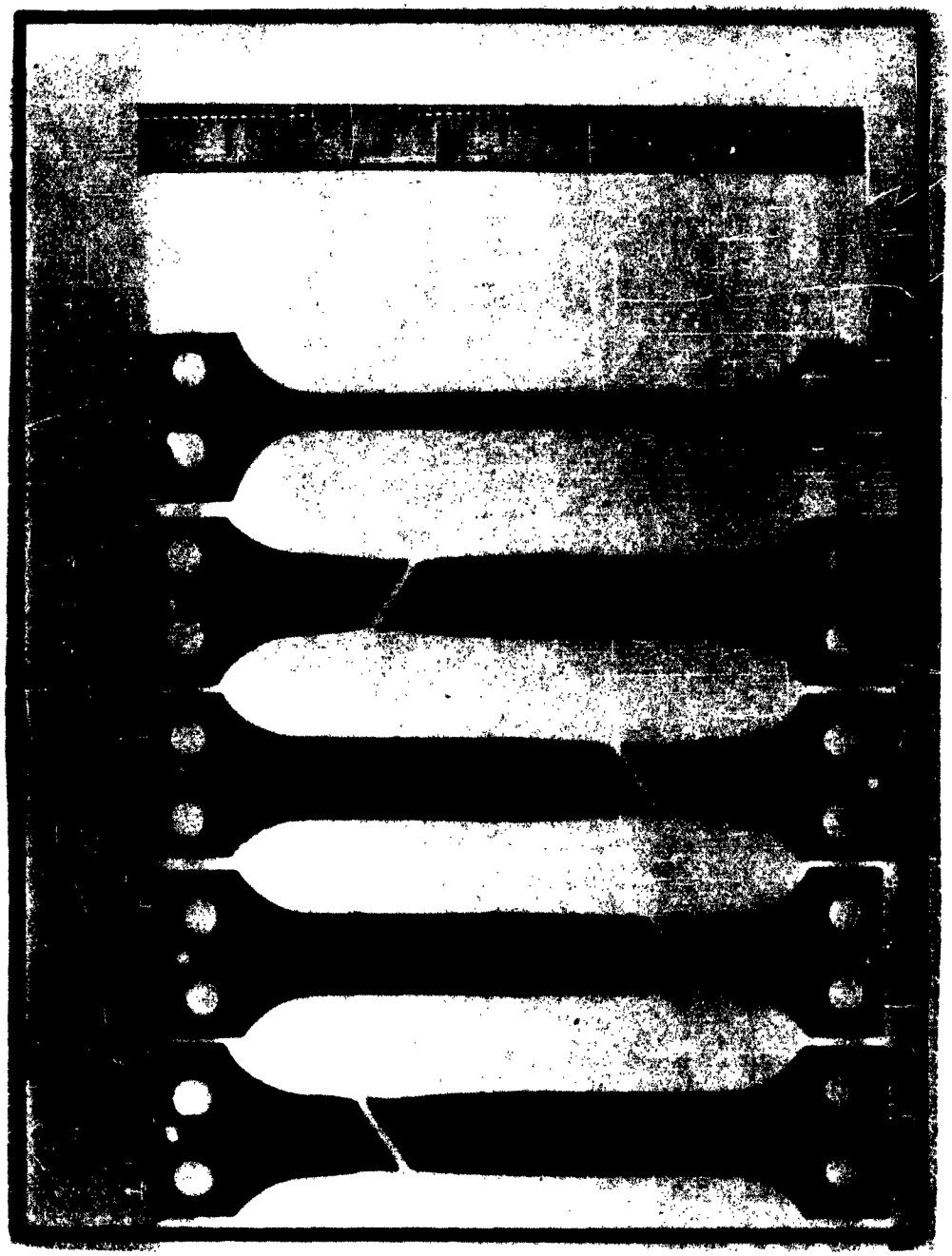

FIGURE 20
PHOTOGRAPH OF DOUBLE-PASS WELD TENSILE SPECIMENS
(.016t, 6Al-4V ANNEALED TITANIUM ROOM-TEMPERATURE TEST)

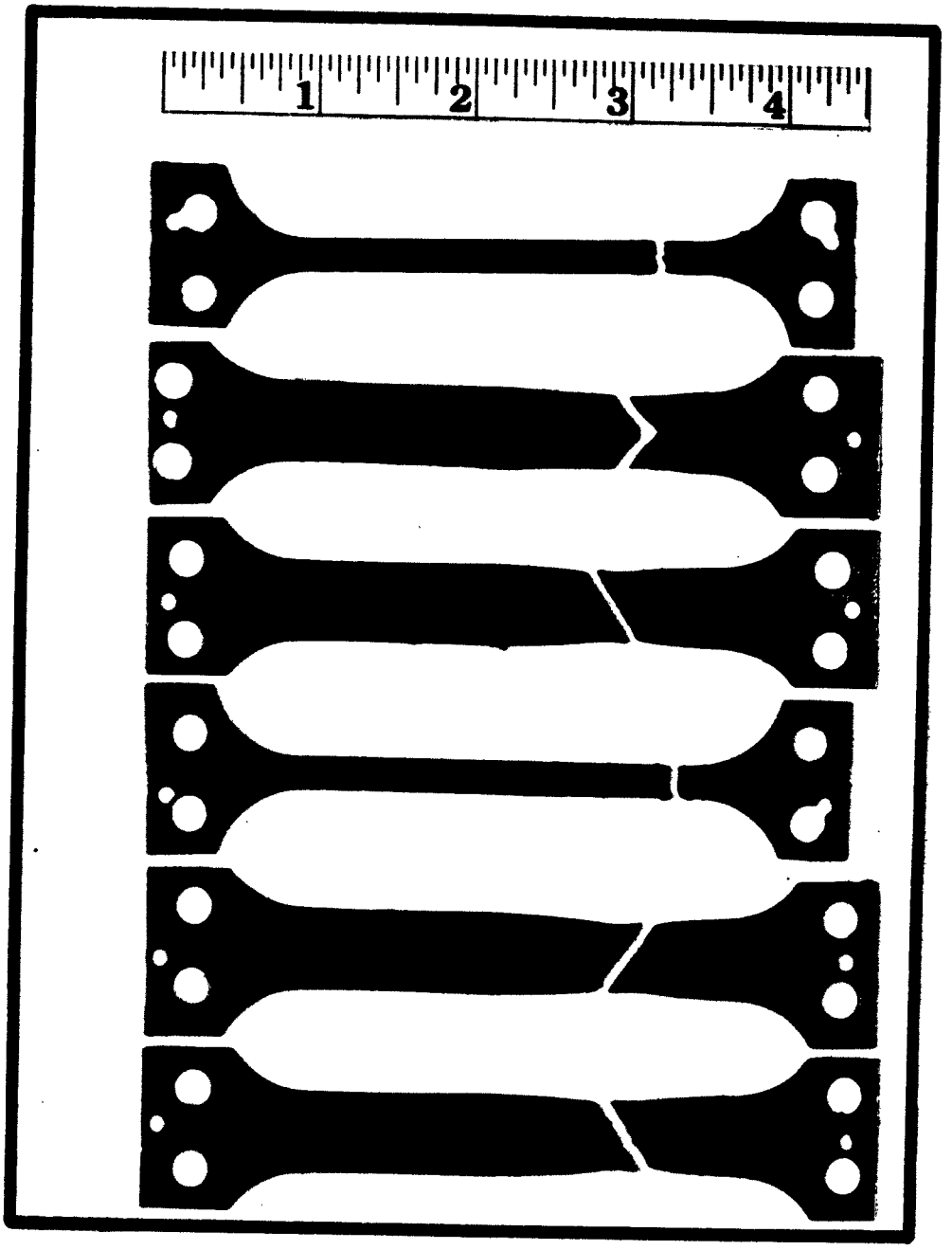

1.2.5 Simulated Weld Porosity Tests

A series of tests was conducted to establish a basis for determining weld acceptability of 6Al-4V titanium alloy. These tests were performed because of the lack of suitable standards regarding acceptability of welded joints containing gas pockets, entrainments and inclusions.

All specimens were prepared and tested in accordance with Beech Specification 7262. An exception was the machining in the test area required to prevent breakage at the holding jaws. Microphotographs at 100X manificiation (Figures 21 and 22) were taken of Specimens T-1-138-197 and B-2-138-98 to determine the exact hole size and shape prior to testing and to identify surface irregularities after a typical bend test. All holes were drilled on a precision drill press operated at 7,000 rpm. Actual drill sizes used were 0.0135, 0.0156, and 0.0180-inch diameters. Bend specimens were tested using a 10t bend radius.

The test specimens were identified as follows:

(a) The first letter, T or B, denotes tensile or bend specimen respectively.

(b) The first number indicates number of holes in specimen.

(c) The second number denotes hole diameter in ten one-thousandths of an inch.

(d) The third number denotes distance that the holes were located from the reference line expressed in hundredths of an inch.

(e) Example: B-3-156-97 is a bend test specimen with three .0156-inch-diameter holes located 0.9700 inch from the references line.

Each bend specimen was thoroughly inspected at 7X magnification and spot checked at 100X magnification. Tables 7 and 8 present the results which appeared generally good. The bend specimens displayed a tendency suspected to be that of grain boundary movement causing some graphs to protrude as surface irregularities. This condition is shown in Figure 22. To prove this supposition correct, the specimen was polished to remove a surface depth of approximately 0.002 inch. This removed the irregularities completely as shown in the microphotograph (Figure 23), and there were no traces of cracks or imperfections.

The tensile specimens were machined to approximately 0.850 inch wide by 2.0 inches long in the test area. The specimens were then tested with satisfactory results except for elongation and yield strength. The low yield strength as noted on most of the specimens is not an accurate reading due to slippage in the jaws. This slippage occurred due to

FIGURE 21
PHOTOGRAPH OF DRILLED HOLE IN
TITANIUM SIMULATED POROSITY SPECIMEN
(100 x size)

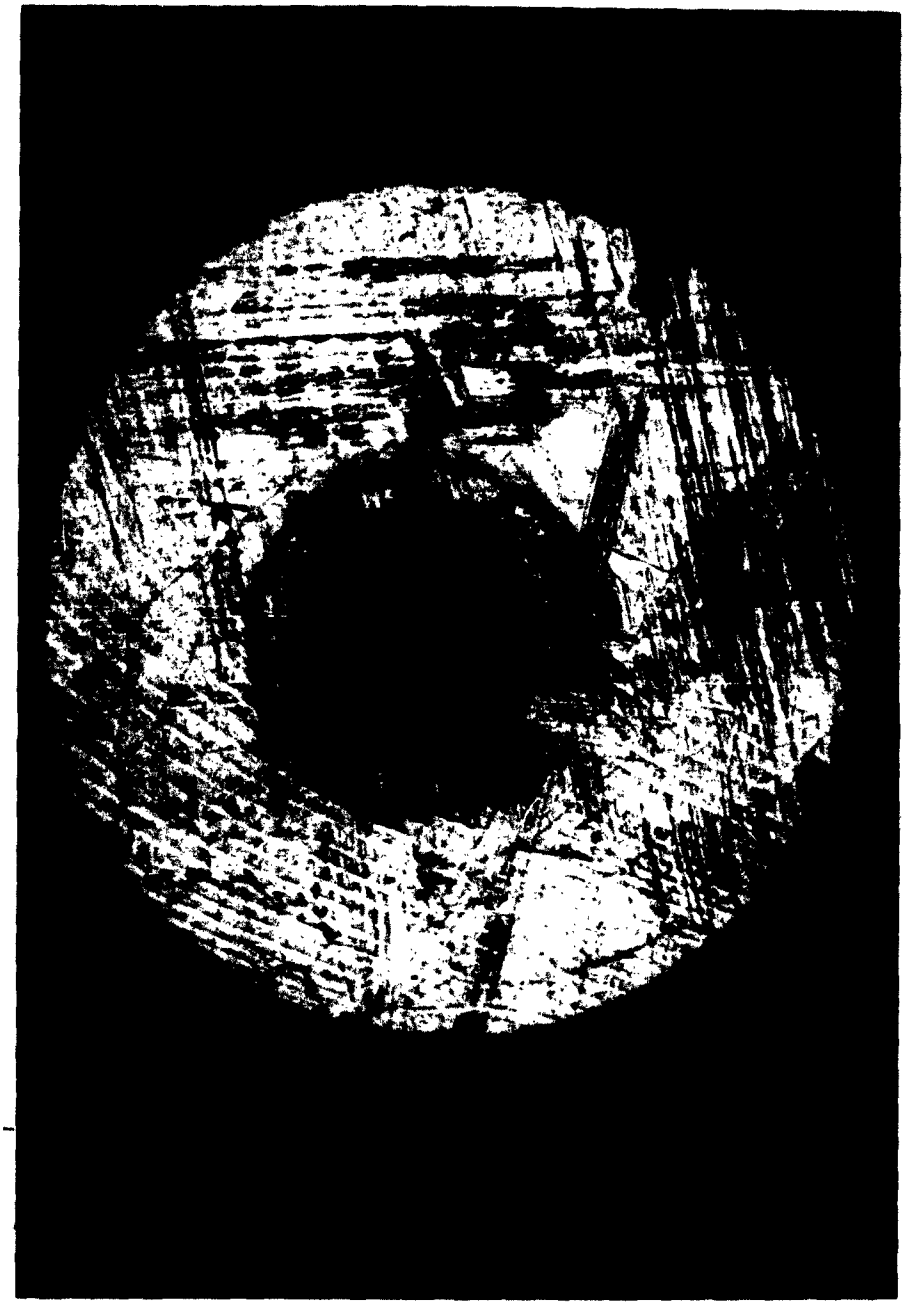

FIGURE 21
PHOTOGRAPH OF DRILLED HOLE IN
TITANIUM SIMULATED POROSITY SPECIMEN
(100 x size)

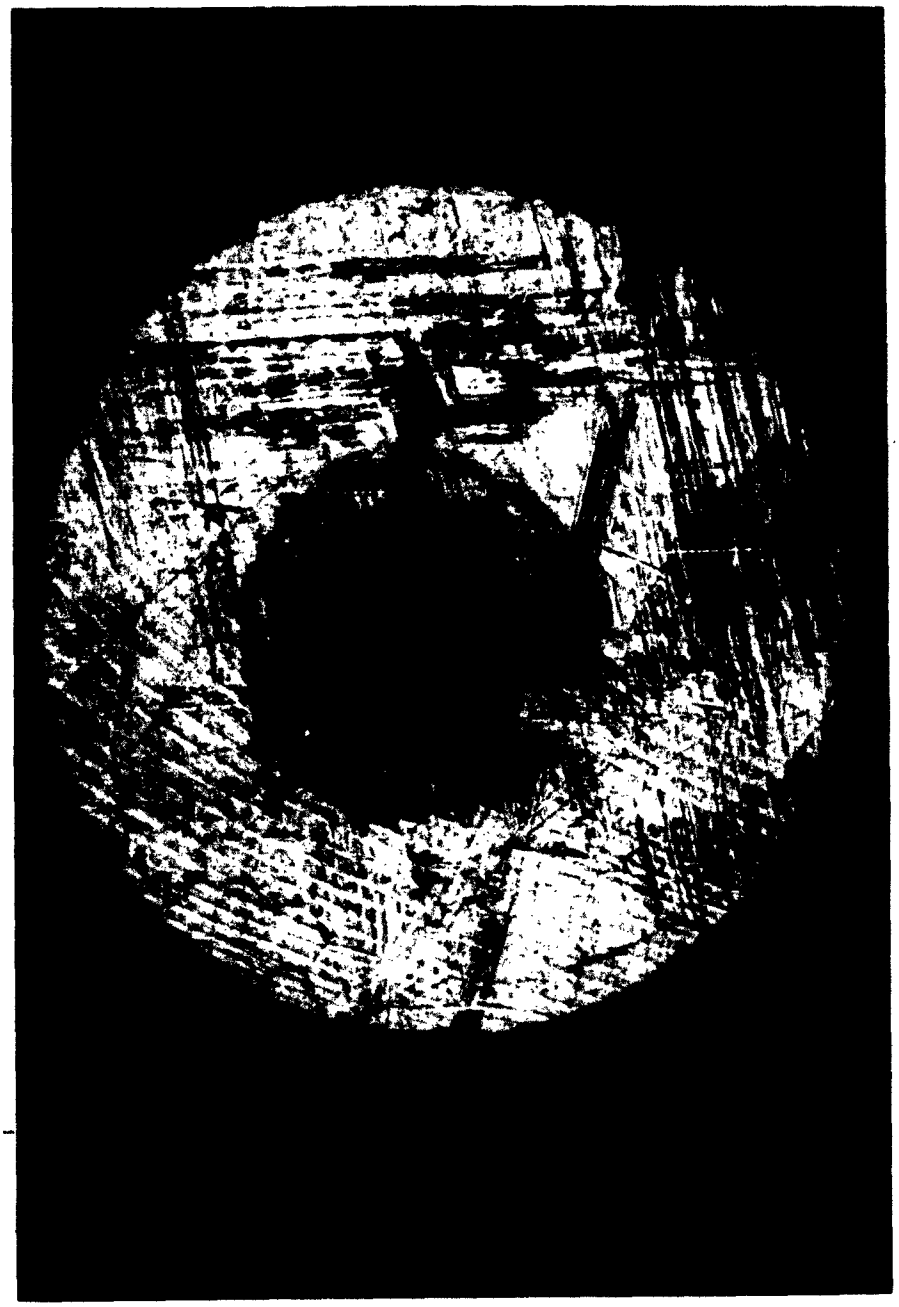

TABLE 7
SIMULATED WELD POROSITY TEST
BEND TEST RESULTS

Sample No.	Results	Sample No.	Results
B-1-138-100	Satisfactory	B-2-159-100	Satisfactory
B-1-138-99	Satisfactory	B-2-159-99	Satisfactory
B-1-138-98	Satisfactory	B-2-159-98	Satisfactory
B-1-138-97	Satisfactory	B-2-159-97	Satisfactory
B-1-138-96	Satisfactory	B-2-159-96	Satisfactory
B-2-138-100	Satisfactory	B-3-159-100	Satisfactory
B-2-138-99	Satisfactory	B-3-159-99	Satisfactory
B-2-138-98	Satisfactory	B-3-159-98	Satisfactory
B-2-138-97	Satisfactory	B-3-159-97	Satisfactory
B-2-138-96	Satisfactory	B-3-159-96	Satisfactory
B-3-138-100	Satisfactory	B-1-193-100	Satisfactory
B-3-138-99	Satisfactory	B-1-183-99	Satisfactory
B-3-138-98	Satisfactory	B-1-183-98	Satisfactory
B-3-138-97	Satisfactory	B-1-183-97	Satisfactory
B-3-138-96	Satisfactory	B-1-183-96	Satisfactory
B-4-138-100	Satisfactory	B-2-183-100	Satisfactory
B-4-138-99	Satisfactory	B-2-183-99	Satisfactory
B-4-138-98	Satisfactory	B-2-183-98	Satisfactory
B-4-138-97	Satisfactory	B-2-183-97	Satisfactory
B-4-138-96	Satisfactory	B-2-183-96	Satisfactory
B-1-159-100	Satisfactory	B-3-183-100	Satisfactory
B-1-159-99	Satisfactory	B-3-183-99	Satisfactory
B-1-159-98	Satisfactory	B-3-183-98	Satisfactory
B-1-159-97	Satisfactory	B-3-183-97	Satisfactory
B-1-159-96	Satisfactory	B-3-183-96	Satisfactory

TABLE 8
SIMULATED WELD POROSITY TEST
TENSILE TEST RESULTS

Sample No.	Yield Strength(psi)	Ultimate Strength(psi)	Elongation % in 2 in.	Location of Fracture
T-1-138-100	130,000	148,000	10.5	Outside Weld
T-1-138-99	128,000	146,000	9.5	Outside Weld
T-1-138-98	137,000	152,000	10.0	Outside Weld
T-1-138-97	131,000	148,000	9.0	Outside Weld
T-1-138-96	133,000	149,000	9.5	Outside Weld
T-2-138-100	133,000	150,000	9.0	Outside Weld
T-2-138-99	132,000	151,000	9.0	Outside Weld
T-2-138-98	128,000	145,000	5.0	In Weld
T-2-138-97	134,000	151,000	7.5	Outside Weld
T-3-138-100	116,000	146,000	6.5	Outside Weld
T-3-138-99	122,000	147,000	12.0	Outside Weld
T-3-138-98	120,000	152,000	8.0	Outside Weld
T-3-138-97	113,000	144,000	9.0	Outside Weld
T-3-138-96	116,000	146,000	9.0	Outside Weld
T-4-138-100	107,000	144,000	4.0	In Weld
T-4-138,99	109,000	144,000	10.0	Outside Weld
T-4-138-98	118,000	144,000	9.0	Outside Weld
T-4-138-97	103,000	144,000	4.0	In Weld
T-4-138-96	118,000	146,000	8.0	Outside Weld
T-1-159-100	Specimen not machined and broke at edge of jaws.			
T-1-159-99	Specimen not machined and broke at edge of jaws.			
T-1-159-98	135,000	149,000	8.0	Outside Weld
T-1-159-97	133,000	148,000	9.25	Outside Weld
T-1-159-96	133,000	148,000	9.0	Outside Weld

TABLE 8 (continued)
SIMULATED WELD POROSITY TEST
TENSILE TEST RESULTS

Sample No.	Yield Strength(psi)	Ultimate Strength(psi)	Elongation % in 2 in.	Location of Fracture
T-2-159-100	145,000	153,000	8.5	Outside Weld
T-2-159-99	133,000	144,000	11.5	Outside Weld
T-2-159-98	133,000	148,000	9.5	Outside Weld
T-2-159-97	122,000	148,000	11.0	Outside Weld
T-2-159-96	118,000	147,000	3.5	In Weld
T-3-159-100	119,000	149,000	8.0	Outside Weld
T-3-159-99	115,000	147,000	9.0	Outside Weld
T-3-159-97	116,000	143,000	8.5	Outside Weld
T-3-159-96	107,000	143,000	9.5	Outside Weld
T-1-183-100	132,000	146,000	8.5	Outside Weld
T-1-183-99	135,000	149,000	10.5	In Weld
T-1-183-98	132,000	147,000	10.5	Outside Weld
T-1-183-97	133,000	148,000	9.0	Outside Weld
T-1-183-96	135,000	148,000	9.0	Outside Weld
T-2-183-100	133,000	148,000	8.0	Outside Weld
T-2-183-99	132,000	147,000	14.0	Outside Weld
T-2-183-98	133,000	148,000	9.0	Outside Weld
T-2-183-97	134,000	148,000	9.0	Outside Weld
T-2-183-96	121,000	147,000	3.5	In Weld
T-3-183-100	106,000	146,000	11.0	Outside Weld
T-3-183-99	111,000	154,000	9.0	Outside Weld
T-3-183-98	109,000	144,000	14.5	Outside Weld
T-3-183-97	105,000	142,000	7.5	Outside Weld
T-3-183-96	101,000	144,000	8.0	Edge of Weld

FIGURE 23
PHOTOGRAPH OF POLISHED SURFACE
REMOVING SURFACE IRREGULARITIES
(100 x size)

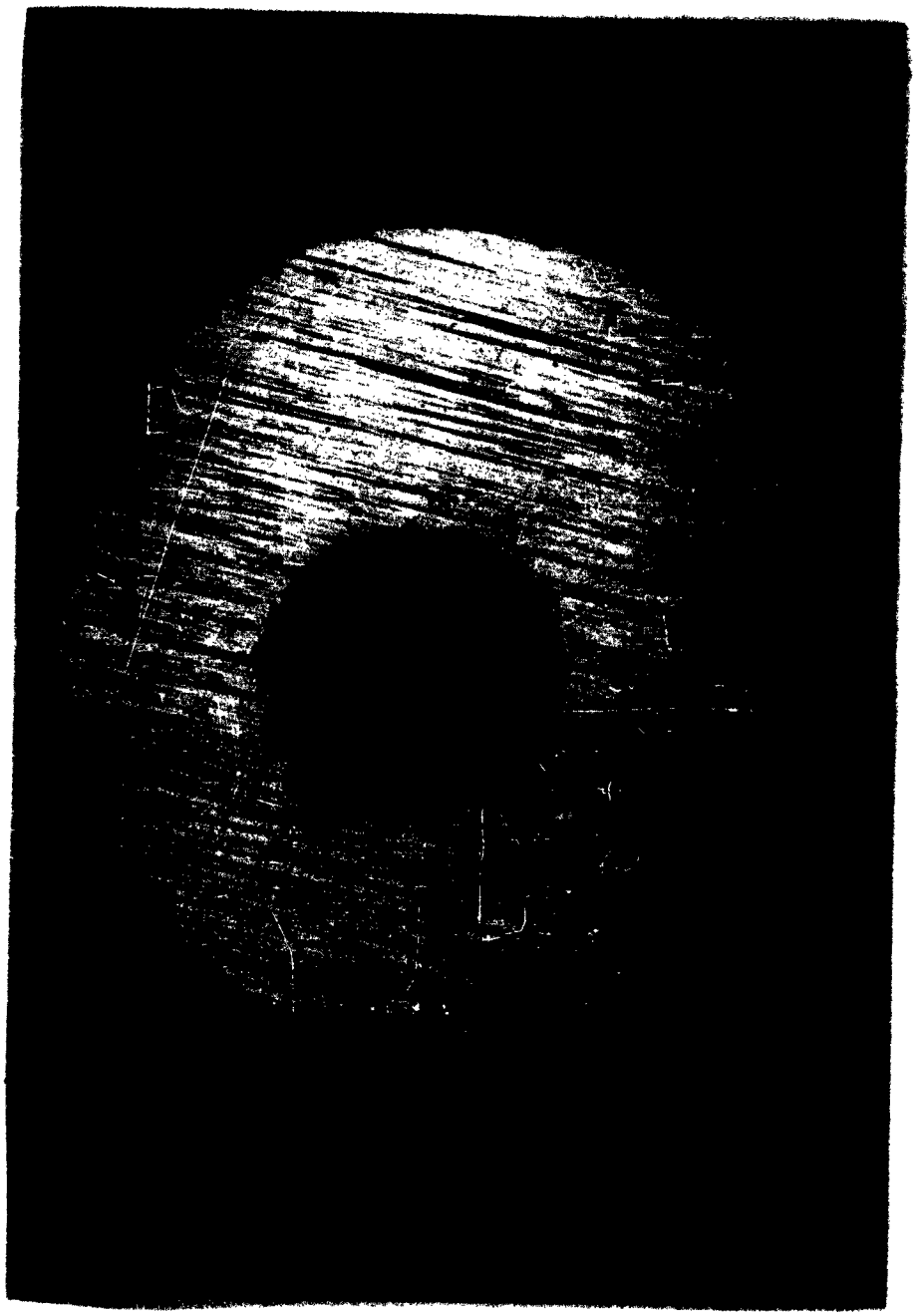

insufficient gripping area. Therefore, it was recommended that all future specimens should be approximately nine (9) inches long to provide adequate "grip area."

In the opinion of the laboratory, the specimens met the minimum requirements for 6Al-4V titanium alloy, except as noted, and are considered acceptable for production welds. Figure 24 illustrates the corrected acceptability limits.

1.3 Fabrication

1.3.1 Heating Treating Study

One of the prime reasons for using 6Al-4V in the mill-annealed condition was to eliminate a heat treatment while still maintaining a good strength-to-weight ratio.

It was judged desirable to have the capability of heat treating large thin-skinned tanks in order to effect higher strength-to-weight ratios. Inquiries were sent to several large heat-treating firms. Several of the companies considered heat treating local weld areas as a possible solution whereby the tank would be fabricated from heat-treated sheets. Lindberg Industrial Corporation considered the construction of a controlled atmosphere furnace 30 feet in diameter by 175 feet long as a feasible solution for the N85-100 propellant tank.

The heat-treating concept was based upon the ability of the tank to support itself. This would require maintaining 3 to 5 psi tank gage pressure. The furnace sections would be assembled around the tank and sealed for atmosphere control. The furnace would require approximately 90 heat control zones. Water nozzles would be required to quench a titanium tank. Heat treating a 422 stainless steel tank was considered simpler than heat treating a 6Al-4V tank due to elimination of the water quench and less critical atmosphere control.

For the smaller 10-ft to 12-ft diameter vessels, Lindberg suggested vertical heat treating chambers similar to the type used for solid propellant cases.

FIGURE 24
RADIOGRAPH INSPECTION LIMITS FOR 6Al-4V TITANIUM WELD
(ANNEALED AND NO FILLER WIRE)

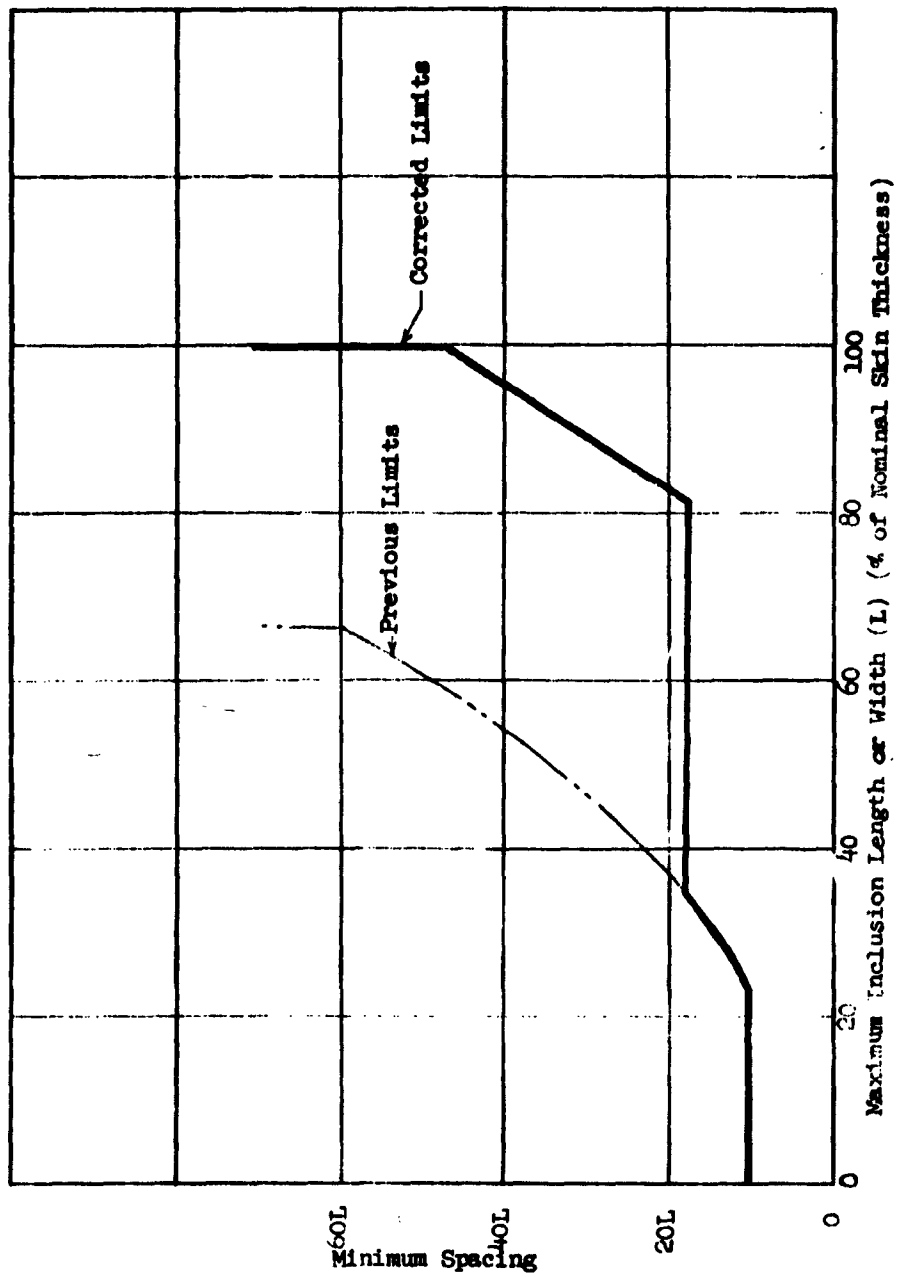

2.0 INSULATION MATERIALS

2.1 Selection of Insulation Materials

The discussions of selection, testing, and fabrication for insulation materials covered in the following sections are limited to liquid hydrogen boost tanks.

Four (4) distinct fields of investigation concerning insulation of cryogenic propellant tanks necessitate engineering studies. The fields are categorized as follows:

Tank Sidewall Insulation	- To minimize tank system weight during flight
Tank End Insulation	- To prevent ice formation during fill and standby
Line and Component Insulation	- To prevent pump cavitation
Auxiliary Ground Insulation	- To prevent excessive losses while on the ground

It is advocated that flight insulation must be employed to minimize the overall net tank-system weight. There are two (2) separate insulation areas, namely, the tank sidewall and the tank ends. These areas have been investigated with respect to their individual design requirements.

The use of a certain amount of insulation mounted on the exterior of the tank sidewall can effect an overall weight savings in the propellant tank system. The insulation accomplishes this by reducing the amount of boil-off and by shielding the structure material from aerodynamic heating, making it possible to design to higher stress allowables. However, there may exist situations in which insulation mounted internally may prove to be more feasible than the external type, perhaps with the use of a high-temperature-resistant tank wall. Any fixed type sidewall insulation that is used must be considered a portion of the fly-away weight. Therefore, it is imperative to employ those insulations that have a high thermal efficiency per unit weight.

Optimum insulation design for liquid hydrogen boost tanks should always give consideration to removable ground-blanket type of insulation for standby requirements used in conjunction with the fixed-type insulation for flight requirements. Also, there may be boost vehicle missions for which a ground blanket by itself would satisfy the insulation requirements.

2.1.1 Tank Sidewall Insulation

Tank sidewall insulation is the key item in obtaining an optimum propellant tank-system weight. As in any cryogenic system, an imposed high

temperature environment over extended periods of time carries with it many stringent design requirements. In order to maintain reasonable boil-off rates of liquid hydrogen under these conditions, a very efficient tank sidewall insulation must be employed or a relatively severe weight penalty incurs. The insulation must also be able to endure high temperatures for short periods of time and still retain good insulating properties.

Several insulation concepts were investigated in References 1 though 7 for sidewall insulation. Among these were the internally mounted insulation, external unevacuated insulation, and external evacuated insulation. The latter type is the most desirable since engineering studies indicate this type is by far the most efficient for minimum tank system weight.

2.1.1.1 External Sidewall Insulation Concept

The basic tank sidewall insulation requirements for the external evacuated type insulations are summarized as follows:

(a) Low conductivity per unit weight.

(b) Low outgassing characteristics since the insulation material must maintain a good vacuum to be effective.

(c) Insulation must be load-bearing since the outer shell or membrane must be supported by the insulation when the insulation is evacuated.

(d) The insulation must be vibration resistant such that rocket engine vibration coupled with acceleration forces will not create detrimental effects upon the insulation.

(e) The material must retain sufficient flexibility to allow the tank structure to expand and contract with pressure and temperature changes.

(f) The insulation must be capable of being encapsulated with an outer skin of lightweight, nonporous material so that the insulation can be evacuated. The outer skin will then prevent air from permeating the insulation and condensing on the tank's metallic surface.

As mentioned earlier, studies have shown that external evacuated insulation is by far the most efficient for minimum tank system weight. This is the type of insulation chosen for the 7,000-gallon test tank and is discussed extensively in the various volumes of this report.

2.1.1.2 Internal Sidewall Insulation Concept

During the initial phase of this program, consideration was given to insulation mounted on the inner surface of a liquid hydrogen tank. A polyester film (Mylar) attached to the inner surface was considered. One design criteria for the Mylar was that it should be of sufficient thickness to prevent air liquefying on the tank wall (temperature above 147.5°R) during standby. Actual thickness, of course, is governed by the mission trajectory and the resulting aerodynamic heating. This concept would be feasible for some types of applications, but it was not recommended for the 7000-gallon test tank.

A more comprehensive discussion of the internal insulation concept may be found in Reference 1. A detailed investigation of this concept was not pursued during the course of this contract for the following reasons:

(a) Obtaining reliable seals for internal insulating materials at liquid-hydrogen temperature presents a major sealing problem.

(b) Fabrication and bonding of the internal type insulations would present major manufacturing problems.

2.1.1.3 Internal Insulation Plus Inner Shell Concept

The inner shell concept proposed the use of foam or some inorganic material as internal tank-wall insulation plus a concentric inner wall to provide a cylindrical torus volume of liquid in contact with the insulation while the bulk of the fuel is being used. The reasoning behind this concept is to eliminate the dry wall as liquid hydrogen is used from the tank. A dry wall results in high-wall temperatures with most trajectories which could melt the foam insulation. It is true that the insulation is no longer needed after the liquid level passes below any particular station on the tank wall. But the melted foam could fall into the remaining liquid hydrogen with disastrous consequences downstream in valves, pumps, etc.

Reference 1 contains a more detailed discussion of the inner shell concept. Further investigation of this concept was not continued during performance of this contract for the following reasons.

(a) Fabrication and bonding of the internal insulations present major manufacturing problems.

(b) Provisions for draining the annular fuel volume conveniently and efficiently would be required.

2.1.1.4 Sidewall Insulation Material Properties

The basic requirements for a tank sidewall insulation are:

(1) Low thermal conductivity

(2) Low weight

(3) Mechanical stability from low to high temperatures

(4) Ease of application

(5) High specific heat

In the investigations for suitable insulation materials, emphasis was directed to the selection of an optimum high-temperature insulation. By using a high-temperature inorganic insulation, a thicker, less dense, and lower "k" material can be used resulting in considerable thermal, weight, and fabrication advantages over the Mylar concept especially under conditions of increased aerodynamic heating.

Initial investigations (Reference 1) included the study of the following insulation materials:

(1) Crystal M Paper (Minnesota Mining and Manufacturing Co.)

(2) Dexiglas (C. H. Dexter and Sons)

(3) Min-K (Johns-Manville)

Min-K insulation satisfied the basic requirements for an optimum insulation concept more completely than the others. This material combines the properties of high-temperature service (1300°F), low thermal conductivity (.2 BTU-in/hr-ft^2 at 200°F) and a reasonable density (10 to 20 lb/ft^3).

The material is a molded solid available in a minimum thickness of 1/8 inch. The thermal conductivity (k) and specific heat (C_p) of some compositions of Min-K are plotted versus temperature in Figures 25 and 26.

The densities available for Min-K range from 10 to 20 lb/ft^3 with a special Min-K filled honeycomb material running approximately 16 lb/ft^3. The densities of Min-K are generally high compared to plastic foams, but they are low compared to such materials as Mylar (87 lb/ft^3) and Crystal-M (70 lb/ft^3).

When evaluating the significance of high specific heat values, it should be noted that the specific heat does not vary appreciably from material to material while density and thermal conductivity may vary from 1-20 lb/ft^3 and .02 to .16 BTU-in/hr-ft^2-°F.

FIGURE 25
SPECIFIC HEAT OF MIN-K INSULATION

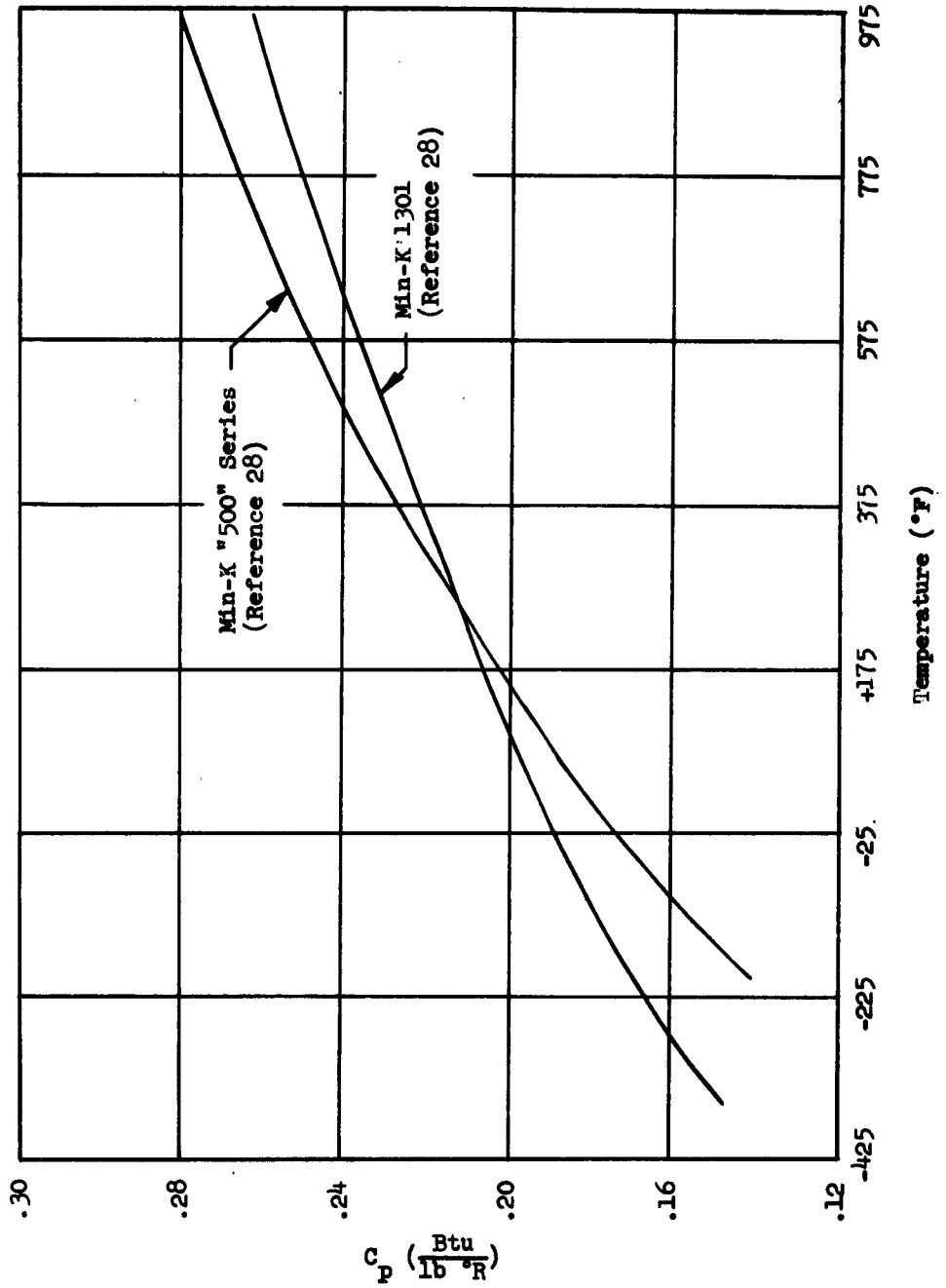

FIGURE 26
THERMAL CONDUCTIVITY OF SEVERAL
MIN-K INSULATION FORMULATIONS

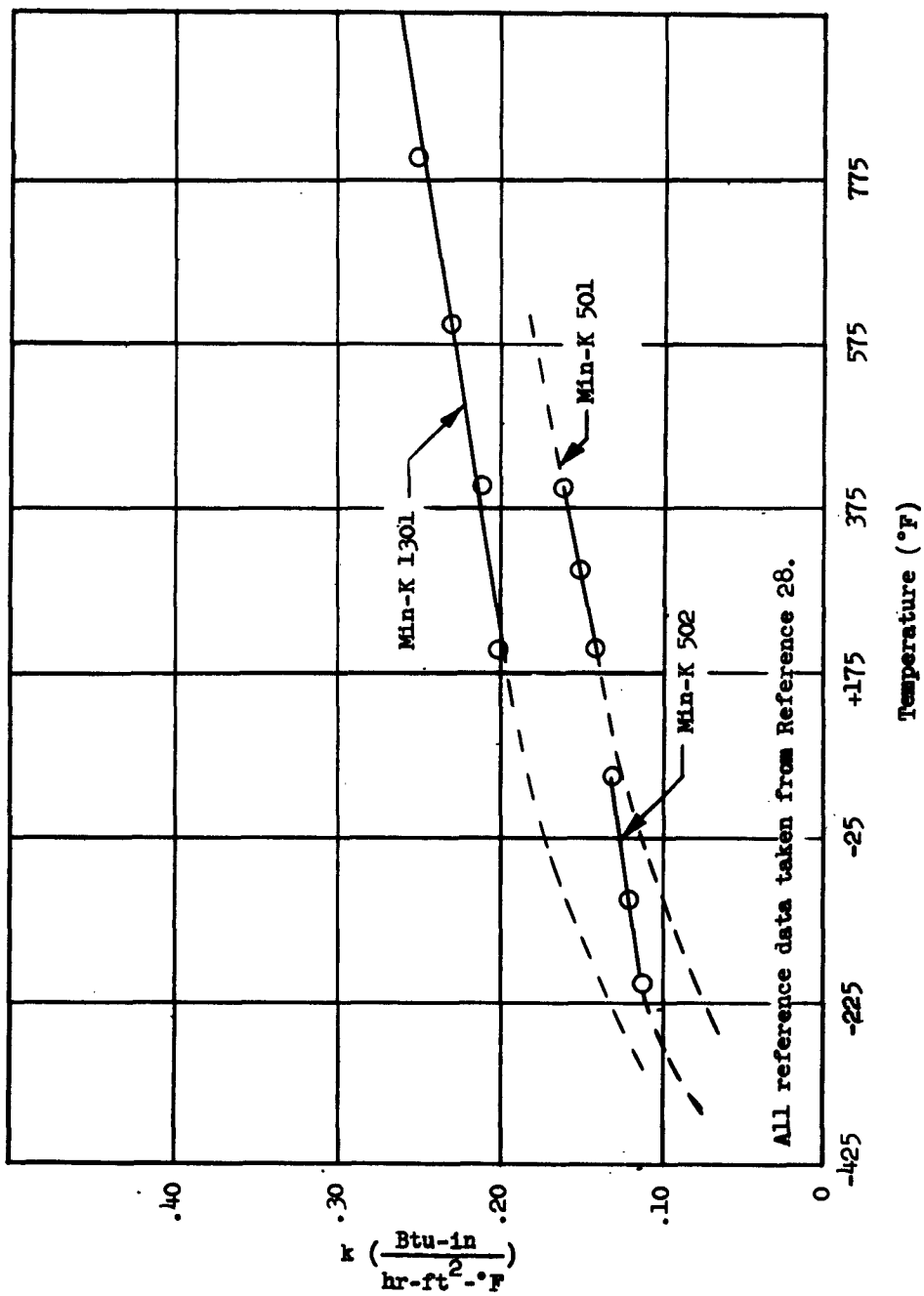

The relationship of thermal conductivity, density, and specific heat defines the relative thermal efficiency of insulating materials. This relationship is called the diffusivity and is $k/\rho C_p$. A low value of diffusivity indicates an efficient insulation. Evacuated Min-K has a low value of thermal diffusivity and was chosen as the insulation for the 7000-gallon test tank.

A comprehensive survey of insulations and adhesives available was accomplished, and the results of the survey were listed in Tables 5 and 6 of Reference 2.

A transient heat-transfer analysis utilizing an active analog computer was accomplished and reported in Reference 3. The purpose of this program was to provide information of acceptable accuracy pertaining to wall temperature profiles and heat transfer rates on tanks related to these studies. The results of the transient heat transfer using various trajectories, various types and thicknesses of insulation, and various thicknesses of tank sidewall (titanium) as variables are set forth in Reference 3. This analysis was extended to the later insulation concepts, Sta-foam AA-602 and LBI-A6 type insulations, and is presented in Section 4.0 of Volume I of this report. The LBI-A6 is a glass fiber, load-bearing insulation developed during this contract and is discussed in subsequent paragraphs.

Also, during the insulation studies major consideration was given to the utilization of plastic foams for tank sidewall insulation. A large coefficient of thermal expansion is the major difficulty which is experienced with cryogenic application of the foam materials. In the proposed application, this difficulty is present because of large temperature differences across small thicknesses of material. It is believed, however, that from the density and thermal conductivity standpoints, these materials warrant additional consideration. The major advantages of foam materials are: (1) they can reduce, or possibly eliminate, the need for an outer sealing membrane such as is required for other insulations and (2) a decrease in insulation system weight can be realized.

Some of the new foam materials that show good promise as tank insulation are discussed below. One is a polystyrene foam of paper thickness and is available in a density of five (5) pounds per cubic foot and in a 14-inch width. Thermal conductivity values for this product are as follows:

Mean Temperature (°F)	Thermal Conductivity (BTU-in/hr-ft^2-°F)
+70	.23
+15	.167
-32	.151
-60	.130
-250	.05

This material can be wrapped on the tank skin to the desired thickness providing the thermal advantages of a number of interfaces as well as being a lightweight insulation.

A second material under investigation is the rigid urethane UMARCO U-200 foam. This is a closed cell, fine grain, 2-3 pound foam with the following thermal conductivities.

Mean Temperature (°F)	Thermal Conductivity (BTU-in/hr-ft^2-°F)
+100	.135
0	.132
-100	.107
-200	.091
-300	.067

This material could be molded to shape in the desired thickness and adhesive bonded to the tank wall in tile segments.

A third foam material is a 2 lb/ft^3 plastic foam (Formulation AA-602 manufactured by the American Latex Division of the Dayton Rubber Company). This plastic foam has an upper temperature limit of approximately 300-325°F and may find use only on low acceleration vehicles.

From the heat transfer analyses performed to select an insulation material for the 7000-gallon test tank, (Reference Section 4.0, Volume I for these heat analyses). insulation material and optimum insulation thickness were determined for use on the 7000-gallon test tank. Maximum insulation temperatures were obtained with evacuated and unevacuated materials. Improved insulating characteristics which result from evacuation resulted in hotter outer surface temperatures under transient heat flow conditions. Encapsulation material requirements are discussed in Section 3.0 for the expected temperature conditions.

During the latter part of the program, work was directed toward investigating the thermal properties of load-bearing insulations (LBI series). For example, the LBI-A6 insulation (a fiberglass insulation that was developed and tested by Beech Aircraft Corporation) has a high service temperature and, thus, could be utilized on the higher acceleration vehicles such as those under LOX-RP boosts. The thermal efficiency of the LBI-A6 is very good; and, as a result, its use in even a practical minimum thickness may produce exterior surface temperatures that would exceed the temperature limits of a Mylar encapsulation. Further discussion of this problem is included in Section 3.1.

2.1.2 Tank End Insulation

The primary purpose for tank end insulation is to preclude the formation of ice and liquid air on the tank ends during the filling and standby

operations. The ice or liquid air, if allowed to accumulate, would impose an additional weight penalty to the vehicle. Also, it would be detrimental to equipment located in the areas adjacent to these tank ends. A secondary effect of this insulation is, of course, to reduce the boil-off losses while on the ground and during boost through the atmosphere.

Since the tank-end insulation is located in the interior of a vehicle, it will not be subjected to high aerodynamic heating rates. The upper temperature limit that the tank-end insulation will witness depends on a number of parameters, such as compartment air conditioning, location of engine, location of auxiliary power units, and location of other internal sources of heat. For the present, it has been assumed that the temperature of the insulation will never exceed 200°F.

Earlier studies have indicated that the use of evacuated plastic foam for the insulation will provide a lightweight method for insulating the tank ends. This concept specifies an insulation thickness such that the outside surface of the foam is maintained just above the freezing point of water. Based on previous tests conducted, the thermal conductivity of the Dayton Rubber Company's Polykoolfoam (a polyisocyanate-type foam) is .069 BTU-in/hr-ft^2-°F. This "k" factor was determined in a cryostat where one side of the foam was exposed to liquid nitrogen (-321°F) and the warm side was at room temperature (80°F).

When liquid hydrogen was used at the cold wall, the apparent mean thermal conductivity was reduced to .048 BTU-in/hr-ft^2-°F. If the more conservative (.069) value is used, the thickness of insulation required to maintain 34°F temperature on the exterior of the foam insulation is 1.93 inches for the upper end and 1.20 inches for the lower end of the 7000-gallon test tank. The method for calculating these insulation thicknesses is fully described in Reference 8.

The foam can be applied to the tank ends by either spraying, pouring, or by molding small size segments and cementing these to the skin with a suitable adhesive. There will be access holes in the foam on the upper end in order to allow exit of the vent line, instrumentation port, and the manhole. (See Figure 27 for details). Once the foam is in position, it will be completely covered with a thin, flexible plastic or latex membrane such that the entire foam end can be evacuated.

In the actual application to the 7000-gallon test tank, pour-in-place Sta-foam C-02 manufactured by the Dayton Rubber Company was poured into the wedge-shaped annulus between the tank heads and tank skirts for added insulation and to prevent the tank skirts from buckling under external pressure when the foam was evacuated. Sta-foam C-02 was also used to insulate the dome areas.

FIGURE 27
TANK END INSULATION DETAILS

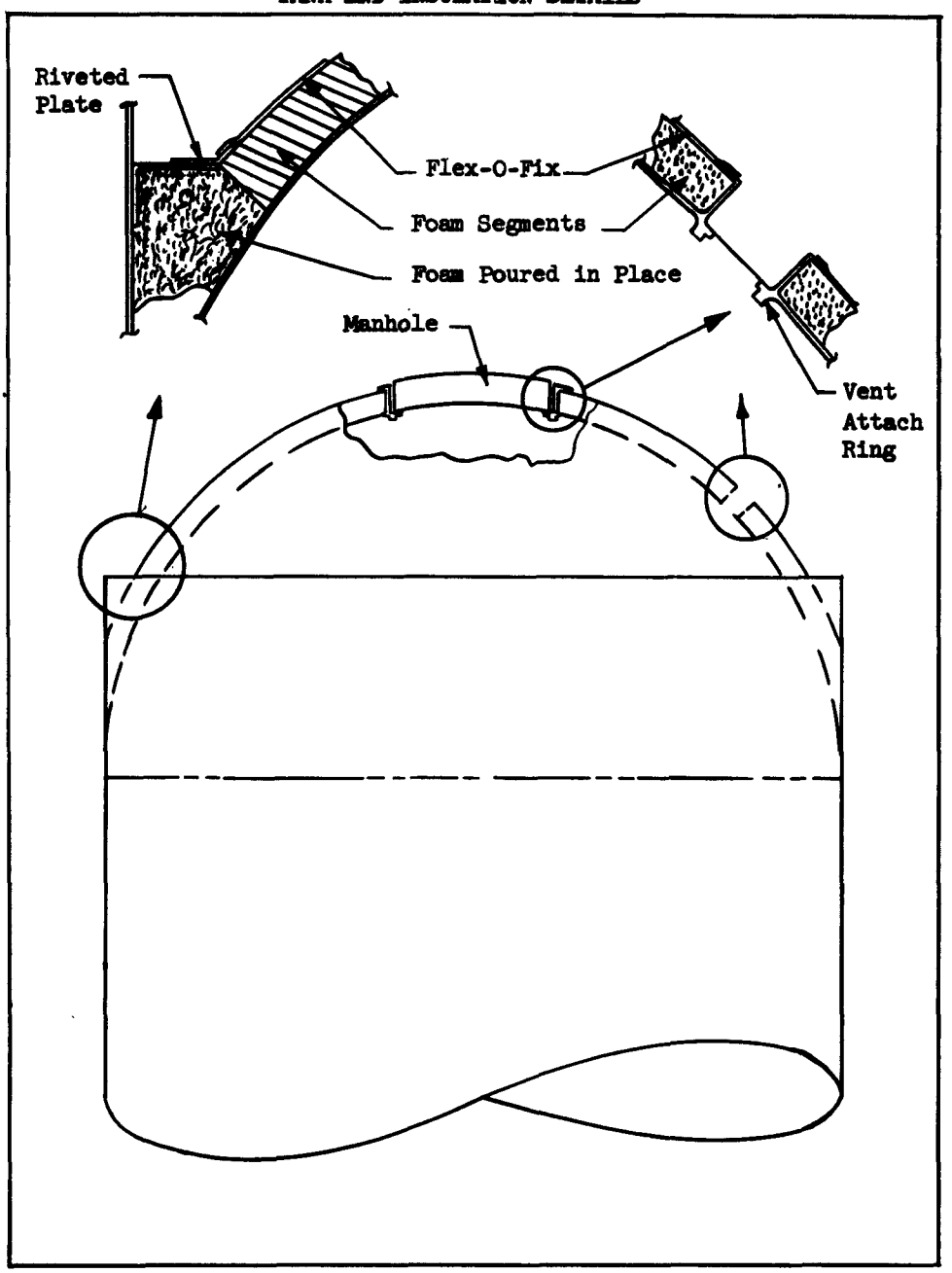

2.1.3 Auxiliary Ground Insulation

The tank sidewall insulation thicknesses, as determined in previous sections and Section 4.0 of Volume I, which satisfy the optimum conditions from a net tank system weight standpoint are too thin to prevent excessive boil-off of the propellant during filling, standby and hold operations. It has, therefore, been recommended that an auxiliary ground insulation blanket be employed to keep the boil-off loss to a minimum.

The design details of the ground insulation concept are described in Reference 11.

The economics of the ground blanket, added flight insulation, or the use of a reliquefier are reported in Reference 3.

A schematic of the tank and how the ground blankets will be used is shown in Figure 28. The ground blankets are constructed of styrofoam with metal stiffeners as indicated in Figure 28.

2.2 Insulation Testing

Tests were performed on selected insulating materials to obtain thermal conductivity curves as a function of temperature throughout the stipulated temperature range. The results of these tests were used in determining the heat inputs required for the heat tower test tank. In addition, optimized performance was calculated using the test results from the insulation program.

An apparatus was designed for measuring the heat capacity of these materials over the temperature range of interest. These data are necessary inputs for transient heat analyses.

2.2.1 Thermal Conductivity Test Apparatus, Basic and Auxiliary

A cryostat for determining low-temperature thermal conductivities of insulating materials was designed and fabricated. It utilizes the standard guard-ring or flat-plate concept which is typical of many instruments used for thermal conductivity measurements. Wilkes and Vershoor, in independent papers, describe a typical apparatus of this type (References 12 and 13).

The test apparatus used in determining the over-all thermal conductivity is shown schematically in Figure 29. The apparatus has a flanged bottom under the sample space that is removable to facilitate a changing of samples. The guard and test chamber move up and down as a unit to accommodate different test sample thicknesses. A pair of O-ring seals near the top of the extended tubes give an adjustable vacuum seal.

In order to prevent error due to the evaporated gas from the test chamber condensing in the fill tube, the guard-ring liquid is maintained at a

FIGURE 28
GROUND INSULATION BLANKET CONCEPT

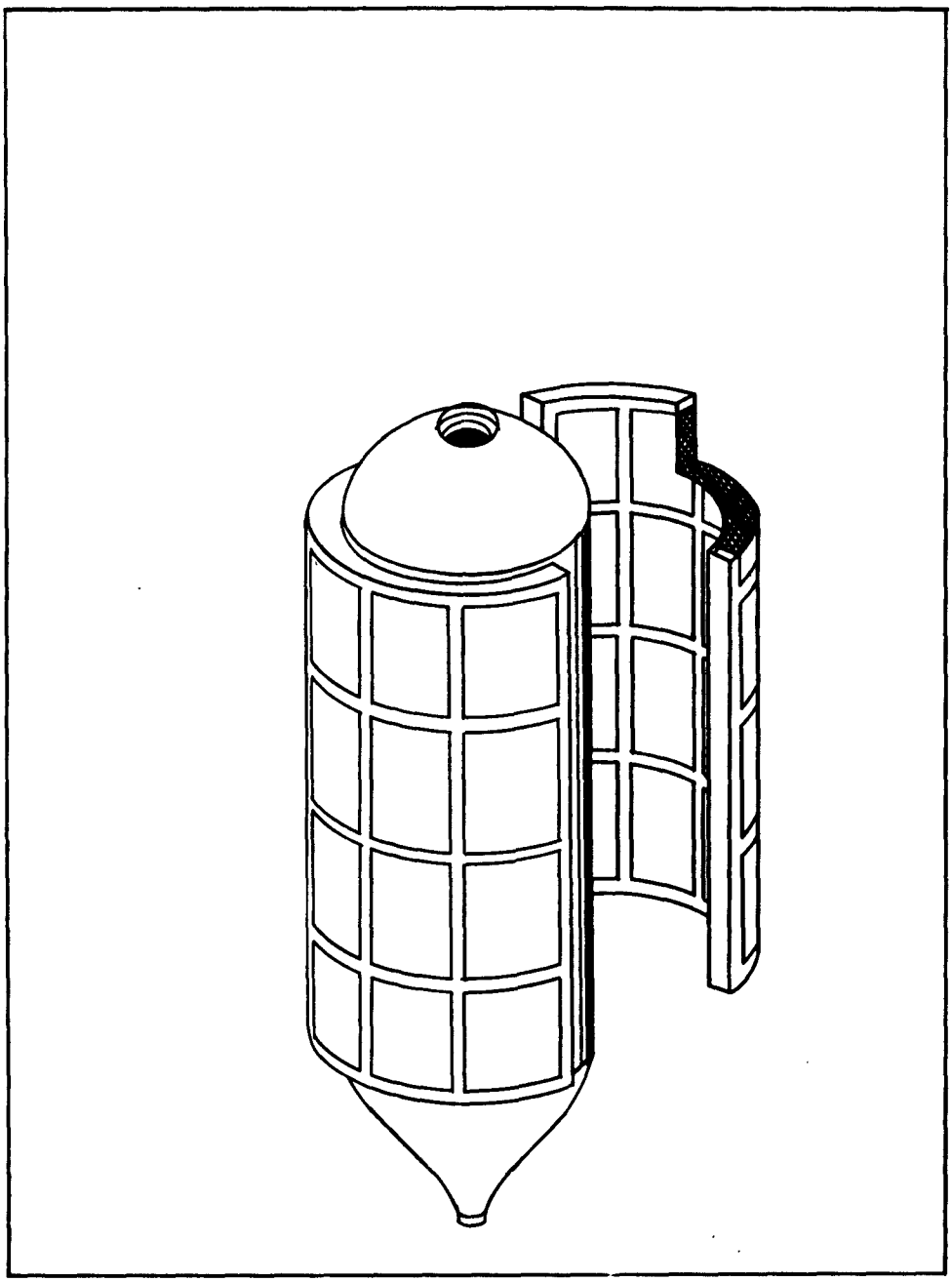

higher pressure and temperature than the test chamber liquid by bubbling the guard-ring vent gas through four (4) inches of water. If any heat is transported because of this resulting temperature difference, it will be into the test chamber causing the resulting $\bar{K}$ values to be slightly high.

The test apparatus used in determining the thermal conductivity versus mean temperature curves is shown schematically in Figure 30. The sample space in the calorimeter is exaggerated to show the location of the thermocouple junctions. If the sample tested is solid, transverse holes are drilled, as indicated, into which thermocouple junctions are inserted. The junction positions, relative to the external surfaces of the sample, were determined by taking X-ray pictures of the instrumented opaque samples.

In order to simulate actual operating conditions, a method of obtaining apparent thermal conductivity data for samples subjected to one (1) atmosphere compressive load was deemed necessary. To obtain these results, the bottom flange of the flat-plate calorimeter was modified as shown in Figure 31. The addition of the rubber diaphragm provides the method of introducing the compressive load.

One of the pumping taps was modified to accommodate the thermocouple wire. Three holes were bored in a rubber stopper and the thermocouple wires were brought out through these holes. Sealing wax was melted and flowed into these holes, thus sealing the pumping tap tightly. A representative thermocouple pair is shown leaving the seal and extending on to the auxiliary apparatus. All three couples actually extended to the reference bath and beyond. A difference of electromotive force is measured with a potentiometer between the two junctions in each circuit. The use of a calibrated table yields the actual temperature differential.

Gold-cobalt versus copper thermocouples were originally chosen for these tests because of their sensitivity near liquid-hydrogen temperature. A gold-cobalt versus copper circuit has a 40-microvolt per degree signal at room temperature and approximately a 15-microvolt per degree signal at liquid-hydrogen temperature. This is contrasted to copper versus constantan circuits which have 40 microvolts per degree at room temperature but fall off to only 6 microvolts per degree at hydrogen temperature. However, during the course of testing, it was determined that the gold-cobalt versus copper thermocouples were unreliable in their operation and did not spot test near published calibration curves. One possible reason for not operating properly could be the temperature history of the gold-cobalt wire. The manufacturer heat treats the wire just above room temperature and any temperature that the wire experiences above this temperature could change the properties, thus yielding erroneous data. The test samples were rewired using copper versus constantan thermocouples even though sensitivity was lost near liquid-hydrogen temperatures.

The various quarterly reports prepared for this contract cover in detail the difficulties experienced with the thermal conductivity test apparatus and give the final solution in making the apparatus function peoperly.

FIGURE 29
THERMAL CONDUCTIVITY TEST CALORIMETER

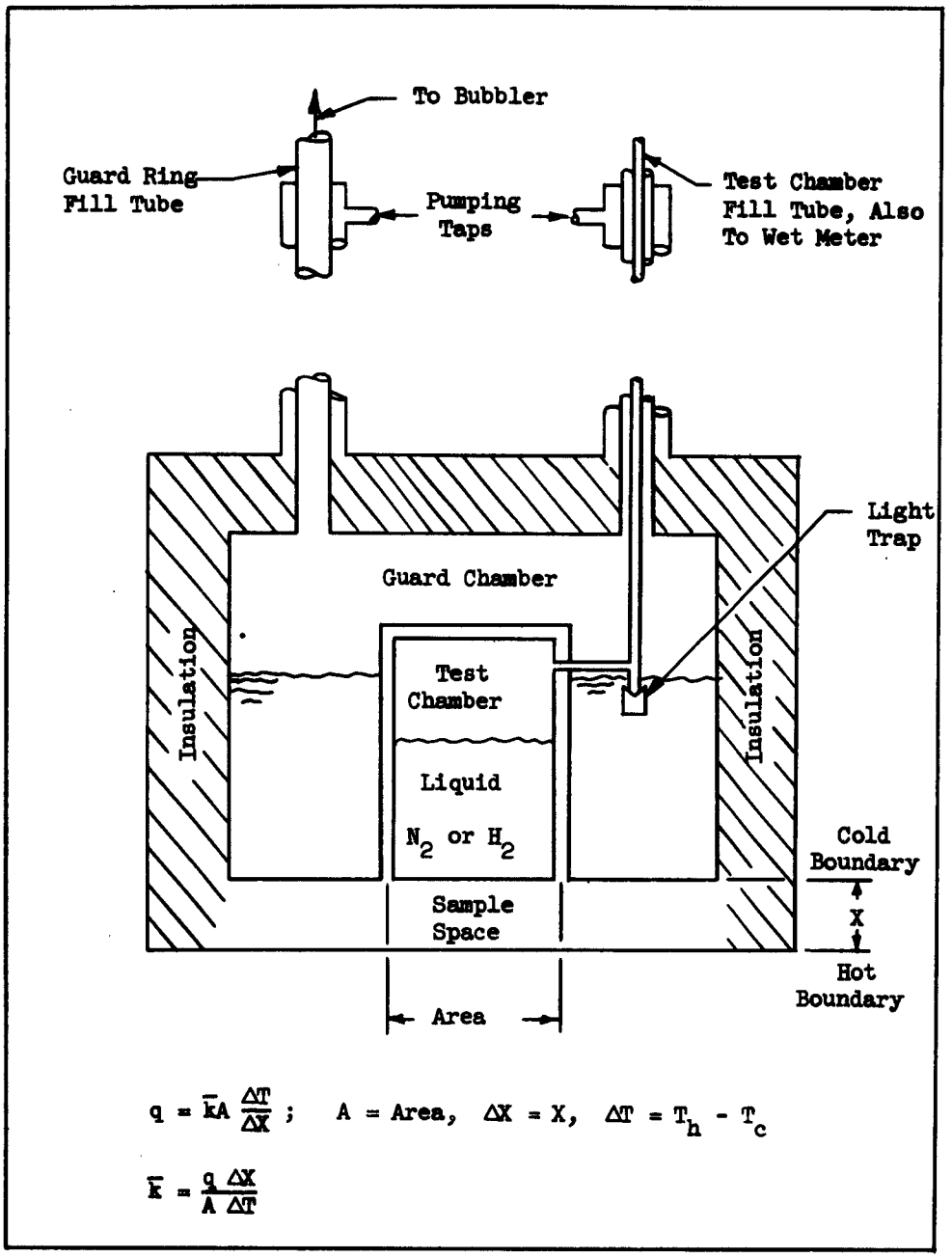

$$q = \bar{k} A \frac{\Delta T}{\Delta X} \; ; \quad A = \text{Area}, \quad \Delta X = X, \quad \Delta T = T_h - T_c$$

$$\bar{k} = \frac{q \, \Delta X}{A \, \Delta T}$$

FIGURE 30
THERMAL CONDUCTIVITY TEST SET-UP

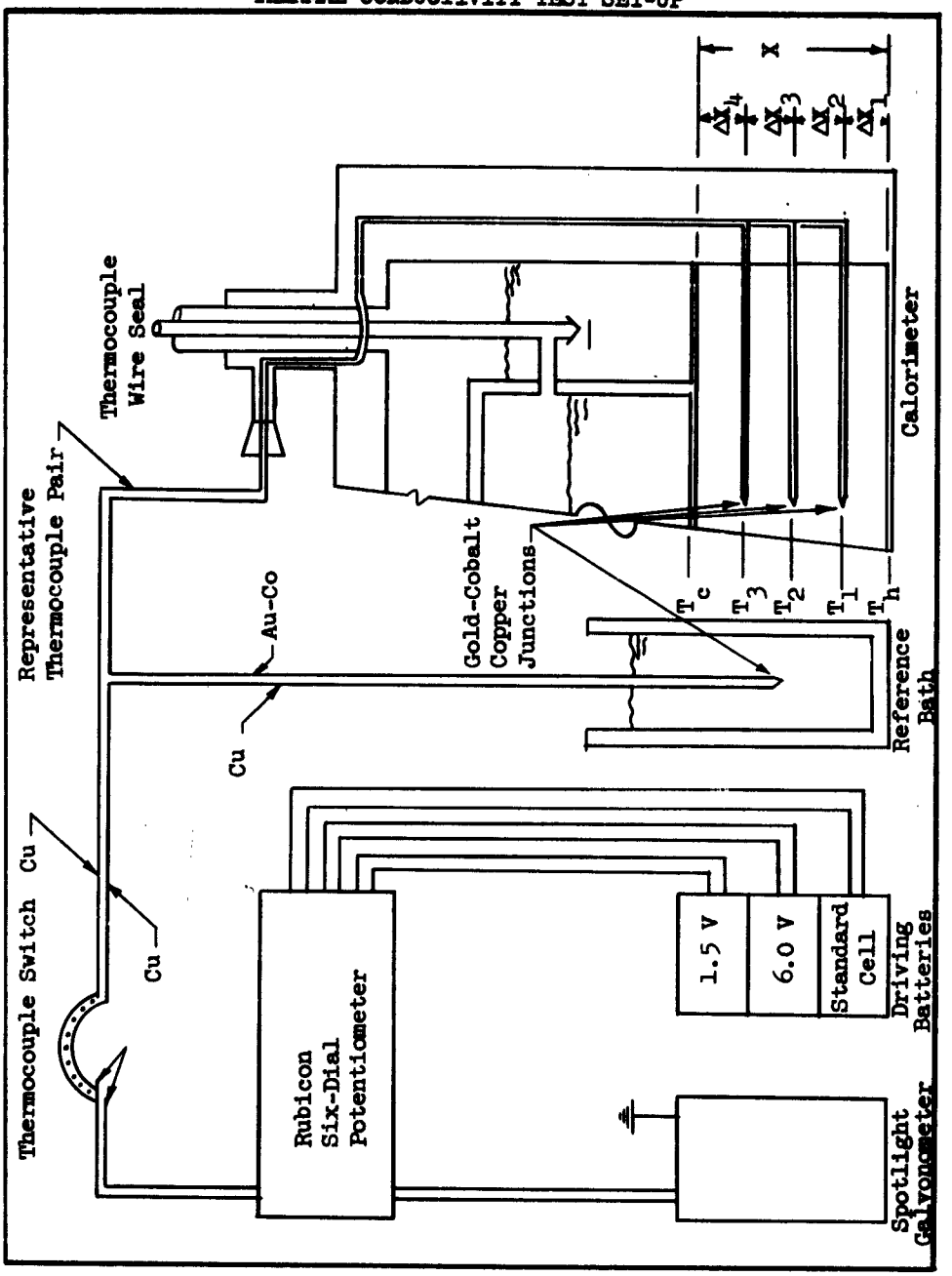

FIGURE 31
MODIFIED FLAT PLATE CALORIMETER SCHEMATIC

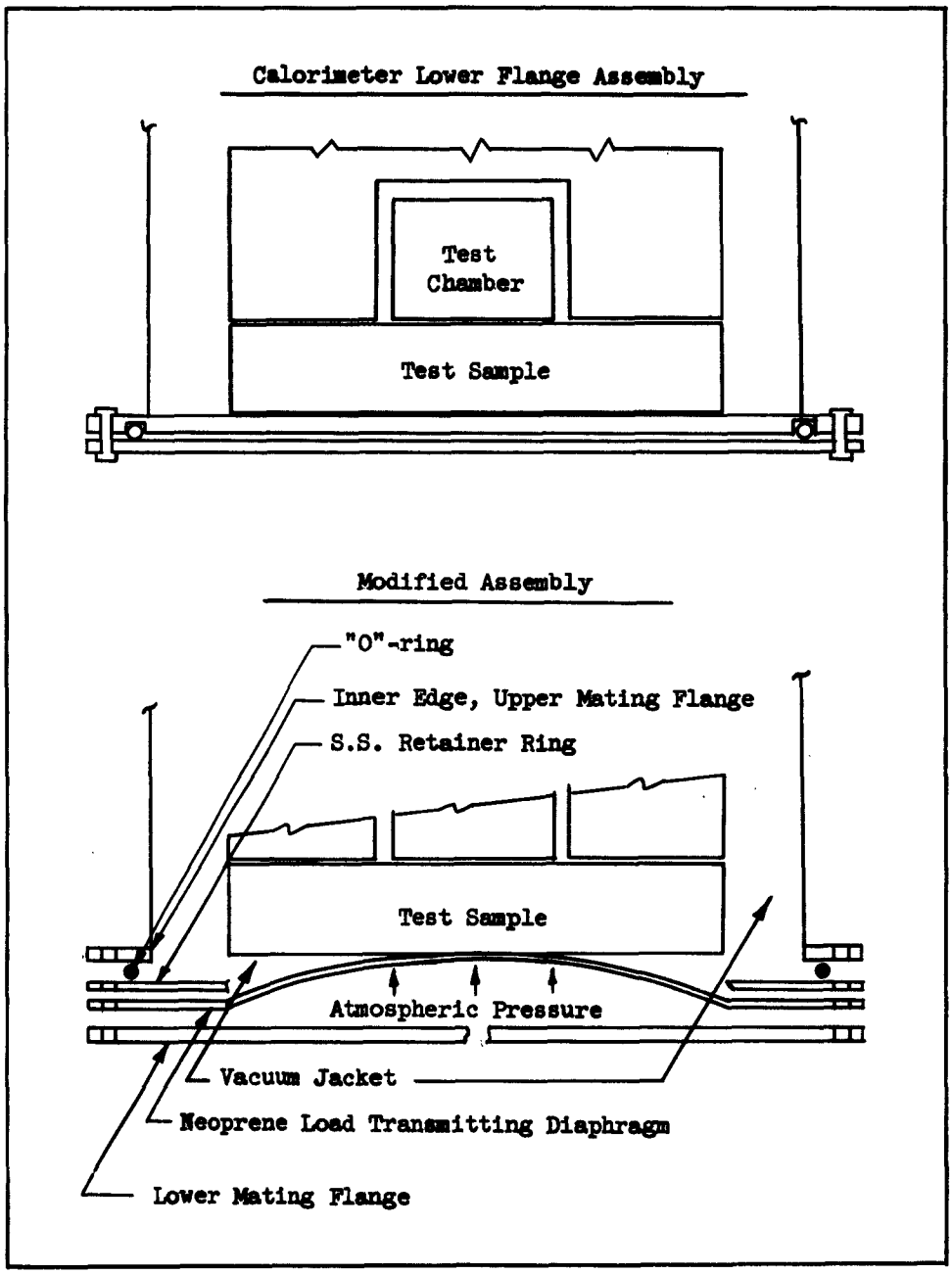

The following auxiliary equipment was also used in the test setup:

(a) Barometer, mercury type.

(b) Wet test meter, Precision Scientific Company, 20 ft^2-hr capacity, accuracy $\pm$ 0.1%, calibrated at low flow rates to $\pm$ 2%.

(c) Rubicon Six-Dial Thermofree Potentiometer - accurate to 1 x 10^{-7} volts.

(d) Standard cell, Eppley Laboratories, Inc., with emf certified by National Bureau of Standards.

(e) Leeds and Northrup spotlight galvonometer.

(f) Leeds and Northrup 13-position thermocouple switch.

(g) 6-volt, 10-milliamp storage battery.

2.2.1.1 Specific Heat Measurements

Obtaining specific heat data of insulations as a function of temperature is necessary for analytical support of the thermal test planning program. Specifically, this data is needed to evaluate thermal diffusivities of various insulations. The program for obtaining these measurements is discussed below.

2.2.1.1.1 Equipment and Apparatus

Figure 32 is a schematic of the test apparatus. Auxiliary equipment not shown in the schematic is a potentiometer circuit and a precision balance.

2.2.1.1.2 Test Procedure

The procedure for determining the specific heat of various insulations is as follows:

(1) Weigh sample on precision balance.

(2) Mount sample in the apparatus and install break-out seal.

(3) Fill test and guard vessels with appropriate liquid.

(4) Regulate gas temperature and flow to the sample by adjusting the gas supply dewar heater.

(5) Observe temperature difference across differential thermocouples. Thermocouple No. 2 is also an absolute reading thermocouple for reading temperature level.

FIGURE 32
SPECIFIC HEAT MEASURING APPARATUS

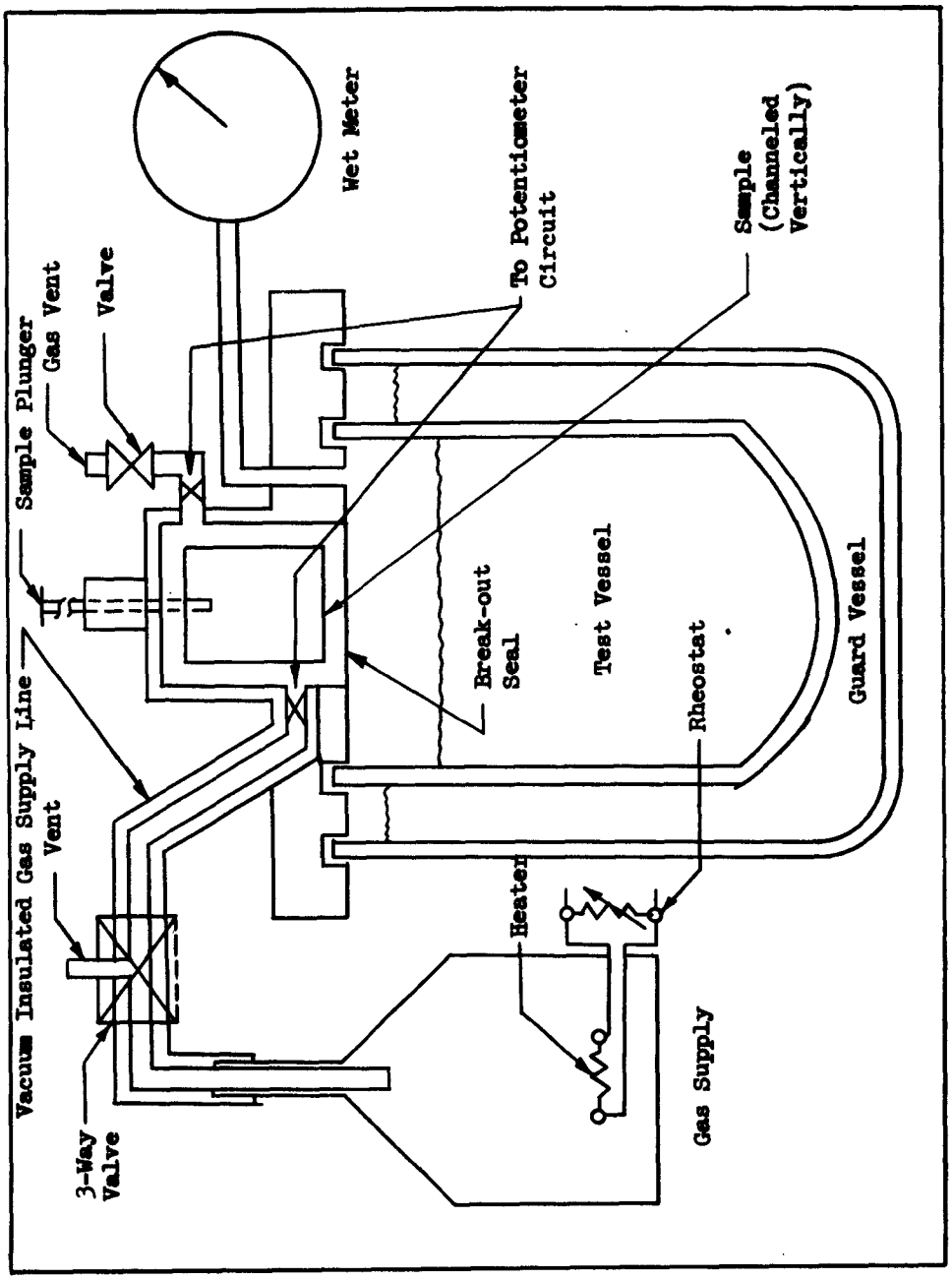

(6) Meter the gas evolving from the test vessel through the wet test meter.

(7) When the differential temperature across the sample is less than 2° Fahrenheit and the temperature level of Thermocouple No. 2 reaches a predetermined level, the 3-way valve is turned to vent, the gas vent valve is closed, and the gas supply dewar heater is turned off. The sample then is ready for immersion.

(8) Push sample through the break-out seal and immerse the sample in the test vessel liquid.

(9) Measure the amount of gas boiled off by the sample with the wet test meter.

The above procedure will constitute a standard method for calibration of the apparatus using a sample of known specific heat.

2.2.1.1.3 Obtaining Specific Heat Data as a Function of Mean Temperature

For each test, as described above, one (1) value for specific heat will be obtained at a given mean temperature. The relationship used to determine this is as follows:

$$C_p = \frac{L_v \, (G.F.) \, Q}{W \, \Delta T}$$

where

C_p is the specific heat of sample

W is the weight of sample

ΔT is the mean gas temperature (also sample temperature) minus temperature of the test vessel liquid

L_v is the latent heat of vaporization

G.F. is a gas conversion factor to obtain standard cubic feet. A detailed explanation is presented in Paragraph 2.2.2.

Q is the quantity of gas evolved

After a sufficient number of tests are performed with various sample and liquid temperatures, a plot of specific heat versus mean temperature can be made.

2.2.2 Obtaining the Thermal Conductivity Coefficient

The Fourier equation

$$q = k A \frac{\Delta T}{X}$$

was used in determining the coefficient conductivity. The parameters are as follows:

A sample of insulation material of known thickness (X) was mounted in the sample space. The area (A) is the area projected by the inner container. The hot boundary was heated by an electrical heater and the heat flow (q) through the insulation was determined from the boil-off gas. The temperature difference (ΔT) between the hot and cold boundaries was measured with thermocouples.

The evaporation rate from the test chamber is obtained by metering the evolved gas through a wet test meter and taking readings at definite time intervals. The heat input to the test chamber is proportional to the amount of gas evaporated during a specific time interval.

$$q = L_v \frac{\text{Boulder ft}^3}{\text{hour}} \text{ gas factor } = L_v \frac{\text{std. ft}^3}{\text{hour}}$$

where

L_v is the latent heat of vaporization of liquid necessary to produce one standard cubic foot of gas. Boulder cubic feet per hour are obtained directly from reading the wet meter at specific time intervals. Converting Boulder cubic feet per hour to standard cubic feet per hour the relationship that follow is used:

$$\text{Gas Factor} = \left(\frac{P - V.P.}{760}\right)\left(\frac{492}{T, {}^\circ R}\right)$$

where P is atmospheric pressure (mm Hg)

V.P. is the partial pressure of water in air, mm Hg, assumed saturated, at T, °R.

T, °R is the abolute temperature of the water in the wet test meter.

Figure 33 is a plot of gas factor versus temperature.

The area, A, and sample thickness, ΔX, are measured directly before inserting the sample. ΔT, or $T_h - T_c$ is obtained by assuming T_c

FIGURE 33
GAS FACTOR PLOT

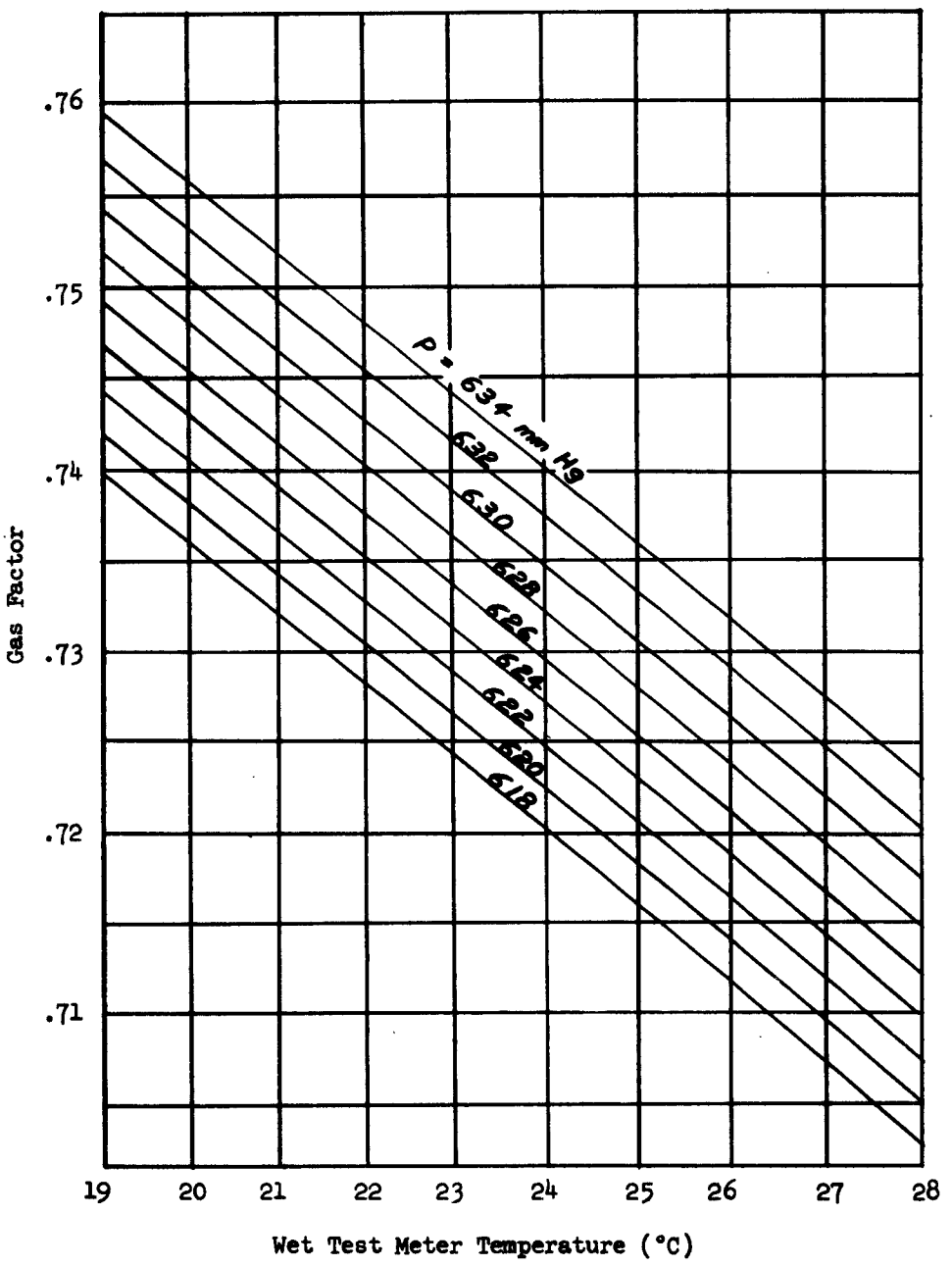

at the equilibrium boiling temperature of the liquid at the known atmospheric pressure, and T_h is measured by a surface pyrometer at the hot wall of the calorimeter.

The equation on Figure 29, $q = \bar{k} A \Delta T/X$, now has all the parameters described except for $\bar{k}$. $\bar{k}$ is the mean thermal conductivity over the indicated temperature range, and solving for $\bar{k}$ gives

$$\bar{k} = \frac{q X}{A \Delta T}$$

This is the relation used in all the conductivity measurements.

2.2.2.1 Obtaining a Thermal Conductivity Versus Mean Temperature Curve

Temperature measurements of the various thermocouple junctions are obtained by use of the potentiometer circuit shown schematically in Figure 30. The potentiometer reads a difference of emf between the sample junction and the reference bath junction. From a calibrated table, the reference emf is found and added to the potentiometer reading, yielding the absolute temperature of the junction. Readings are taken immediately after each wet meter reading is taken. After equilibrium is reached, a $\bar{k}$ versus mean temperature curve is obtained. Since q, and similarly q/A are constant throughout the sample, the auxiliary equations that follow may be used to determine $\bar{k}$ versus mean temperature (T_m). T_m is the average temperature of any of the given ranges, ΔT is the temperature difference obtained from the potentiometric measurements, and ΔX is the distance between the thermocouple junctions as shown in Figure 30.

$$\bar{k} \Big]_{T_1}^{T_h} = \frac{q \Delta X_1}{A \Delta T_{h-1}}$$

$$\bar{k} \Big]_{T_2}^{T_1} = \frac{q \Delta X_2}{A \Delta T_{1-2}}$$

$$\bar{k} \Big]_{T_3}^{T_2} = \frac{q \Delta X_3}{A \Delta T_{2-3}}$$

$$\bar{k} \Big]_{T_c}^{T_3} = \frac{q \Delta X_4}{A \Delta T_{3-c}}$$

2.2.3 Insulating Material Testing

The selected materials for consideration were all evaluated as to their overall thermal conductivity. In addition, some of the following tests were performed on some of the materials: thermal conductivity versus mean temperature over the range of interest; outgassing characteristics over extended time periods; and the effect of prolonged dynamic evacuation on the conductivity.

Each material and the tests performed on thermal conductivity are discussed in the following sections.

Table 9 is a tabulation of the thermal conductivity tests on Min-K 504, Sta-foam AA-602, and the LBI (Load-Bearing Insulation) series.

2.2.3.1 Min-K 504

The thermal conductivity of Min-K 504 was determined at low temperatures. Some data were available from work performed at the Armour Research Foundation, Chicago, Illinois, and from the manufacturer, Johns-Manville. Figure 34 presents their reported results graphically. From the obvious disagreement of these data, an independent measuring program was deemed necessary. These data, generated on this contract, are also shown in Figure 34. Several possible reasons for deviation of the data may be offered such as, moisture content, or orientation of the samples in the calorimeter. It must be emphasized that the Armour Research data reflects their initial attempts at measuring the conductivity of Min-K 504 and is thus inconclusive.

Because Min-K 504 is a very opaque material, X-ray pictures of the prepared sample were taken after drilling holes and inserting the thermocouples. The measurement of the thermocouple junction distance from the edges was determined by including a standard 1 inch opaque object, and facing each sample edge with opaque pointers. These X-ray pictures yielded the information necessary for obtaining thermal conductivity versus mean temperature data, using the method outlined in Section 2.2.2.1.

The relative ease of evacuation and the outgassing characteristics of Min-K 504 were tested to determine how much pumping time would be required for evacuation of a known volume of the material, with resulting low pressure rise under static vacuum conditions.

It has been previously shown that the thermal efficiency of Min-K insulation is greatly increased by evacuation. When the 7000-gallon test tank insulated with Min-K 504 is in the heat tower, it will be subjected to an external vacuum condition provided by the vacuum bell assembly. As a matter of economics in reducing boil-off losses, the vacuum bell is evacuated before filling the tank. Prior to evacuation of the vacuum bell, the encapsulated tank sidewall insulation must also

TABLE 9
RESULTS OF INSULATION TESTS

Insulation	Nominal Insulation Thickness (in)	Load on Sample	Heat Flux ($Btu/hr\text{-}ft^2$)	$\bar{k}$ ($Btu\text{-}in/hr\text{-}ft^2\text{-}°F$)
Min-K 504	1.0	atm	26.7	0.07
Sta-Foam AA-602	1.0	atm	47.4 to 52.8	0.124 to 0.138
LBI A-2	0.017	atm	166	*0.00352
LBI A-4	0.048	atm	64.7	*0.0042
LBI A-5 (big F.P.)	0.028	0	4.4	*0.00032
LBI A-6	0.016	atm	10.8	*0.0010

*For use only with identical conditions (see Section 2.2.3.3).
Refer to Figure 37 for the conditions.

FIGURE 34
THERMAL CONDUCTIVITY OF MIN-K 504

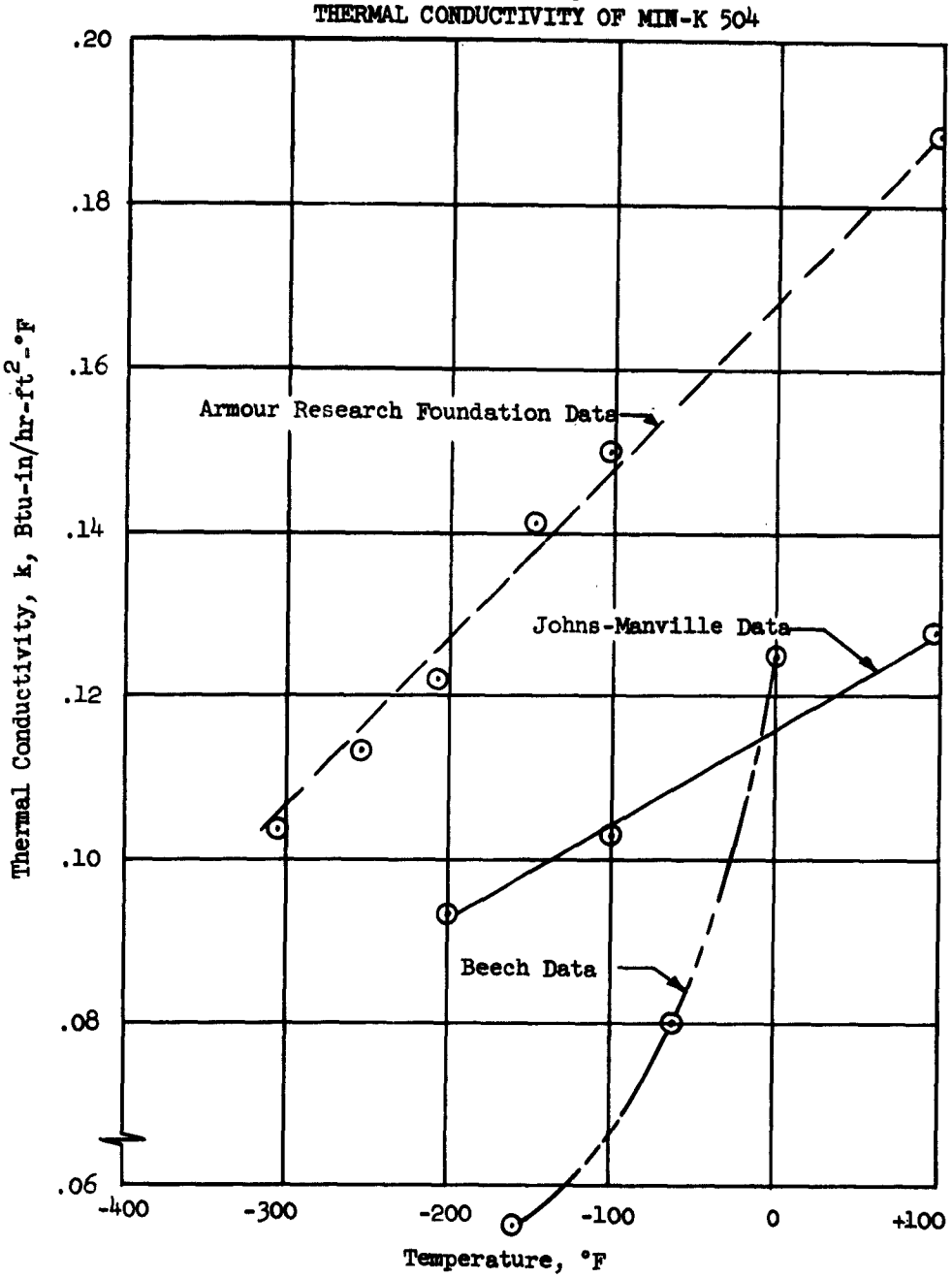

be evacuated in order to prevent ballooning of the encapsulating material. Immediately upon filling the tank, the pressure in the insulation material will be further reduced by condensation or "freeze-out" of the remaining entrained gases and moisture. This is another reason for evacuating the insulation because if the moisture and gaseous content of the Min-K is not substantially reduced, the frozen moisture and gases will create a solid conduction path which will reduce the thermal efficiency of the insulation. This insulation efficiency will be impaired when the frozen vapors and gases are possibly evaporated by the heat lamps during the thermal test. Either the solid or the gaseous term can reduce insulating efficiency, and the removal of this heat leak source is desirable.

The measurements reported here were made at room temperature, utilizing the test apparatus shown in Figure 35. A test sample 9-5/8" in diameter and one inch thick was enclosed in a modified bell jar. The bell jar was evacuated with a Welch Duo-Seal 1405 mechanical pump and the pressure monitored with a 0 to 1000-micron-range thermocouple gauge.

The results of these tests may be seen in Figures 36 and 37, which plot pump-down and outgassing pressure versus time. Pump-down runs 1, 2, and 3 were continued for a period of three (3) hours, starting from atmospheric pressure. The first run was obviously the most effective in removing water vapor since the second run pumped down to 500 microns in about thirty (30) minutes compared to three (3) hours for the first run. A total pumping time of 56 hours was consumed in reducing the pressure to less than ten (10) microns during ten (10) separate pump-down periods. Between each pump-down the sample was allowed to outgas and readings were taken of the increasing pressure.

Conclusions drawn as a result of this investigation are as follows:

(1) Min-K 504 can be evauated to a pressure of less than 10 microns in a relatively short time. (Similar experiments with a number of foam plastics consumed weeks of pumping time.)

(2) After reaching a pressure of approximately ten (10) microns, the outgassing rate is low for Min-K 504.

The pumping time on the sample of Min-K 504 to attain a low pressure is felt to be quite conservative if applied to the 7,000-gallon tank insulation thickness since the sample is approximately eight (8) times thicker than the proposed insulation thickness.

The thermal expansion properties of Min-K must be known in order to establish compatible fabrication techniques for bonding the insulation to the tank wall. Significant work has been done in this area by R. P. Dengler at NASA, Cleveland, Ohio, with Min-K1301. A summary of this work indicates that Min-K 1301 contracts when heated from

FIGURE 35
PUMP-DOWN AND OUTGASSING TEST APPARATUS

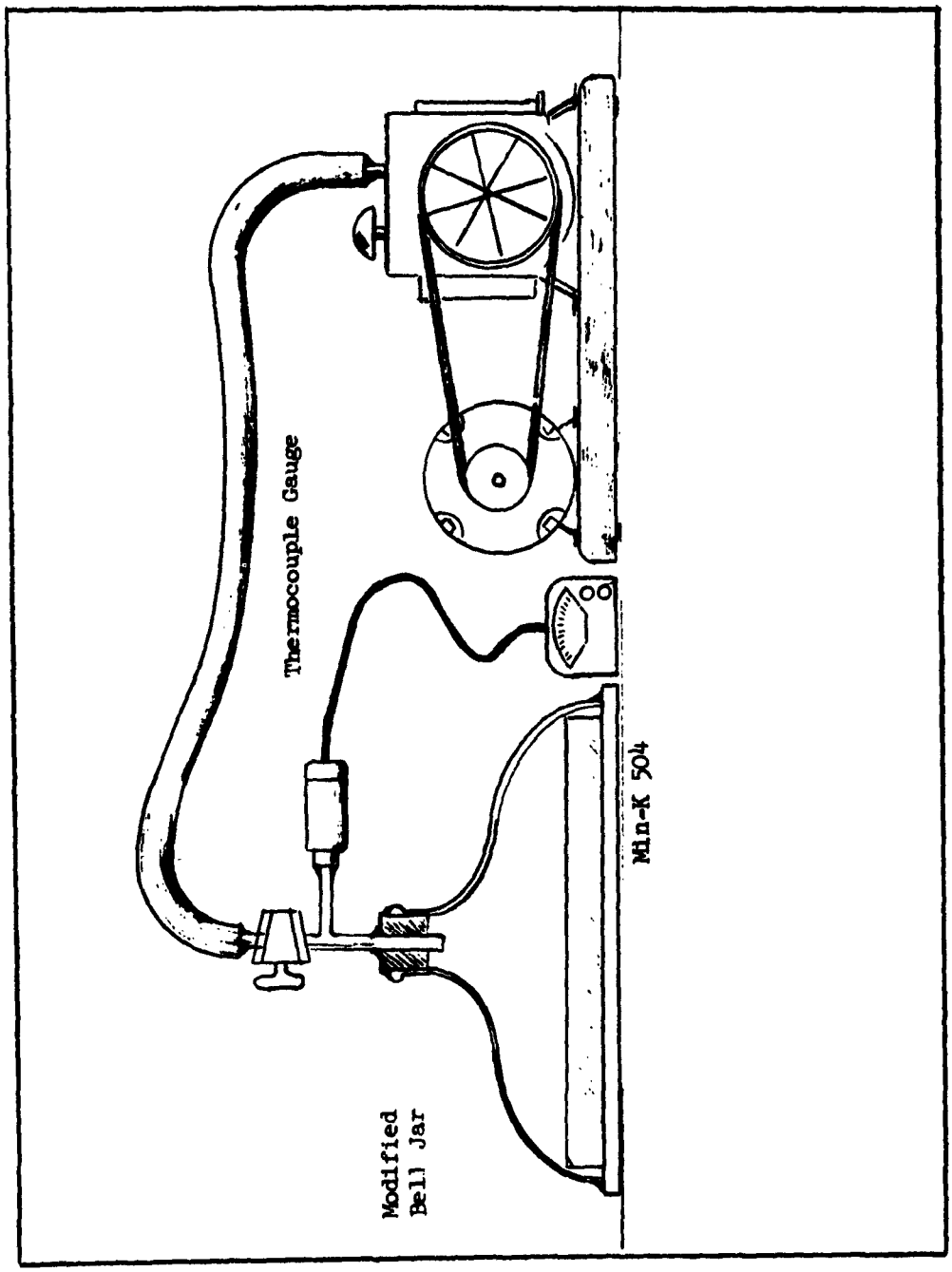

FIGURE 36
PUMP-DOWN CURVES
MIN-K 504

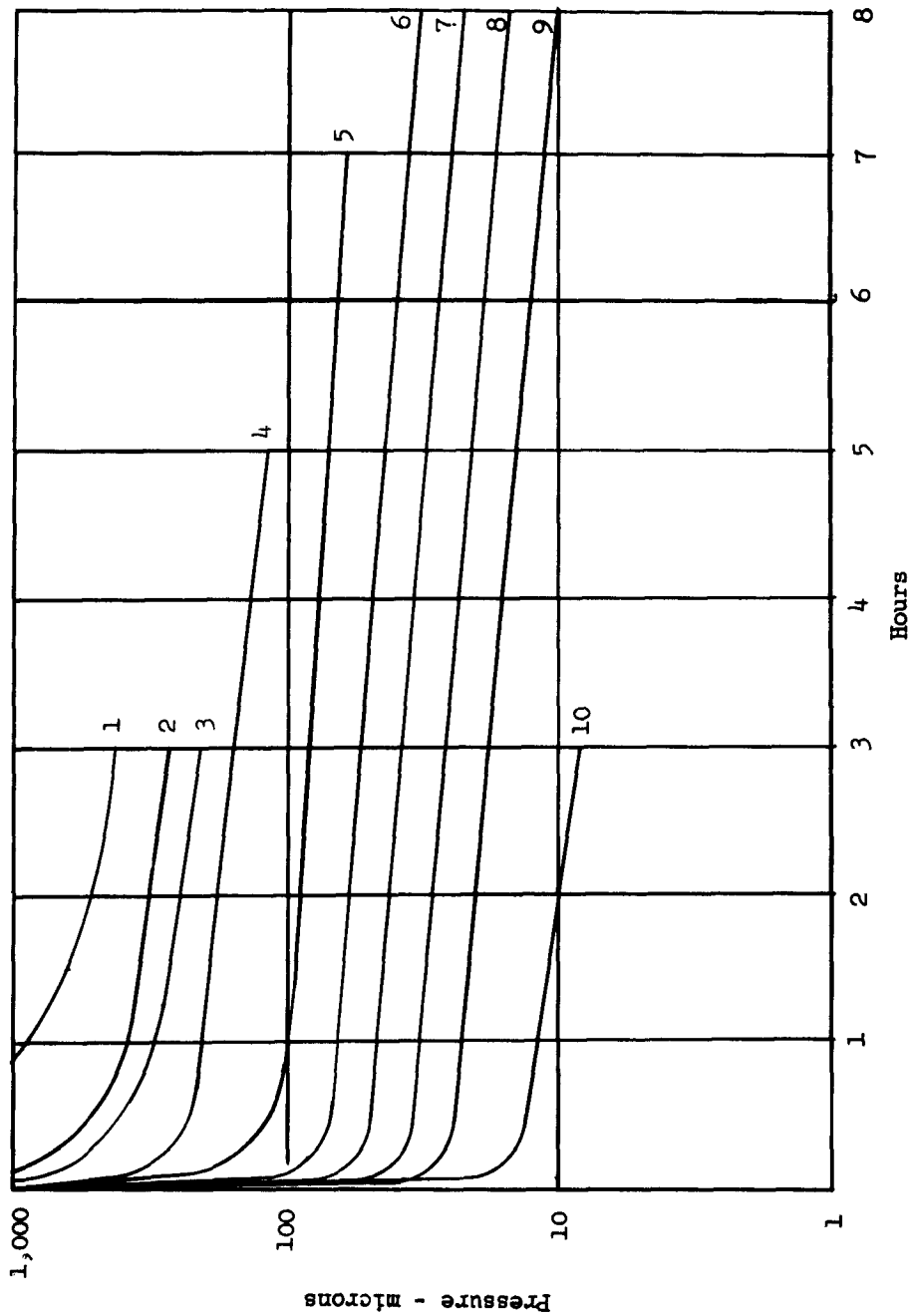

FIGURE 37
OUTGASSING CURVES
MIN-K 504

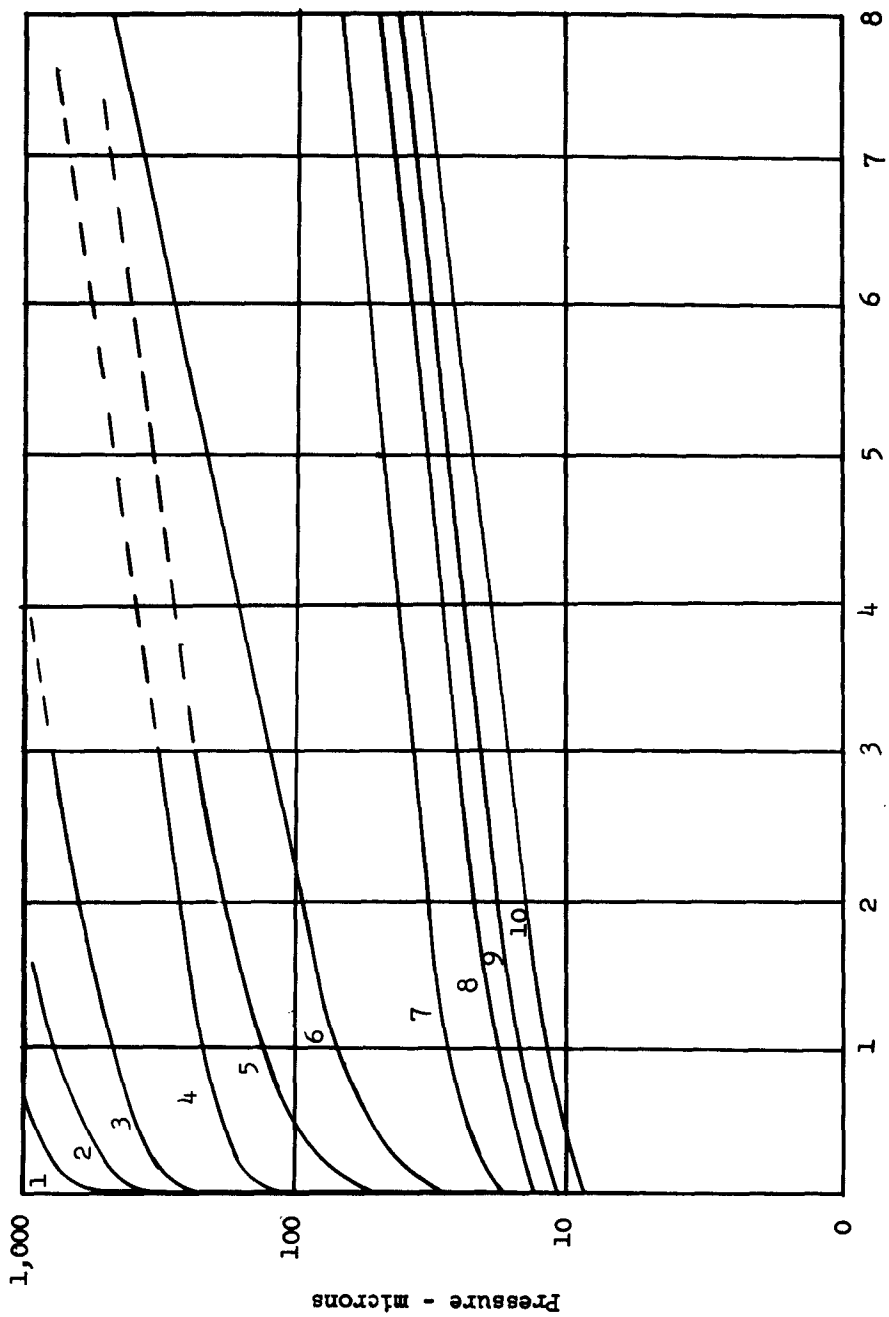

room temperature to 1500°F and that this contraction is a permanent set which is not recoverable upon cooling to room temperature. When subjected to a cooling cycle from room temperature to -310°F and back to room temperature, the material exhibits no dimensional change. The thermal coefficient of expansion values obtained from this work are as follows:

Temperature °F	Mean Coefficient/°F
70 to 1100	-4.92×10^{-6}
1100 to 1580	-21.3×10^{-6}
70 to -320	0

While the material tested in this instance was Min-K 1301, the overall similarity of Min-K 504 to 1301 is such that one would expect nearly identical thermal expansion properties for the two materials. The relative thermal expansion stability of Min-K insulation over the above wide range of temperatures is an advantageous property for rocket vehicle insulation applications.

2.2.3.2 Sta-Foam AA-602

Apparent thermal conductivity figures for Sta-Foam AA-602, when under a one (1) atmosphere load, were obtained from two (2) series of tests. The first test yielded apparent thermal conductivity versus mean temperature data (Figure 38) obtained from thermocouple measurements of temperature versus distance in the sample (Figure 39). The second test was for the purpose of determining if the apparent thermal conductivity decreased after the sample had been evacuated. The magnitude of this reduction is shown in Figure 40. Apparently, Sta-Foam AA-602 is a relatively closed cell foam, and evacuation of the intercellular gas is difficult. After pumping on the sample for nine (9) days, the conductivity was decreased only 10%.

2.2.3.3 LBI (Load-Bearing Insulation) Tests

Tests were conducted on LBI insulation samples (Figure 41) and the performance of the insulations discussed in the following paragraphs. The total heat transported through the LBI series is compounded of three (3) heat transporting mechanisms.

(a) Heat carried by radiation
(b) Heat carried by solid conduction
(c) Heat carried by gas conduction

Gas conduction in an insulation on a liquid hydrogen container will probably be very small if the insulation is sealed airtight. The amount of surface area at 36°R exposed to the interstitial gas will be sufficient

FIGURE 38
APPARENT THERMAL CONDUCTIVITY
AS A FUNCTION OF MEAN TEMPERATURE
STA-FOAM AA-602 SAMPLE (1.0")

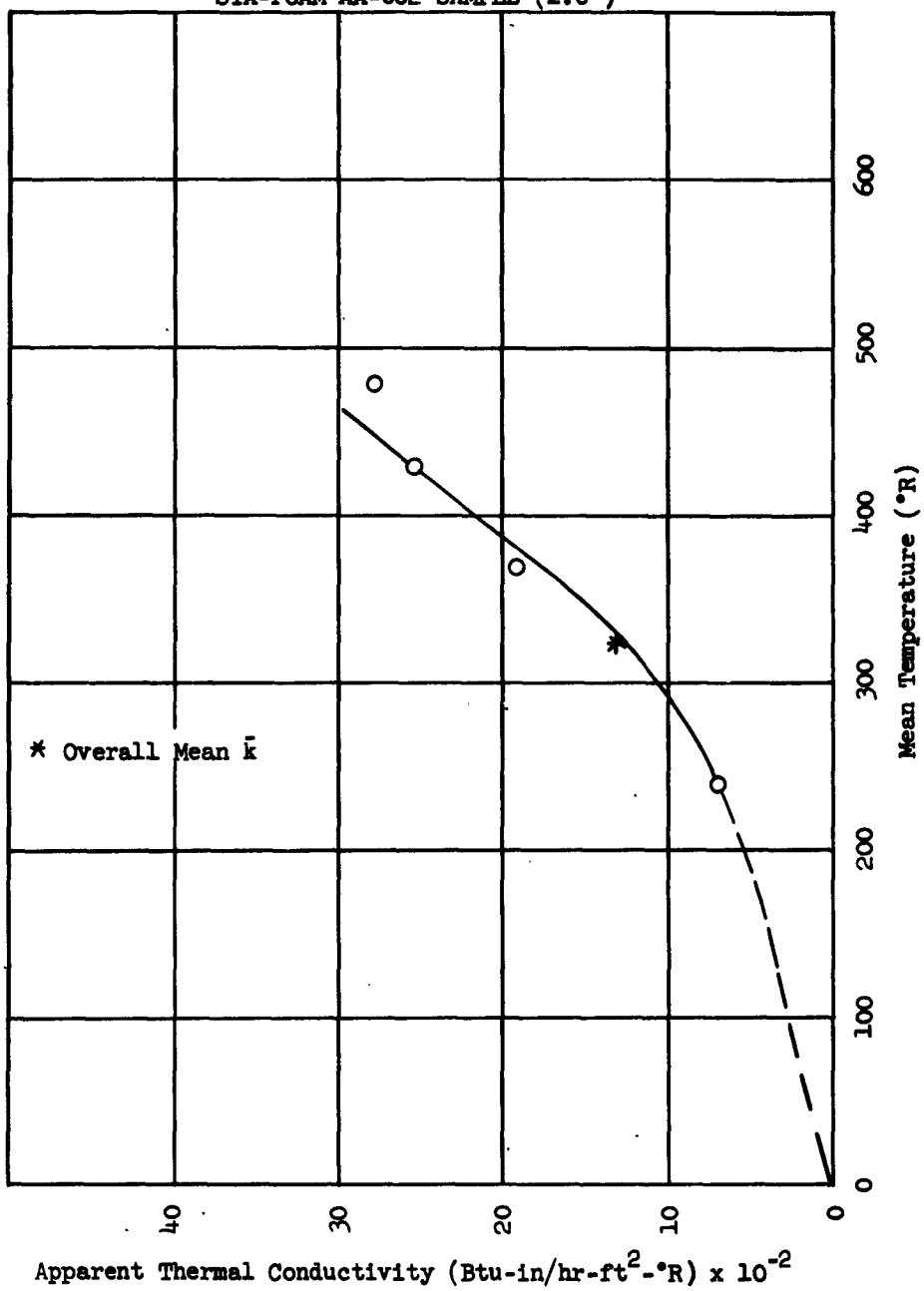

FIGURE 39
TEMPERATURE VERSUS DISTANCE
STA-FOAM AA-602 FOAM SAMPLE (1.0")

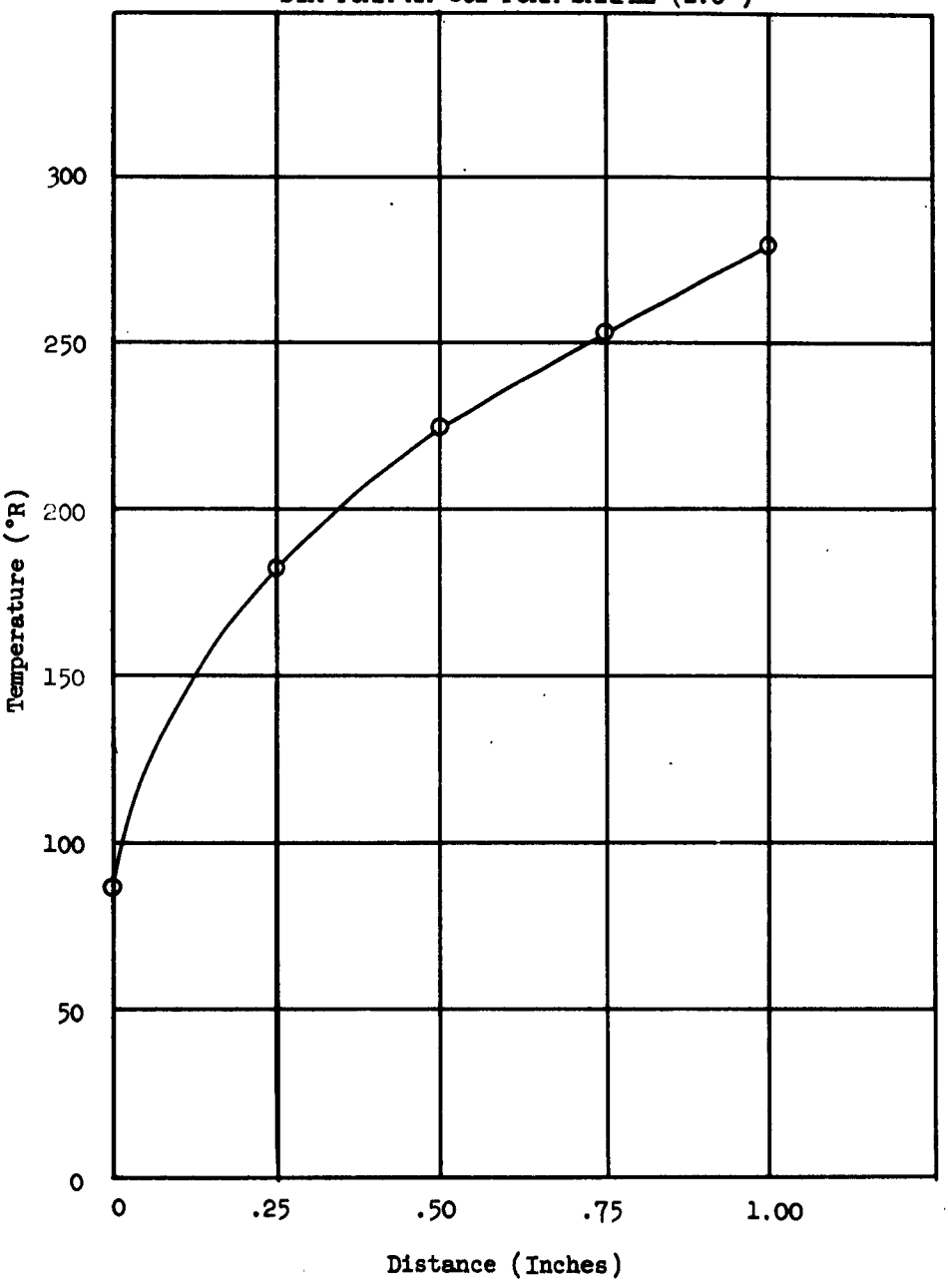

FIGURE 40
REDUCTION OF APPARENT THERMAL CONDUCTIVITY
AS A FUNCTION OF DAYS PUMPED (AA-602)

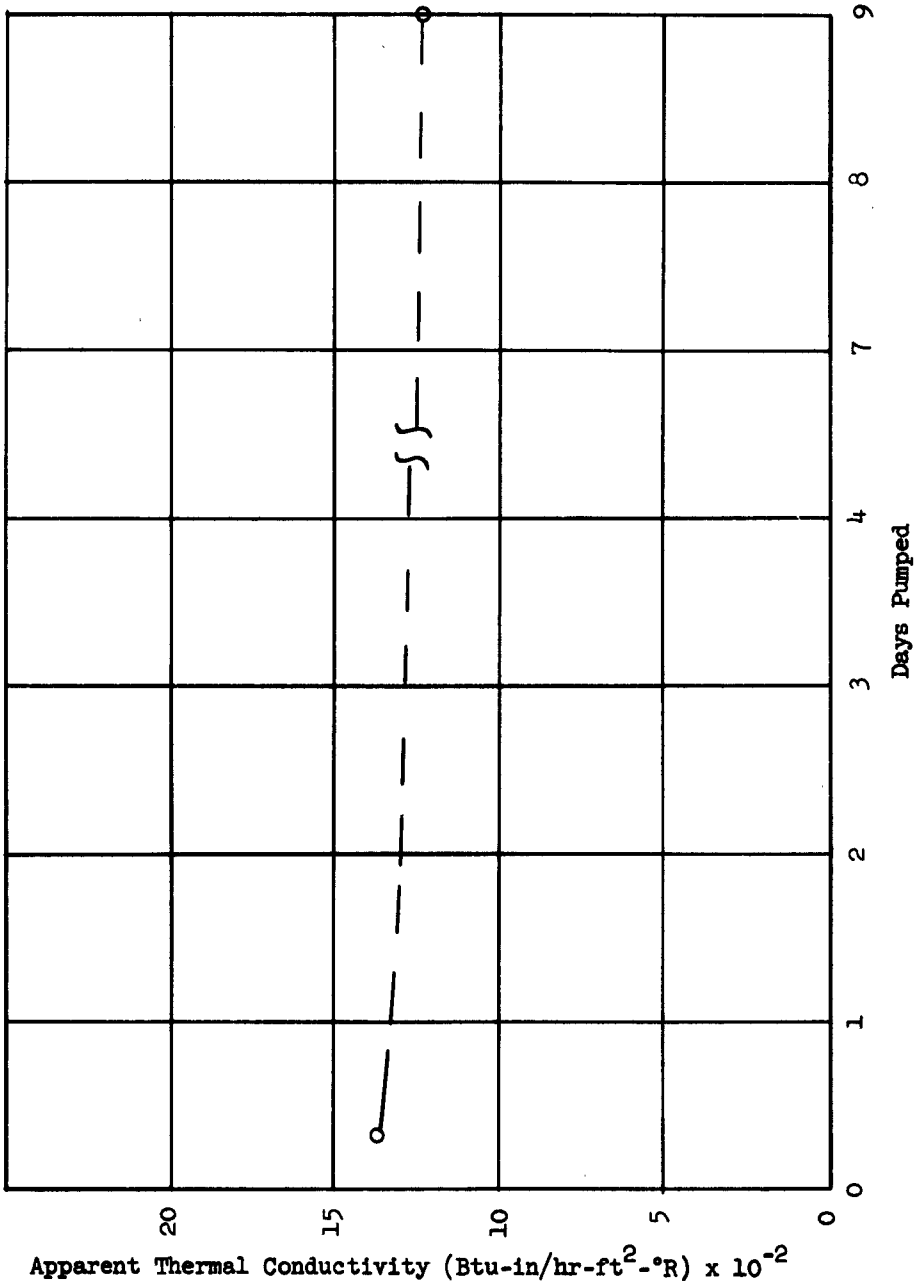

FIGURE 41
BEECHCRAFT LOAD-BEARING INSULATION

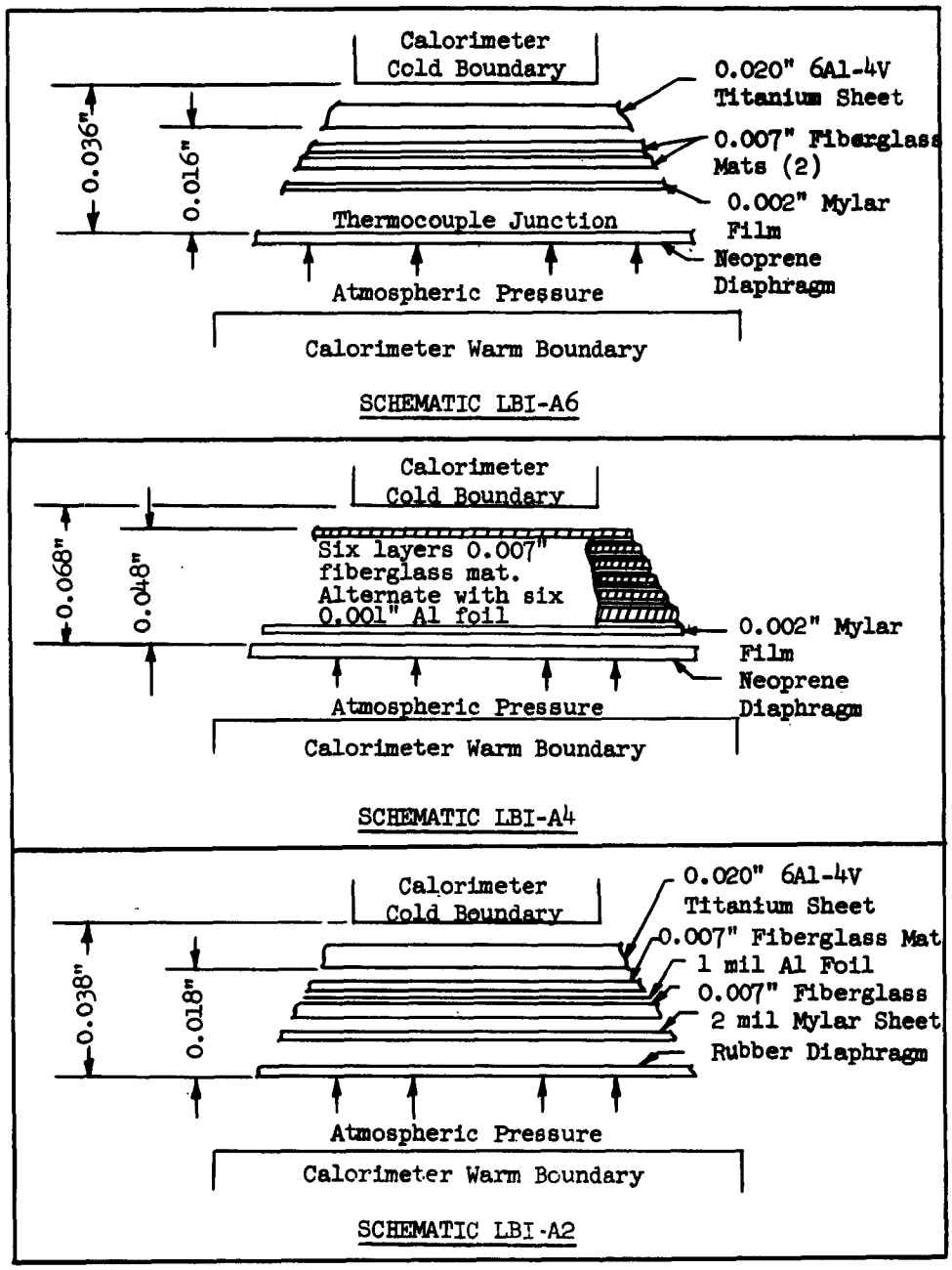

to "evacuate" the gas by condensation without any prior gas evacuation. A high vacuum, at least 10^{-6} mm Hg, can be realized by this condensation process thereby rendering the amount of heat carried by gas conduction negligible.

Heat carried by solid conduction can be reduced to a minimum by choosing a material with low thermal conductivity. The choice of material to "insulate" liquid hydrogen or rather to act as a warm boundary layer support should be based on the solid conduction coefficient. Glass fibers with the fibers oriented perpendicular to the heat flow were chosen because of their low inherent solid conductivity (References 14 and 15). Another reason for choosing glass fibers as the boundary separators was the transparency to long-wave radiation (Reference 16).

Radiation heat transfer is the final and largest heat-carrying component. By inserting the glass fibers between the warm and cold temperature boundaries, the low solid conduction term inherent to the glass is utilized and its transparency to long-wave radiation enables efficient reflection to occur at the cold surface. This combination of properties results in the low apparent thermal conductivity figures in Table 9.

The results obtained during the LBI insulation tests were different than the anticipated performance. The primary difficulty was a small leak in the calorimeter which opened up at low temperatures. The thermal conductivity for LBI-A6 shown in Table 9 was obtained for a comparatively short time interval. As the leak opened up, the thermal conductivity increased considerably. If any air condenses on the test surface, the amount of heat transferred to the test liquid increases radically. Considering the small insulation thickness, gas conduction across the space can also increase markedly. The apparent thermal conductivity quoted was obtained with an interstitial gas pressure below 1×10^{-4} mm Hg. The interstitial gas pressure increased to 5 to 6×10^{-4} mm Hg when the low temperature leak opened and resulted in higher thermal conductivities. For extremely thin insulations, such as the LBI series, the number of interstitial gas molecules and their mean free path becomes quite important to the gas conduction. The following analysis is made to describe their effect.

From Reference 17 an equation giving the mean free path is

$$L = 0.86 \times 10^{3} \frac{n}{p} \left(\frac{T}{M} \right)^{1/2}$$

where

L is the mean free path in cm

n is the viscosity of the gas in poises

P is the pressure in microns of mercury

T is the temperature in degrees kelvin

M is the molecular weight

The values assumed for purposes of estimation are:

$n = 0.000171$ poises

$M = 28$

$T = \frac{290 + 76}{2} = 183°K$

$P = 0.5$ microns (5×10^{-4} mm Hg)

then

$$L = 0.86 \times 10^{3} \left(\frac{0.000171}{0.5}\right) \left(\frac{183}{28}\right)^{1/2}$$

$L = 0.75$ cm $= 0.3$ in

From this calculation, the mean free path of the gas molecules is seen to be considerably larger than the distance between the hot and cold surfaces. In this case, the gas molecules move for the most part directly between the hot and cold walls without collisions with other gas molecules. The ability of gas in this situation to carry heat between the walls is proportional to the number of molecules present. Therefore, gas conduction is directly dependent upon gas pressure.

To observe the magnitude of this effect, Sample A-5 was tested in another similar calorimeter that was completely vacuum tight. The results of this test show a conductivity only 1/3 that previously tested for LBI-A6. While the boundary emissivities were different and the sample was not under a compressive load, the amount of reduction of heat leak is very indicative that gas conduction was significant in the LBI-A6 test. Furthermore, condensation of gases on the cold wall could have caused an increase in system emissivity which would increase the radiation component. Samples LBI-A2 and LBI-A4 were also influenced by this varying sample gas pressure.

The radiation sensitivity of the LBI series is an important quality. The transparency of the glass fibers used in this insulating scheme coupled with their low inherent solid conductivity causes the insulation system to be influenced primarily by radiation. Other experimenters (Reference 18, 19, and 20) have found radiation a major heat leak in evacuated insulations.

The total heat leak may be considered to consist of a solid conduction term, a gas conduction term, and a radiation term, or:

$$Q_T = Q_R + Q_G + Q_S$$

where

Q_T is the total heat

Q_R is the radiated heat

Q_G is the gas conducted heat

Q_S is the solid conducted heat

If the gas pressure is very low and the solid conduction very low, the total heat is nearly proportional to the radiation term, or:

$$Q_T \approx Q_R$$

Examination of the parameters affecting Q_R reveals the following relationship:

$$Q_R = \sigma \epsilon A (T_H^4 - T_C^4)$$

where

σ is Stefan-Boltzmann constant

ϵ is net system emissivity

A is shape factor

T_H and T_C refer to the hot and cold temperature boundaries, respectively

This equation is independent of distance or thickness, but the thermal conductivity is a function of thickness as proved experimentally and shown analytically below. Apparent thermal conductivity test results must be used only with their particular insulation thicknesses.

Tests on LBI-A2 and LBI-A4 indicate the validity of the above analysis. The LBI-A4 test sample was thicker than the LBI-A2 sample and its apparent thermal conductivity was greater. The reason being, if a given radiation component is the same in two instances, with the system emissivity and other parameters remaining constant and only the insulation thickness varied, the total heat leak across both systems will remain the same (ignoring the small solid conduction term for the present).

Placing these heat leaks into a Fourier equation results in a linear relationship between conductivity and insulation thickness. Algebraically,

$$Q_T = Q_R + Q_S$$

where

$$Q_S \approx 0$$

and

$$Q_R = \sigma \epsilon A (T_H^4 - T_C^4)$$

using

$$Q_T = \bar{k} A \frac{\Delta T}{\Delta X}$$

where

k is apparent thermal conductivity

Q_T is heat transferred

ΔT is temperature difference

ΔX is insulation thickness

All other notation is as previously described.

Therefore,

$$\bar{k} A \frac{\Delta T}{\Delta X} = \sigma \epsilon \bar{A} (T_H^4 - T_C^4)$$

Since all the other parameters were assumed constant and only ΔX varied, $\bar{K}$ is proportional to ΔX. The results of the tests on LBI-A2 and LBI-A4 support these assumptions.

To apply a relationship to a transparent insulating system, such as the LBI series, where the system emissivity is the controlling total heat leak factor, an effective system emissivity would be a far better choice than the Fourier relationship. The LBI series would then be described by Christiansen's formula, which is,

$$\epsilon_{net} = \frac{\epsilon_o \epsilon_i}{\epsilon_o + \epsilon_i (1 - \epsilon_o) \rho}$$

where

ϵ_{net} is the net system emissivity

ϵ_o is hot boundary emissivity

ϵ_i is cold boundary emissivity

ρ is ratio of cold surface area to warm surface

Applying this relationship to the radiation equation, the following is obtained.

$$Q_T = \sigma \epsilon_{net} A (T_H^4 - T_C^4)$$

In the above relationship, if an increase in temperature occurs on either wall, the resulting increase in the net system emissivity can cause the amount of heat flowing between boundaries to increase. When the Fourier equation is used, this phenomena causes an increase in apparent thermal conductivity. The former statement is obvious in the case of an increase in temperature of the hot wall, but also true for an increase in temperature of the cold wall. That is to say, that for a small temperature increase of the cold wall the inherent increase of the cold wall emissivity can increase the ϵ_{net}, and thus the heat transport, more than the decrease in heat transport caused by the smaller temperature difference between walls.

Because of the foregoing reasoning, the heat transferred between boundaries is a function of both the temperature difference and the emissivity of the system, and the emissivity is dependent upon the temperature levels.

Realizing the shortcomings involved when a radiation sensitive insulation's thermal performance is described by an apparent thermal conductivity, the use of the Fourier relationship is acceptable only if it is used with a given thickness.

2.3 Application of Insulation

The mechanical properties of an insulation and the method by which it lends itself to application on the tank wall are essential considerations in the choice of insulation material. For a given tank configuration, the contraction and expansion can be calculated. Mechanical application of the insulation may be the only alternative if the tank material, wall thickness, wall length, and environmental conditions are such that large dimensional changes occur. On the other hand, if the tank has good dimensional stability, the insulation could be bonded to the tank wall with adhesives.

As a molded solid, Min-K 1301 is particularly adapted to adhesive bonding but could be attached by mechanical means. Min-K 504 has little or no mechanical strength and does not lend itself to either method but finds utility as a filling material for honeycomb structures.

Foams come in a variety of forms and can be attached by either mechanical methods or adhesives.

Insulation applications using bonding techniques must use an adhesive and insulation that can withstand the dimensional changes occasioned by large temperature changes and changing internal tank pressure. It has been determined that a maximum circumferential elongation of less than 1% takes place on the proposed test tank during typical heat tower test run. The differential expansion between metal and insulation is slight. The subject of low temperature adhesive bonding is treated in some detail by McClintock and Hiza (Reference 21), and McClintock and Van Gundy (Reference 10).

Laboratory tests determined a proper adhesive for use in bonding Min-K to metal. Armstrong's A-4 Epoxy Resin is suitable. The adhered samples were dunked in liquid nitrogen to determine if differential expansion rates would cause adhesive failure. The tests were negative from which this adhesive was deemed suitable for use. Section 2.2.1.2.3 of FTRDI MR 60-2 details the application of Min-K 504 to the 7,000-gallon stainless steel test tank.

Two prime possibilities are evident when considering Min-K 504 and 1301 as mechanically attached insulations: (1) Min-K 504 filled phenolic honeycomb, and (2) asbestos filled phenolic plastic facing bonded to Min-K 1301. The first insulation utilizes a large cell phenolic honeycomb structure filled with Min-K 504 and faced on both sides with a thin asbestos-filled phenolic sheet (Figure 42). This material can be performed in 90° segments to fit a given tank radius. This combination provides a material with a density of approximately 16 lb/ft^3 and a "k" factor of .16 BTU-in/hr-ft^2-°R, both of which are superior to Min-K 1301. The phenolic facing also eliminates the problem of surface sealing which is necessary to prevent cryogenic pumping through a porous material.

The second insulation possibility utilizes the product Min-Klad which incorporates a layer of Min-K 1301 bonded to a thin asbestos filled phenolic sheet. This material can be either bonded or mechanically attached to the tank. Specific values of density and thermal conductivity will depend on the thickness of the phenolic sheet and the Min-K 1301; however, they will be higher than an equivalent thickness of the honeycomb filled with Min-K 504.

While these materials continue to show increased promise for cryogenic tank application, they cannot be considered as the optimum insulation material, since only preliminary computer analysis has been completed.

2.3.1 Methods of Adhesive Insulation Application

Two (2) methods of adhesive bonding are under consideration and are illustrated in Figures 43 and 44. Figure 43 shows the preformed Min-K or honeycomb structure bonded to the tank over its entire surface. This method assumes that the extremes of dimensional change can be withstood by the adhesive bond and the insulation material. The need for joint and end sealing of the segments is largely eliminated by this method.

Figure 44 shows an adhesive bonding method which would allow the insulation to "work" with the tank through the overlapping joints of the segments. This concept requires some method of flexible sealing along the joints and ends of the segments in order to prevent air condensation between the insulation and the tank wall.

2.3.2 Methods of Mechanical Insulation Application

Any method of mechanical attachment must allow the insulation to move in conjunction with tank expansion and contraction. Several methods of mechanical attachment were studied and one of these is depicted in Figure 45. This method would attach a filled honeycomb structure to the tank wall by means of short metal studs. The studs would be spaced down the center of each 90° segment and would protrude only through the inner face of the honeycomb where a locking nut would be applied. The segment joints would be overlapped and sealed.

FIGURE 42
MIN-K FILLED HONEYCOMB

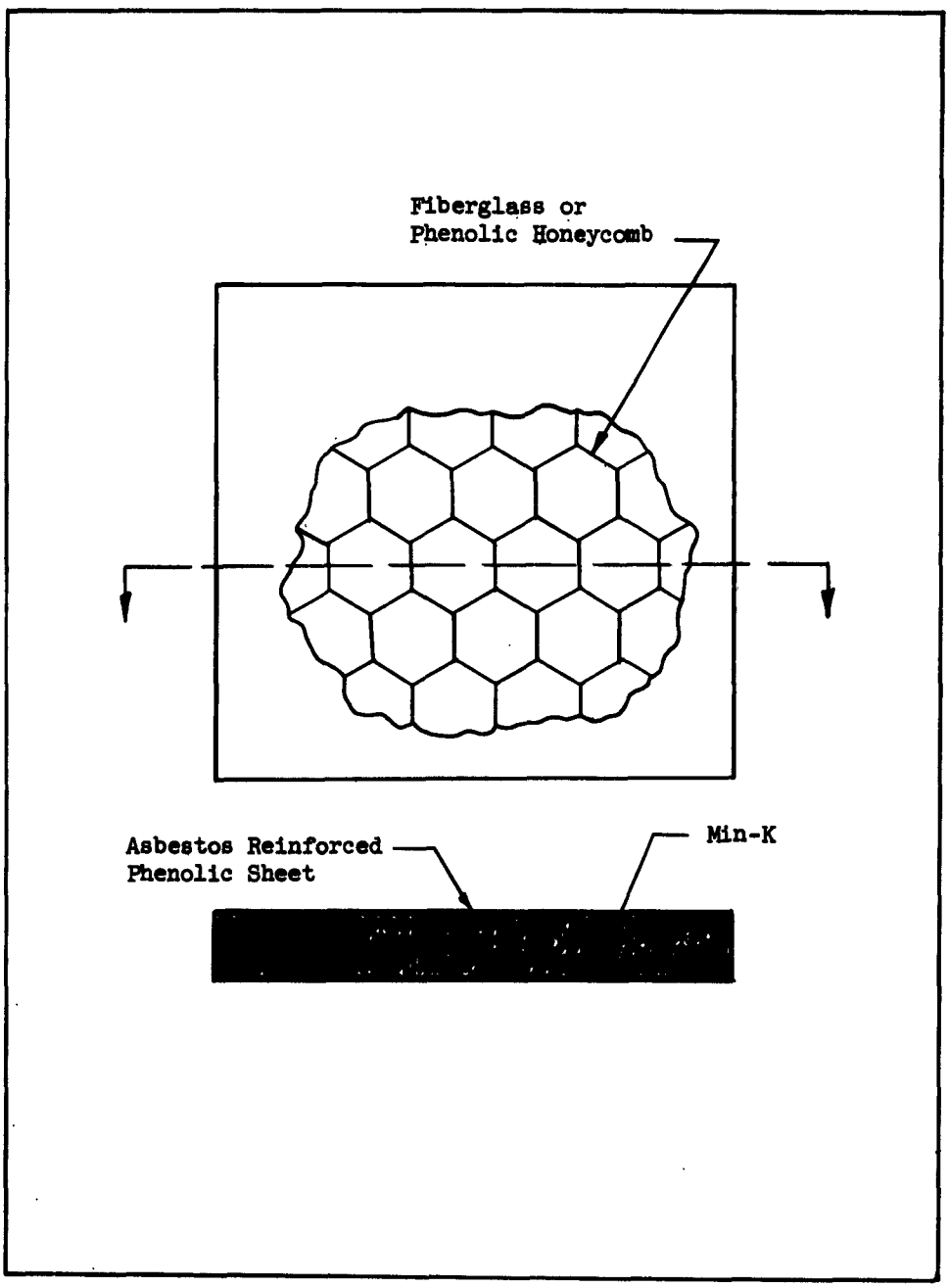

FIGURE 43
ADHESIVE BONDING OF MIN-K INSULATION
(ENTIRE SURFACE BONDED)

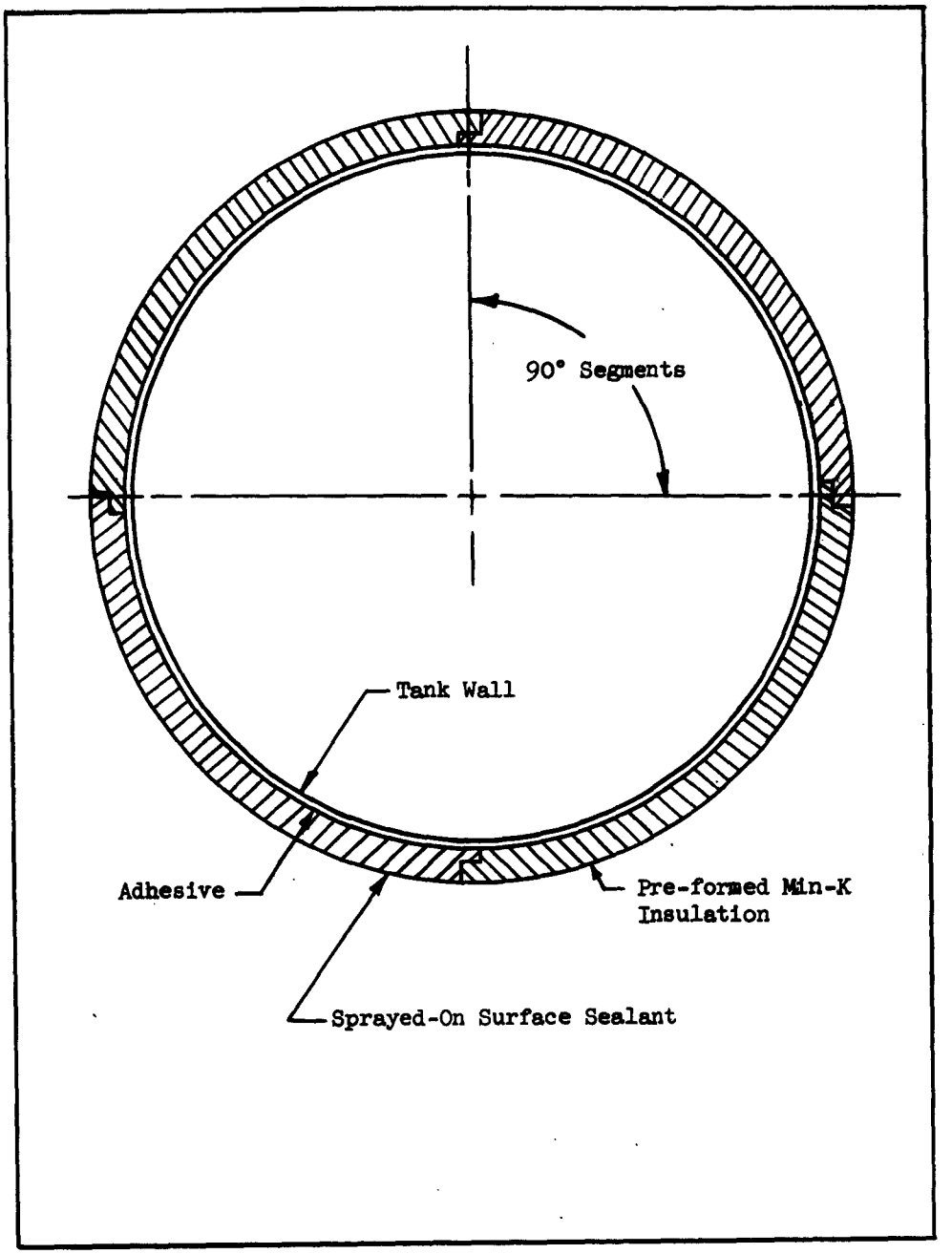

FIGURE 44
ADHESIVE BONDING OF MIN-K INSULATION
(STRIP BONDED)

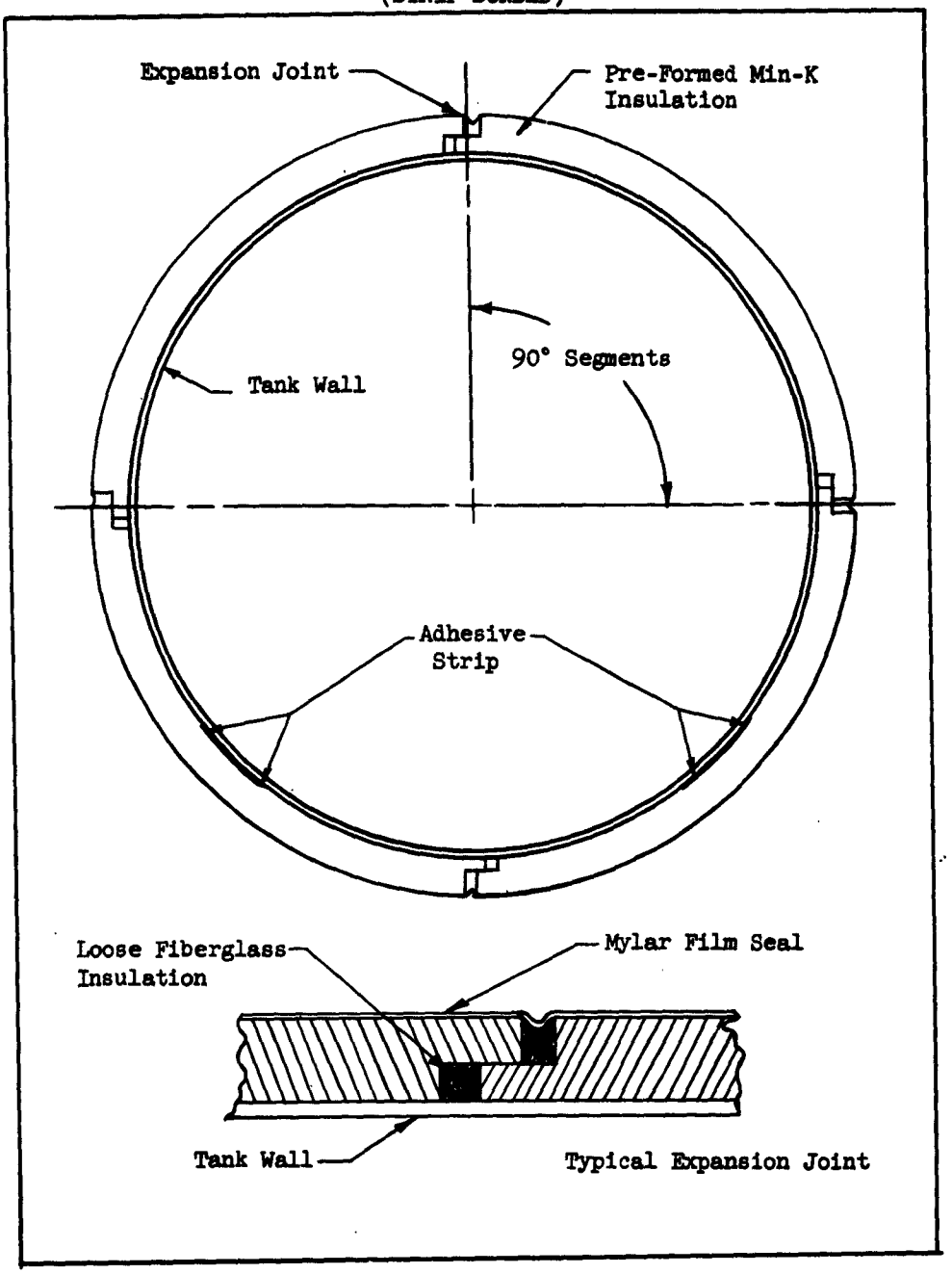

FIGURE 45
MECHANICAL ATTACHMENT OF
MIN-K HONEYCOMB INSULATION

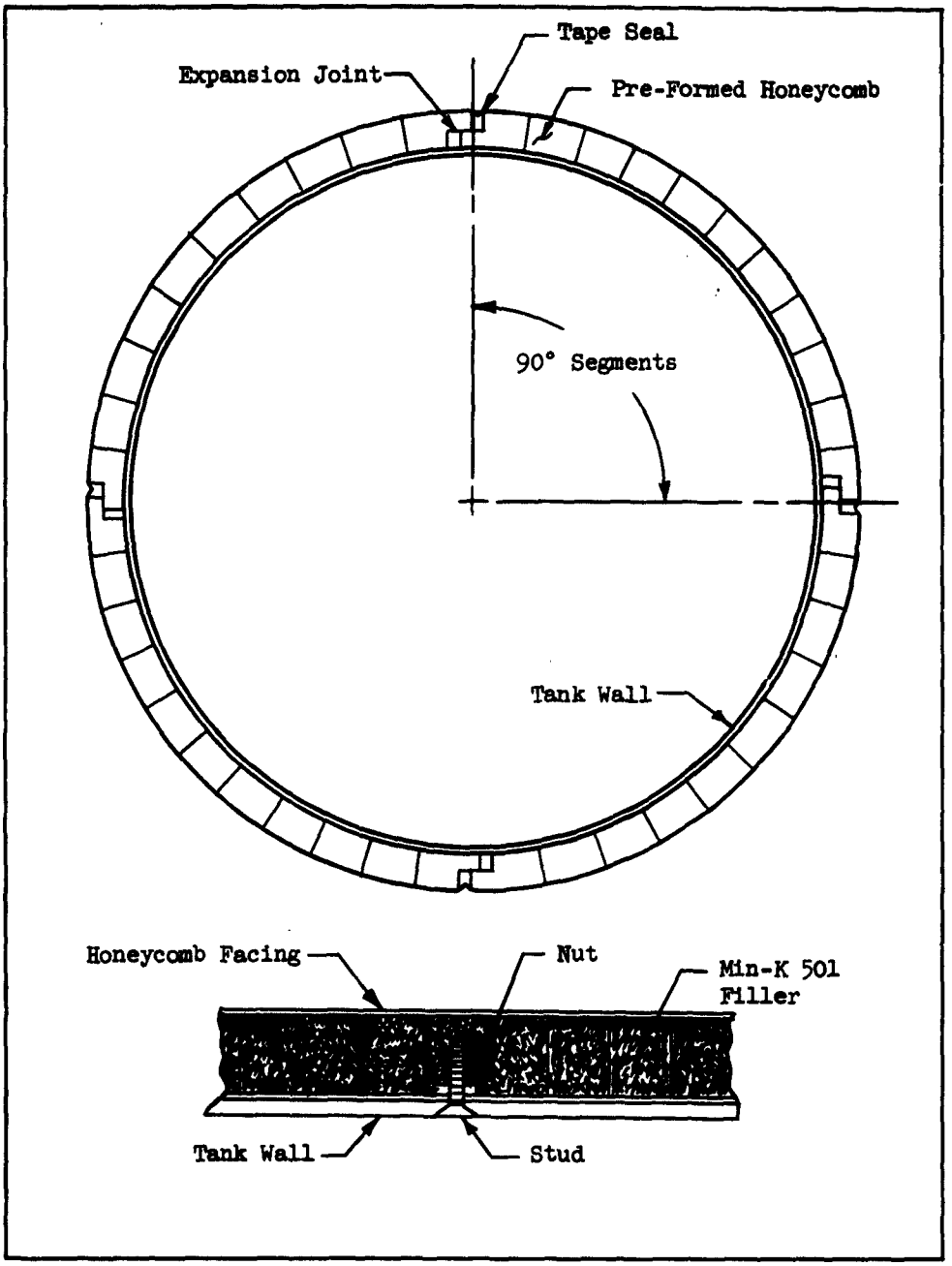

3.0 ENCAPSULATION MATERIALS

3.1 Selection of Encapsulation Materials

An optimum encapsulation material should be thin, lightweight, and of low porosity capable of withstanding high surface temperatures.

The use of high thermal efficiency insulations produces exterior surface temperatures that would exceed the temperature limits of Mylar and some other organic materials. Therefore, other methods and materials were considered such as silicone rubber and plastic laminates.

With the use of metal encapsulations such as stainless steel, the expected temperatures will be below material operating limits. The stainless steel encapsulation also provides a weldable material thereby ensuring a positive seal for evacuation purposes. This type of encapsulation could be provided with corrugations or beads to allow the tank structure to expand or contract from pressure and temperature changes. Other beneficial effects from the metal encapsulations include protection from meteorite penetration, cosmic radiation (radiation having a pronounced detrimental effect on plastics, elastomers and organic materials), and a probable lessening of the acoustic fatigue problem. In regard to the latter, the metal encapsulation in conjunction with the tank sidewall insulation would serve as "panel damping" of the acoustical vibration from high-sound pressure levels generated by large rocket engines and, thus, would protect primary tank structure.

3.1.1 Encapsulation Concepts

Several encapsulation concepts were studied for the 7000-gallon tank designed for the Flight Simulation Test Program. A preliminary study revealed that the use of a thin silicone rubber sheeting formed and vulcanized into an undersized cylinder which could be stretched over the tank sidewall would have temperature capabilities of 500-600°F. Another method studied was the use of thin strips of glass reinforced plastic that would be spiral wrapped around the tank in a manner such that each wrap lapped over the previous wrap by approximately one-half the width of the strip. The strip would be bonded at the overlap with a high-temperature adhesive. This system would have a temperature range of about 600-700°F. Another method was to use aluminum foil strips spiral wrapped around the tank and bonded to itself where it overlapped on each turn.

It was expected that the optimum thickness of the initial insulations encountered in the insulation study would not produce surface temperatures that would require a metallic encapsulating sheath or require the high-temperature materials mentioned above. Therefore, a Mylar film encapsulation was given major consideration.

3.2 Mylar Encapsulation

The first choice for an encapsulation material for the 7000-gallon test tank was Mylar. This material when heated to approximately 350°F shrinks a considerable amount. Calculations were performed to determine the ideal shrinkage so that the fabricated cylindrical bag of Mylar could be made the correct oversize. This cylinder was then to be shrunk fit on top of the Min-K insulation. Later test results of the cylinder shrink tests appear in Section 3.2.2.

The proposed method of shrinking the Mylar encapsulation on the test tank was as follows: The Mylar cylinder was fabricated two percent oversize in diameter and four feet in length. Extra size allowance in length was used to attach a hoop-type weight on the lower end so the cover could be placed in tension while heat shrinking. When shrinking was completed, the ends of the shrunk Mylar cylinder would then be trimmed and bonded to the tank sealing anvils.

Difficulties were experienced with shrink tests of the Mylar cover, so this material was abandoned as an encapsulation for the 7,000-gallon test tank. Temperature control and non-uniform shrinkage were the difficulties encountered.

3.2.1 Mylar Encapsulation Laboratory Tests

A shrink test of a sample of Mylar material was performed to confirm available manufacturer's data concerning the bag. A rectangular section of 0.002-inch Mylar, 17-7/8 inches by 20-15/16 inches, was measured and marked as shown in Figure 46. This sample was subjected to 350°F temperature in an oven, and the sample shrank to the dimensions shown in Figure 46. The lengthwise shrinkage was 3% and 3.5% long and short, respectively. These results agreed reasonably well with the manufacturer's shrinkage vs. temperature data.

To obtain a suitable method for shrinking the large test tank encapsulating bag, the test described below was made with the idea of using infrared bulbs to apply the heat. The experimental device is shown in Figure 47. Careful temperature control was obtained by continuously reading the thermocouples and adjusting the height of the infrared bulb mounting board. The Mylar sample was painted with Super-flake conductive coating, scribed with measured grid lines, and taped to the mounting box to assure a constant distance to the heating bulbs. Results from the tests were erratic as the conductive coating was incapable of diffusing the heat from the infrared bulbs. Spots opposite the bulbs were puckered from shrinkage making overall shrinkage measurements unrealistic. From these laboratory tests, it was concluded that a more uniform method of heat application was necessary.

FIGURE 46
LABORATORY TEST
(MYLAR SHRINKAGE)

Mylar heated at 350°F, one (1) hour

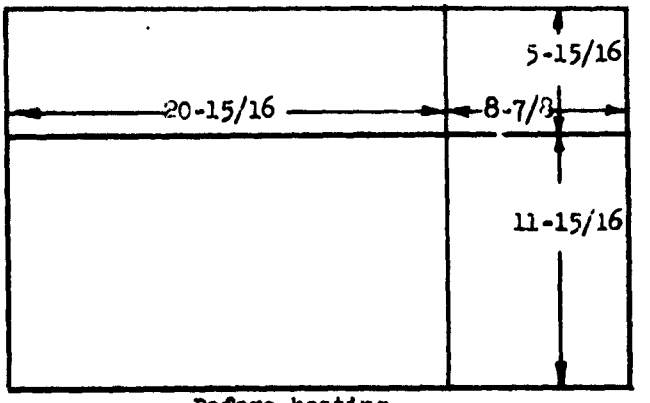

Before heating

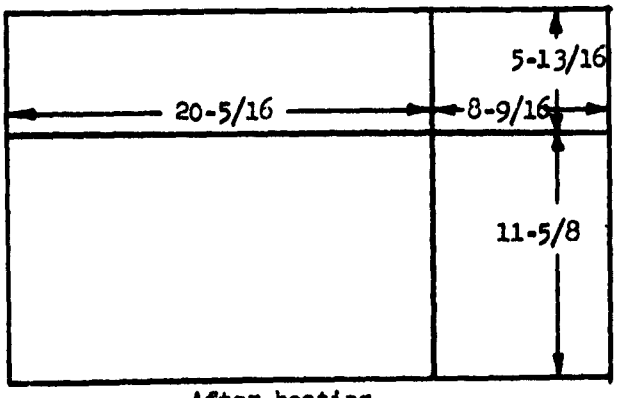

After heating

Scale: 1-1/2" = 1'

FIGURE 47
MYLAR SHRINK TEST APPARATUS

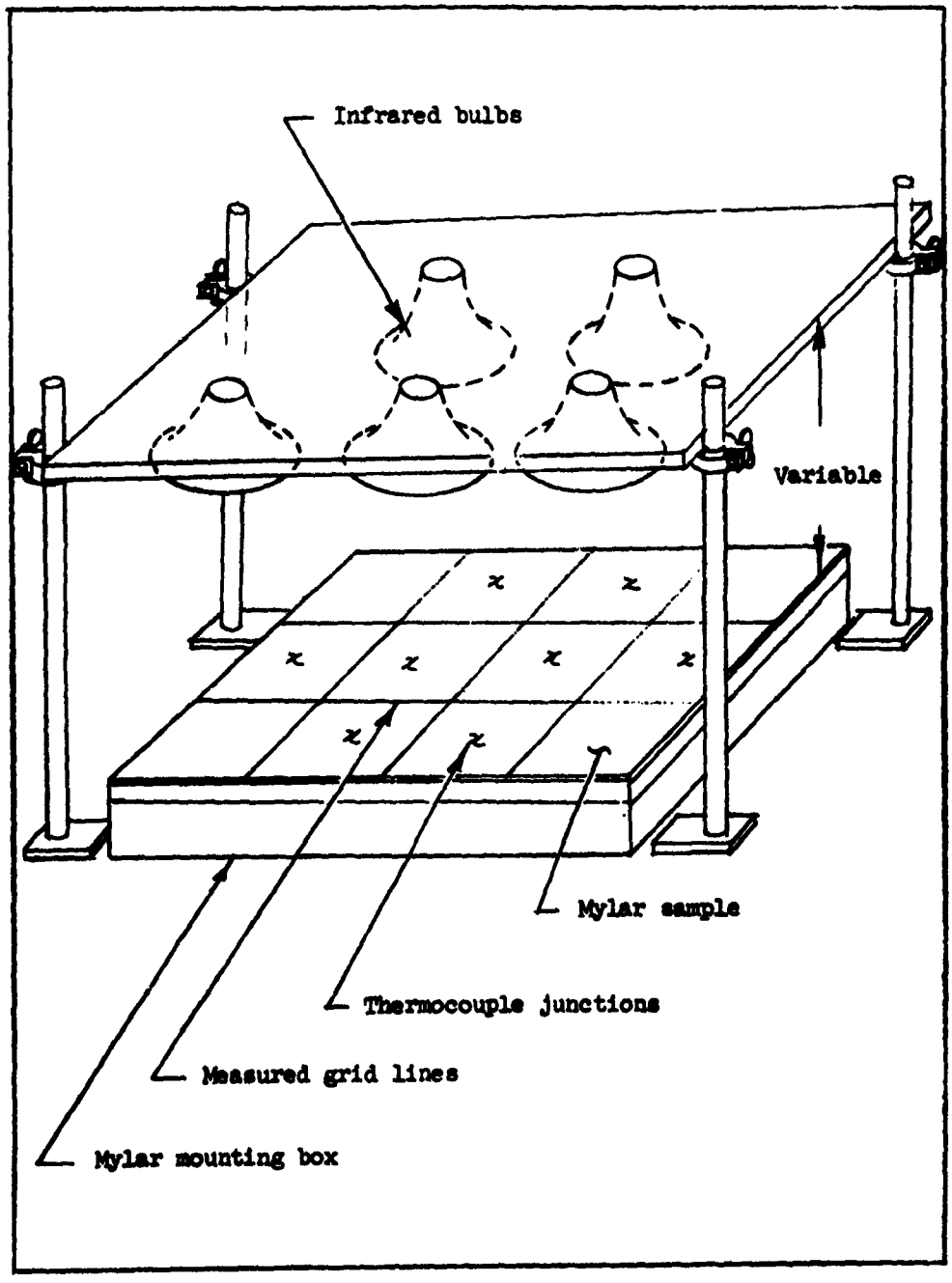

3.2.2 Heat Tower Tests on Mylar Bag

Sample sections of the Mylar bag were mounted on the stainless steel practice cylinder for testing in the heat tower. It was felt this would give the uniform heat necessary to shrink the Mylar.

One large Mylar bag was cut into short cylinders for the tests. First, an unpainted cylindrical sample four feet high was taped to the stainless steel practice cylinder and placed adjacent to the upper four heat zones of the heat tower. Heat was programmed into these four zones by manual control of the heat-rate controllers. The upper dome of the vacuum bell was left off.

Temperature readings up to 400°F from the thermocouples on the stainless steel test cylinder were necessary to cause shrinkage. The Mylar temperature probably lagged because of the transparency of the Mylar. Overall results indicated that the heating of the Mylar was not uniform because of uneven shrinking.

For the next test, another four-foot-high cylinder of Mylar was used. The Mylar was painted with Super-flake conductive coating, and the control thermocouples were fastened to the outer side of the Mylar bag directly exposed to the heating lamps. Five banks of heating lamps were used. The heat-rate controllers were programmed with prepared graphs. The program called for gradually increasing the temperature up to 200°F. The temperature was held constant at this point for the remainder of the ten-minute program. During this test, Zone 3 had a malfunction and flashed brightly for one to two seconds. This completely vaporized the Mylar opposite Zone 3.

Similar programs were run with peak temperatures of 250°F, 275°F, and 300°F. Shrinkage results of these tests are shown in Table 10. A graph of shrink vs. temperature was drawn to compare with the manufacturer's data (Figure 48).

For the final test, the remainder of the Mylar bag was used. The stainless steel test tank was supported one foot above its normal position in the heat tower. The Mylar bag upper end was taped to the stainless steel cylinder opposite Zone 8. A steel hoop was attached to the bottom end of the Mylar bag placing the Mylar in tension. The control thermocouples were mounted on the outside of the Mylar. Heat-rate controller programs were drawn gradually increasing the temperature to 350°F. The temperature was maintained constant for 10-minute intervals starting at 200°F and at each added 25°F increment.

When the temperature reached 310°F, the tensioning hoop ring dropped onto the bottom tank rest. The test was discontinued temporarily to inspect the upper tape bond. Satisfied that the tape had not released, heat was

TABLE 10
MYLAR CYLINDER SHRINK TEST (THERMAL FACILITY)

Program No.	Program Duration (min)	Maximum Temperature	Circumference (in)	Shrinkage from Original (in)	Shrinkage from Original (%)
0		Ambient	296		
1	10	200°F	296	0	0
2	10	250°F	292	4	1.4%
3	10	275°F	289-1/2	6-1/2	2.2%
4	10	300°F	289	7	2.3%

FIGURE 48
RESULTS OF THERMAL FACILITY MYLAR SHRINK TESTS

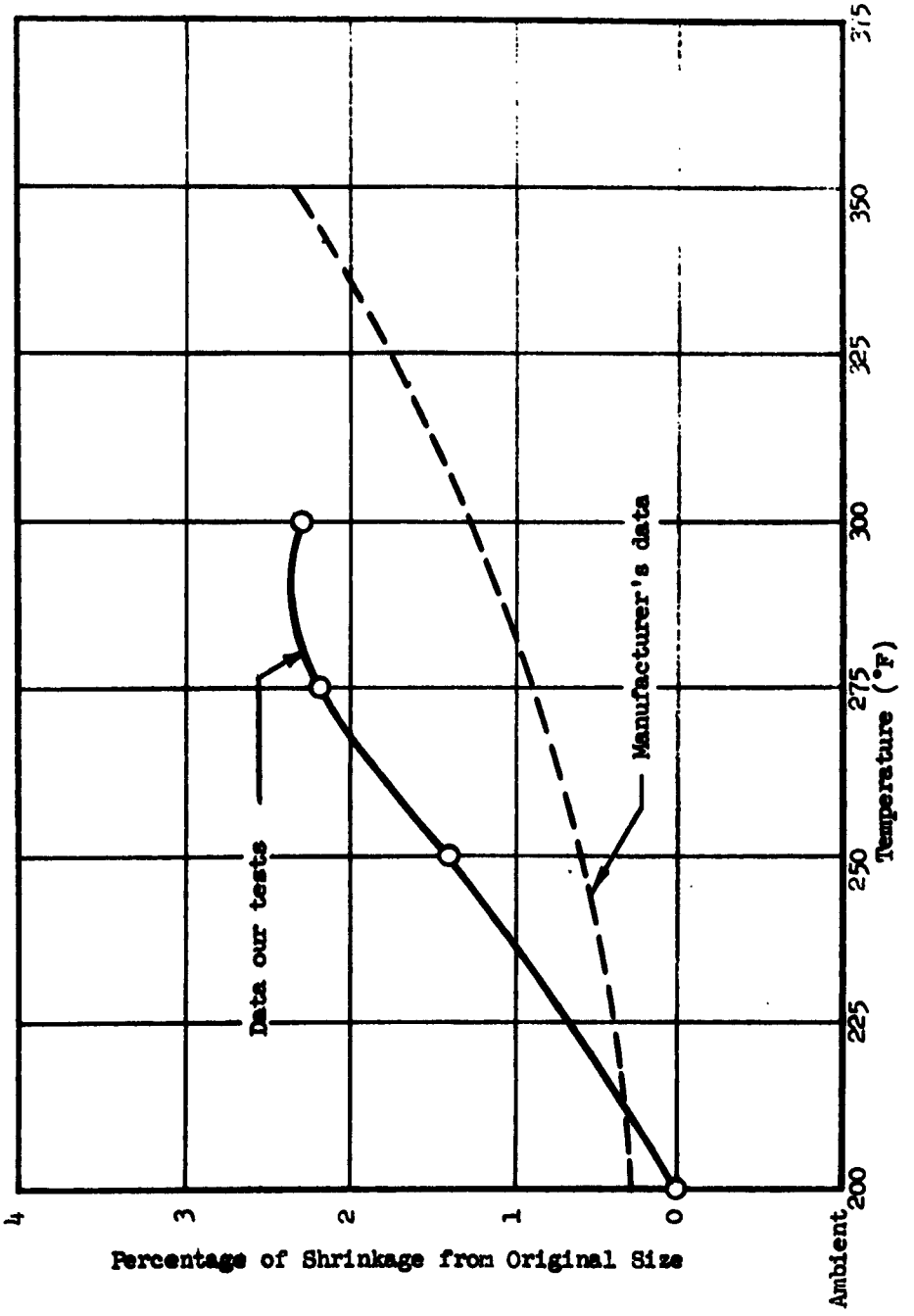

again programmed in. The Mylar and paint started to smoke, indicating excessive Mylar temperatures before attaining 300°F indication on the control thermocouples. The test was discontinued, and the sample was removed for inspection.

Inspection from all the heat tower tests indicated the Mylar was exposed to uneven heating and excessive temperatures. Because of this, uneven shrinkage and some heat damage was encountered on all the test samples.

The difficulties encountered with Mylar as an encapsulating material resulted in abandoning it for an encapsulation material for the 7,000 gallon test tank.

3.3 Silicone Rubber Impregnated Fiberglas Encapsulation

The encapsulation sheath that was actually used to enclose the Min-K 504 insulation of the 7,000 gallon test tank was silicone rubber impregnated fiberglas and aluminum foil. This encapsulation consisted of an aluminum foil layer of 2-mil thickness layed on top of the Min-K followed by two layers of fiberglas wrapping alternated with sprayed-on silicone rubber for a total thickness of .030 inches.

In order to predict the behavior of the silicone rubber encapsulation with changes in tank pressure and temperature, an elastic analysis was performed for the encapsulation subject to the environment of the 7,000 gallon test tank. Preliminary tests indicated that the coefficient of thermal expansion (contraction) of the encapsulating material was considerably higher than the metal tank wall. Therefore, the analysis was made to determine the encapsulation temperature and tank pressure that produces meridional tension stresses in the encapsulation equal to the allowable tensile stress.

Equations were derived for finding the minimum allowable encapsulating temperature, the limit tensile circumferential load in the encapsulating material, and the limit shear load at the sealing anvil. These equations were programmed into the Bendix G-15 digital computer along with a program to read out the margins of safety against shear at the anvil, tensile failure at the anvil, and tensile failure around the tank circumference. Several assumptions were made regarding the derived equations so the calculations could proceed. They are as follows:

(1) Compressibility of the Min-K insulation does not vary significantly within the low-temperature range.

(2) The modulus of elasticity of the encapsulating material is directly proportional to the ultimate stress with varying temperature.

(3) The average coefficient of thermal contraction of the encapsulating material from +80°F to -320°F (liquid-nitrogen temperature) is applicable for the range +89°F to -424°F (liquid-hydrogen temperature).

(4) Ultimate stress and critical stress vary linearly with temperature.

(5) Sliding friction is negligible.

Tests of the encapsulating material were conducted to determine the modulus of elasticity and thermal coefficient of expansion at room and liquid nitrogen temperatures. Also, compression tests were conducted to determine whether the Min-K 504 insulation would compress and relieve some of the stress in the encapsulating material. Compression of the insulation was found to be negligible, and little or no stress relief can be expected.

The results of this analysis produced the following values:

(1) Minimum allowable encapsulating temperatures = -215°F

(2) Limit tensile circumferencial load = 70.6 lb

(3) Limit shear load at the sealing anvil = 20.0 lb

(4) Pressure exerted on tank wall by encapsulation = 1.5 psi

(5) Margin of safety of shear at the sealing anvil = 0

(6) Margin of safety in meridional direction = +5%

(7) Margin of safety in circumferencial direction = +6%

The conclusions that can be drawn from the results are:

(1) The encapsulation material will fail (rupture) if the temperature is allowed to go below -215°F.

(2) This imposes an operation limitation on the test tank such that it cannot be allowed to set very long with liquid hydrogen with the vacuum bell evacuated or the encapsulation will become too cold.

(3) The vacuum bell should not be evacuated when filling with liquid hydrogen because this will decrease the allowable hold time before the encapsulation will become too cold.

3.4 Bonded Aluminum Foil Encapsulation

The second encapsulation covering that actually was tested on the 7,000 gallon test tank involved the use of one mil aluminum foil. This concept specified for the tank to be wrapped with three (3) layers of aluminum foil in a spiral manner. Each wrap would overlap the previous wrap approximately 50% of its area and be bonded together by a film of silicone rubber to form a vacuum tight sheath.

Calculations were performed to check the stresses in the cover as it cooled down and contracted. From this investigation, the amount of slack to be built into the cover was determined. Some assumptions had to be made since complete information was not available that applied to the actual conditions to be imposed on the cover. However, it appeared the cover would stand the stress levels imposed upon it if our assumptions proved to be reasonably accurate.

The cover was tested for vacuum tightness and was deemed capable of protecting the insulation and tank wall from the liquefying of air.

Several thermal tests were performed on this encapsulating concept with the tank full of liquid hydrogen. After several fill and drains were performed, the cover failed by splitting open from top to bottom. Apparently, the built-up layers of silicone rubber had contracted considerably more than data indicated and had overstressed the aluminum foil causing it to fail.

Since the thermal tests to be conducted on the tank itself and its insulation specified a highly reflective cover, a single wrap of aluminum foil was installed with the seams sealed by aluminum pressure sensitive tape. However, the cover was not intended to be evacuated but only to provide a reflective cover so tests on the tank itself could continue.

Beech Aircraft Corporation

SPECIFICATION

SPECIFICATION FOR TESTING WELDED
THIN-SHEET TITANIUM ALLOY AT EXTREME
TEMPERATURE (-423°F to 1000°F)

BEECH AIRCRAFT SPECIFICATION - 6157

APPENDIX I

ISSUED 4 November 1958

REVISED 3 November 1959

James E. Bell
Lead Engineer
Boulder Division

C. W. Spieth
Group Engineer
Boulder Division

E-78A

Beech Aircraft Corporation

SPECIFICATION BS 6157

PAGE 1 OF 15

TITLE Specification for Testing Welded Thin-Sheet Titanium Alloy at Extreme Temperature (-423°F to 1000°F) ISSUED

WRITTEN BY J. E. Bell REVISED

1.0 SCOPE

This specification is submitted to Titanium Metals Corporation of America in conjunction with testing of a thin-sheet titanium alloy at various temperature conditions. It is intended that Beech Aircraft Corporation and Titanium Metals Corporation of America will jointly pefform the specifications as outlined under Section 3.0 requirements.

2.0 INTRODUCTION

Beech Aircraft Corporation is presently conducting a material evaluation program for anticipated use with large thin-gage pressure vessels. Preliminary investigations indicate that titanium alloys provide many good characteristics which are particularly favorable for the pressure vessel design program.

The purpose of this specification is to outline specific tests which must be performed prior to an actual design program. The following factors are considered as a basis for the test specification.

1) Available manufacturers' data is not considered applicable to welded thin-skin techniques.

2) Available manufacturers' data does not include extreme temperature properties of welded material.

Since the Beech application is concerned with extreme temperature conditions (-423°F to 1000°F), it becomes evident that sample materials under simulated conditions must be tested prior to actual fabrication.

The outlined tests listed in this specification will be utilized as basic data with which Beech can launch a preliminary design program. The test data will not be construed to mean it can be published as qualified design data; but, rather, a specific condition that must be verified for Beech.

TITLE Specification for Testing Welded Thin-Sheet Titanium Alloy at Extreme Temperature (-423°F to 1000°F) ISSUED

WRITTEN BY J. E. Bell REVISED

3.0 REQUIREMENTS

It is anticipated that a minimum of 72 test specimens as illustrated in Figures 1 and 3 will be utilized during the test program. Titanium alloy Ti-6Al-4V in the annealed condition will be furnished to Beech whereby proficient welding techniques will be determined for the thin-sheet application. Upon completion of this phase, a portion of the welded sheet specimens will be returned to TIMET for sizing and tensile testing as outlined in Section 3.1.1.

Prior to shipment to TIMET, the tensile specimens shall be X-ray inspected and leak checked whereby the welding shall be considered acceptable. This inspection, in addition to bend testing, impact testing and specified tensile testing as outlined in Sections 3.1.1, 3.1.2 and 3.1.3, will be performed by Beech Aircraft Corporation.

3.1 Test Program

Test specimens of annealed Ti-6Al-4V sheet will conform to ASTM, ASME or testing facility standards. Tests to be performed are tensile, bend and impact as outlined below.

3.1.1 Tensile Tests

Test specimens will be cut from a welded sheet of annealed Ti-6Al-4V at an angle with the weld as specified in Figure 1. This will allow tensile tests with three weld directions: longitudinal, transverse and 45° angle.

3.1.1.1 Tensile Tests Required

Tensile Tests A, B and C are considered essential as preliminary design data and should be completed at an early date. Tensile Tests D, E and F will supplement the previous tests for additional design data. Tensile

TITLE Specification for Testing Welded Thin-Sheet Titanium Alloy at Extreme Temperature (-423°F to 1000°F)

ISSUED

WRITTEN BY J. E. Bell

REVISED

FIGURE 1
TENSILE AND BEND TEST SPECIMEN LAYOUT

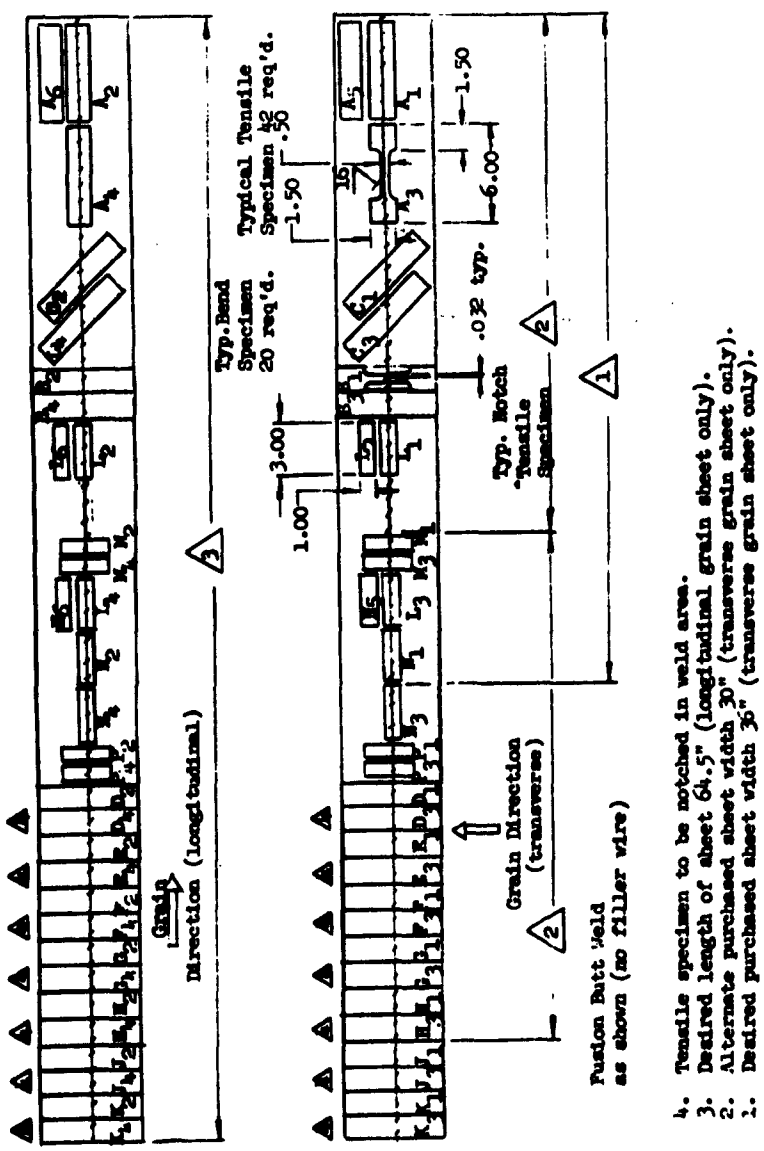

tests G, H, J and K will be performed for future required data which covers the complete temperature range of the Beech application.

Test A - Four (4) longitudinal welded specimens and two (2) nonwelded specimens of .016"-thickness Ti-6Al-4V annealed sheet shall be tested at 1000°F temperature. Parent metal grain direction shall be tested as shown in Figure 1, Specimens A_1 through A_6.

Test B - Four (4) transverse welded specimens of .016"-thickness Ti-6Al-4V annealed sheet shall be tested at 1000°F temperature. Two (2) of the welded specimens (B_3 and B_4) shall be notched .032 inch on each edge of the weld area. This modification is to assure the weld will fracture, thus providing tensile and ductility data on the weld proper. Parent metal grain direction shall be tested as shown in Figure 1, Specimens B_1, B_2, B_3 and B_4.

Test C - Four (4) 45° angle welded specimens of .016"-thickness Ti-6Al-4V annealed sheet shall be tested at 1000°F temperature. Parent metal grain direction shall be tested as shown in Figure 1, Specimens C_1, C_2, C_3 and C_4.

Test D - Four (4) transverse welded specimens of .016"-thickness Ti-6Al-4V annealed sheet shall be tested at -180°F temperature. Two (2) of the welded specimens (D_3 and D_4) shall be notched .032 inch on each edge of the weld area. Parent metal grain direction shall be tested as shown in Figure 1, Specimens D_1, D_2, D_3 and D_4. A suggested method of attaining this temperature is to mix liquid nitrogen with ethyl alcohol until a slush mixture is formed.

TITLE Specification for Testing Welded Thin-Sheet Titanium Alloy at Extreme Temperature (-423°F to 1000°F) ISSUED

WRITTEN BY J. E. Bell REVISED

Test E - Four (4) transverse welded specimens of .016"-thickness Ti-6Al-4V annealed sheet shall be tested at -321°F temperature. Two (2) of the welded specimens (E_3 and E_4) shall be notched .032" on each edge of the weld area. Parent metal grain direction shall be tested as shown in Figure 1, Specimens E_1, E_2, E_3 and E_4. Liquid nitrogen may be used to attain this temperature.

Test F - Four (4) transverse welded specimens of .016"-thickness Ti-6Al-4V annealed sheet shall be tested at -423°F temperature. Two (2) of the specimens (F_3 and F_4) shall be notched .032 inch on each edge of the weld area. Parent metal grain direction shall be tested as shown in Figure 1, Specimens F_1, F_2, F_3 and F_4. Liquid hydrogen should be used to attain this temperature. Beech will perform this test.

Test G - Four (4) transverse welded specimens of .016"-thickness Ti-6Al-4V annealed sheet shall be tested at room temperature. Two (2) of the specimens (G_3 and G_4) shall be notched .032 inch on each edge of the weld area. Parent metal grain direction shall be tested as shown in Figure 1, Specimens G_1, G_2, G_3 and G_4.

Test H - Same as Test G, except at 200°F temperature per Figure 1, Specimens H_1, H_2, H_3 and H_4.

Test J - Same as Test G, except at 600°F temperature per Figure 1, Specimens J_1, J_2, J_3 and J_4.

Test K - Same as Test G, except at 800°F temperature per Figure 1, Specimens K_1, K_2, K_3 and K_4.

3.1.2 Bend Tests

Suitable size test specimens will be cut from a welded sheet of annealed Ti-6Al-4V. See Figure 1. Each test will be a guided bend type conducted on a 105° vee block as shown in Figure 2. These tests will be performed with the bend specimens in longitudinal and transverse directions and are intended to provide weld ductility data. The bend tests will be conducted prior to the tensile tests to assure the welding is void of defects.

3.1.2.1 Bend Tests Required

Test L - Four (4) longitudinal welded specimens, Figure 1, Specimens L_1, L_2, L_3 and L_4 and two (2) nonwelded specimens, Figure 1, Specimens L_5 and L_6, of .016"-thickness Ti-6Al-4V annealed sheet at room temperature.

Test M - Four (4) transverse welded specimens, Figure 1, Specimens M_1, M_2, M_3 and M_4, of .016"-thickness Ti-6Al-4V annealed sheet at room temperature.

Test N - Four (4) longitudinal welded specimens, Figure 1, Specimens N_1, N_2, N_3 and N_4 and two (2) nonwelded specimens Figure 1, Specimens N_5 and N_6, of .016"-thickness Ti-6Al-4V annealed sheet at -321°F temperature.

Test P - Four (4) transverse welded specimens of .016"-thickness Ti-6Al-4V annealed sheet at -321°F temperature. Figure 1, Specimens P_1, P_2, P_3 and P_4.

3.1.3 Impact Tests

Test specimens will be prepared from welded sheet for the V-notch Charpy im-

TITLE Specification for Testing Welded Thin-Sheet Titanium Alloy at Extreme Temperature (-423°F to 1000°F) ISSUED

WRITTEN BY J. E. Bell REVISED

FIGURE 2
105° VEE BLOCK FOR BEND TESTS

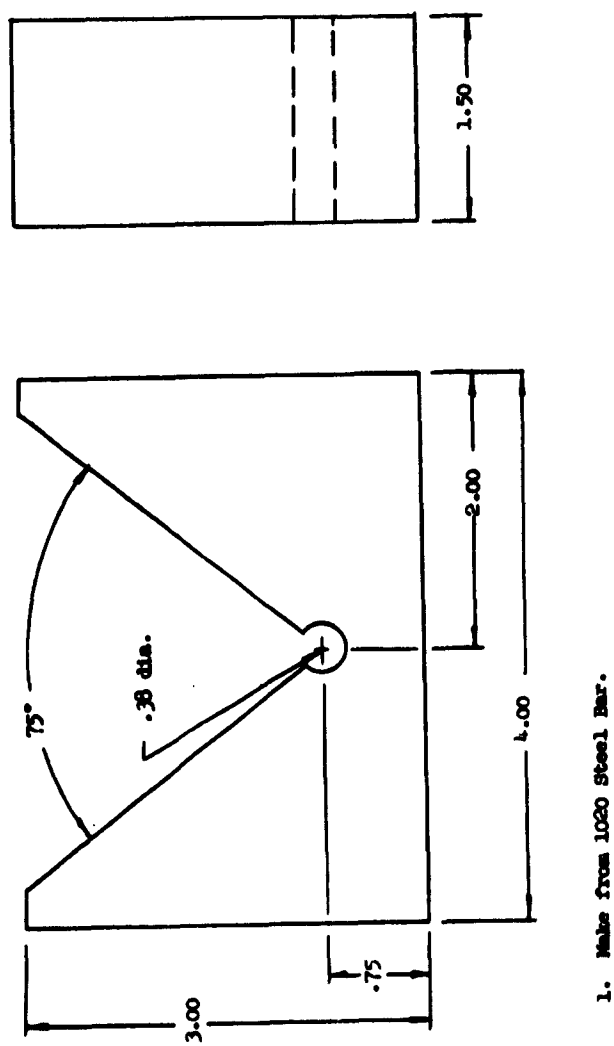

pact test. The purpose of this test is to establish the quality of the weld under impact at the extreme temperature levels. These tests will be performed with the weld in various positions to the parent grain direction. (Figure 3)

3.1.3.1 Impact Tests Required

Test A - Four (4) transverse welded specimens and two (2) nonwelded specimens of .098"-thickness Ti-6Al-4V annealed sheet at -423°F temperature, Figure 3, Specimens A_1 through A_6.

Test B - Two (2) adjacent to weld, nonwelded specimens of .098" Ti-6Al-4V annealed sheet at -423° temperature, Figure 3, Specimens B_1 and B_2

Test C - Two (2) adjacent to weld, welded specimens of .098" Ti-6Al-4V annealed sheet at -423°F temperature, Figure 3, Specimens C_1 and C_2.

3.1.4 Welding Tolerance Test Required

Tensile tests R, S, T, U, V, W and X will be performed to verify the maximum allowable fabrication tolerances.

Test R - Four (4) transverse welded specimens of .016"-thickness Ti-6Al-4V annealed sheet shall be tested at room temperature. Parent metal grain direction and mismatch tolerances shall be in accordance with Figure 4, Specimens R_1, R_2, R_3 and R_4.

Test S - Same as Test R. Figure 4, Specimens S_1, S_2, S_3 and S_4.

TITLE Specification for Testing Welded Thin-Sheet Titanium Alloy at Extreme Temperature (-423°F to 1000°F) ISSUED

WRITTEN BY J. E. Bell REVISED

FIGURE 3
IMPACT SPECIMENS

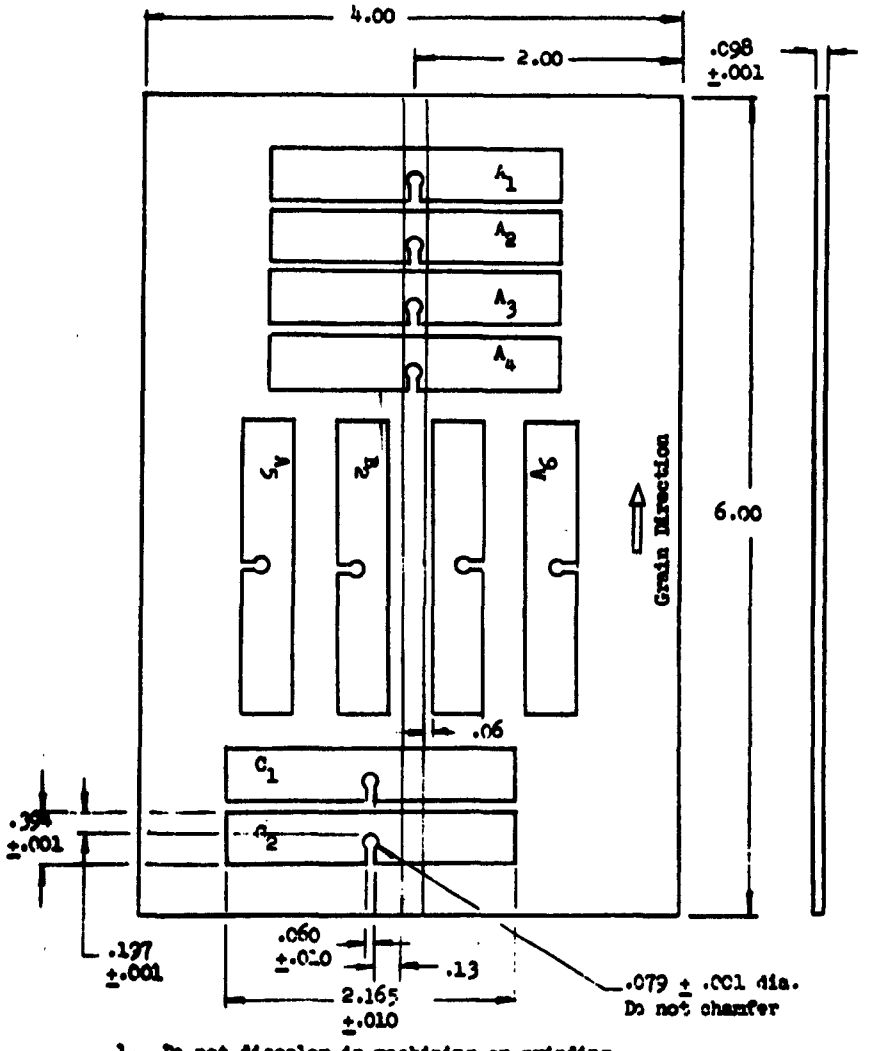

1. Do not discolor in machining or grinding.
2. All surface finish 16-64.
3. Refer to ASME Boiler and Pressure Vessel Code Sec. VIII, U68d.
4. Machine and sandbelt weld to .098 ± .001 sheet thickness.

TITLE Specification for Testing Welded Thin-Sheet Titanium Alloy at Extreme Temperature (-423°F to 1000°F)

ISSUED

WRITTEN BY J. E. Be..

REVISED

FIGURE 4
MISMATCH WELDED TENSILE SPECIMENS

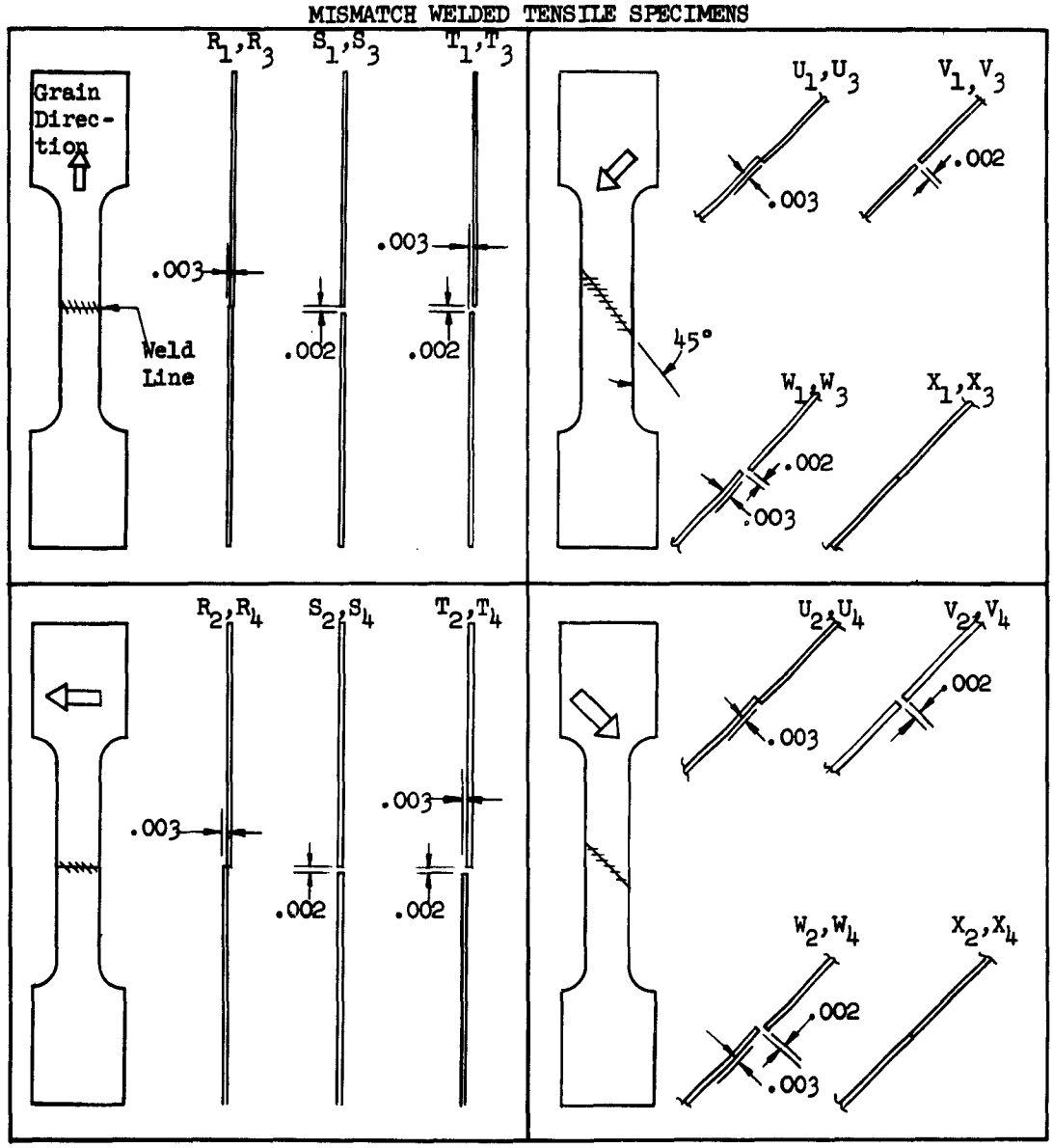

Test T - Same as Test R. Figure 4, Specimens T_1, T_2, T_3 and T_4.

Test U - Four (4) 45° angle welded specimens of .016"-thickness Ti-6Al-4V annealed sheet shall be tested at room temperature. Parent metal grain direction and mismatch tolerances shall be in accordance with Figure 4, Specimens U_1, U_2, U_3 and U_4.

Test V - Same as Test U. Figure 4, Specimens V_1, V_2, V_3 and V_4.

Test W - Same as Test U. Figure 4, Specimens W_1, W_2, W_3 and W_4.

Test X - Same as Test U. Figure 4, Specimens X_1, X_2, X_3 and X_4.

Tensile test results shall be in accordance with Sections 3.2 and 3.2.1.

3.1.5 Hydrogen Embrittlement Tests Required

Tensile Test Y is considered essential in determining strength effects of 6Al-4V titanium exposed to hot hydrogen gas atmosphere at specified temperature and time elements.

Test Y - Forty (40) transverse welded specimens of .016"-thickness Ti-6Al-4V annealed sheet shall be prepared according to detail of Figure 5. The specimens in pairs shall be placed into a 100% H_2 gas-environment sealed test tube. Eight (8) test tubes, No 1 through No. 9, shall then be exposed to a temperature of 200° ± 25°F as outlined in Table 1. Specimens contained in tubes No. 10 through No. 18 shall be held to room temperature as outlined in Table 1.

TITLE Specification for Testing Welded Thin-Sheet Titanium Alloy at Extreme Temperature (-423°F to 1000°F) ISSUED

WRITTEN BY J. E. Bell REVISED

FIGURE 5
HYDROGEN EMBRITTLEMENT SPECIMENS

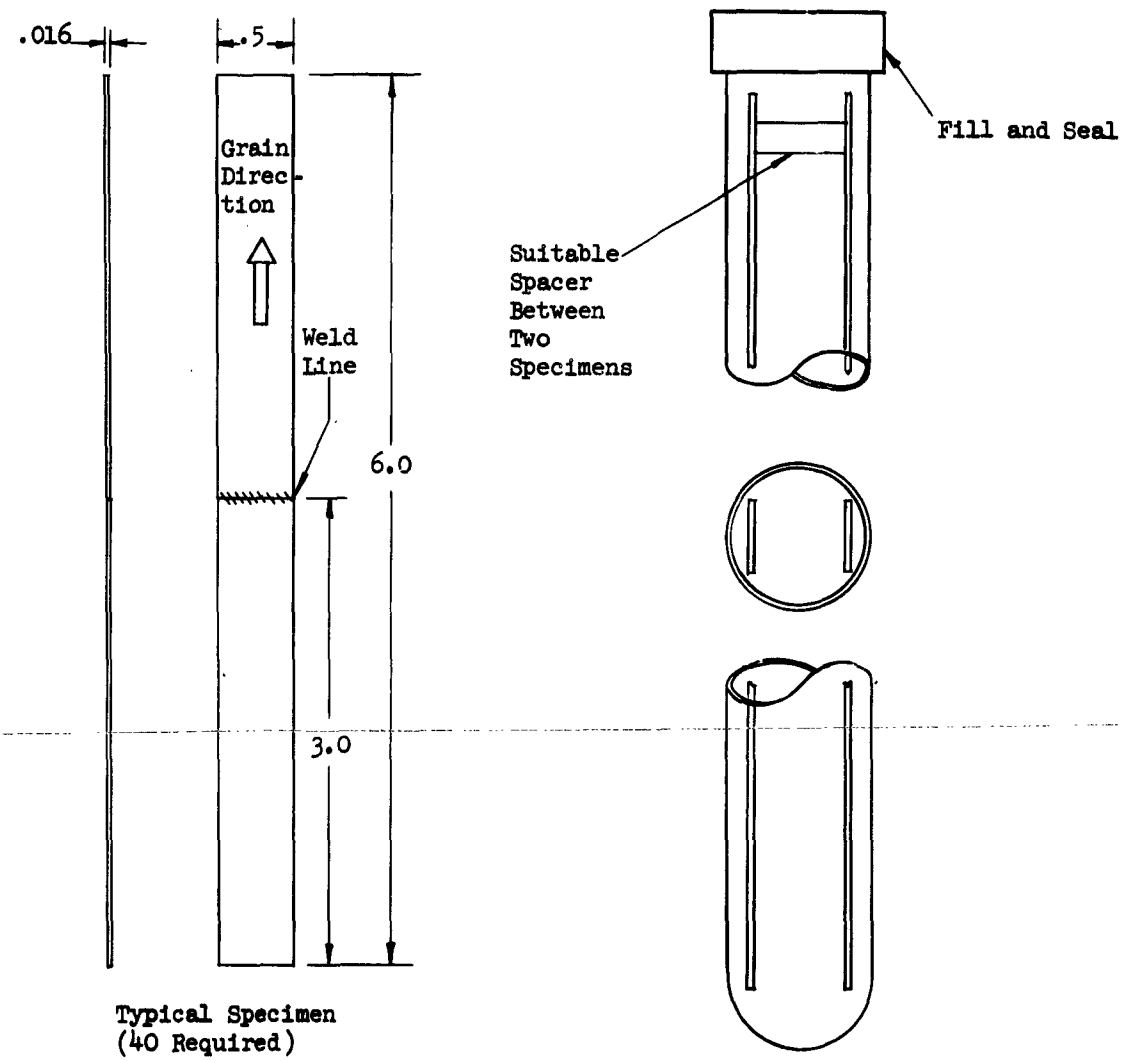

TITLE Specification for Testing Welded Thin-Sheet Titanium Alloy at Extreme Temperature (-423°F to 1000°F)

ISSUED

WRITTEN BY J. E. Bell

REVISED

Specimens Y_1, Y_2, Y_{21} and Y_{22} are included to test the normal qualities of the welded material before being exposed to the hydrogen gas. These specimens will be compared to known data to insure the welding and parent metal are of good quality.

The specimens shall be removed from the H_2 atmosphere immediately after completing the exposed time period. Tensile tests results shall be in accordance with Sections 3.2 and 3.2.1.

Tube Number	Specimen Number	Time at Temperature
-	Y_1 and Y_2	Non-H_2 exposed at R. T.
1	Y_3 and Y_4	1 Hr. at 200° ± 25°F
2	Y_5 and Y_6	4 hrs. at 200° ± 25°F
3	Y_7 and Y_8	8 hrs. at 200° ± 25°F
4	Y_9 and Y_{10}	24 hrs. at 200° ± 25°F
5	Y_{11} and Y_{12}	48 hrs. at 200° ± 25°F
6	Y_{13} and Y_{14}	96 hrs. at 200° ± 25°F
7	Y_{15} and Y_{16}	168 hrs. at 200° ± 25°F
8	Y_{17} and Y_{18}	216 hrs. at 200° ± 25°F
9	Y_{19} and Y_{20}	264 hrs. at 200° ± 25°F
-	Y_{21} and Y_{22}	Non-H_2 exposed at R. T.
10	Y_{23} and Y_{24}	8 hrs. at R. T.
11	Y_{25} and Y_{26}	24 hrs. at R. T.

Tube Number	Specimen Number	Time at Temperature
12	Y_{27} and Y_{28}	48 hrs. at R. T.
13	Y_{29} and Y_{30}	96 hrs. at R. T.
14	Y_{31} and Y_{32}	168 hrs. at R. T.
15	Y_{33} and Y_{34}	264 hrs. at R. T.
16	Y_{35} and Y_{36}	432 hrs. at R. T.
17	Y_{37} and Y_{38}	768 hrs. at R. T.
18	Y_{39} and Y_{40}	1440 hrs. at R. T.

3.2 Results and Documentation

The results shall be recorded in a reliable engineering procedure. This procedure shall utilize graphs, tables, photographs and familiar methods of clearly conveying the results to a potential reader. All of the compiled data will eventually be supplemented to existing known data; thus, all terms and units used should be consistent with existing data.

3.2.1 Tensile Test Results

Tensile test results shall include yield strength .2% offset-psi, ultimate tensile strength-psi and percent elongation in 2 inches of the parent metal and the weld.

3.2.2 Bend Test Results

Bend test results will be visually observed and recorded. Any weld or parent metal defects will be analyzed for reason of defect. These tests will be performed prior to tensile and impact tests to verify the apparent ductility of the welds.

TITLE Specification for Testing Welded Thin-Sheet Titanium Alloy at Extreme Temperature (-423°F to 1000°F) ISSUED

WRITTEN BY J. E. Bell REVISED

3.2.3 Impact Test Results

Impact test results shall include the foot-pounds of impact absorbed by the test specimens at the required temperature.

Beech Aircraft Corporation

SPECIFICATION

SPECIFICATION FOR
TESTING SIMULATED POROSITY IN 6Al-4V TITANIUM ALLOY WELDS

Beechcraft Specification - B. S. 7262

APPENDIX II

ISSUED November 18, 1959

REVISED _____

L. R. Stoecker
Lead Engineer
Boulder Division

J. H. Rodgers
Assistant Manager of Engineering
Boulder Division

C. W. Spieth
Group Engineer
Boulder Division

A. L. Clark
Manager - Engineering & Sales
Boulder Division

e-78A

Beech Aircraft Corporation

SPECIFICATION BS 7262

PAGE 1 OF 4

TITLE Specification for Testing Simulated Porosity in 6Al-4V Titanium Alloy Welds

ISSUED

WRITTEN BY L. R. Stoecker REVISED

1.0 SCOPE

The purpose of this specification is to define the method of approach in establishing a lower limit for determining the weld acceptability in 6Al-4V titanium alloy welded joints. Because of a lack of suitable standards regarding acceptability of welded joints containing gas pockets, entrainments and inclusions, it has been decided to conduct sufficient tensile and bend tests on specially prepared specimens which would, in effect, duplicate the above noted defects.

2.0 REQUIREMENTS

It shall be required that a tensile test and a bend test be conducted on each of the proposed test specimens as outlined in Section 3.0. Complete records of testing standards, methods and results shall be maintained and returned along with all test specimens to Boulder Engineering at the completion of the test program.

2.1 Tensile Tests

All tensile tests shall be conducted with a speed of .05 in/in-min. Tensile test results shall include ultimate tensile strength (psi), .2% yield strength (psi), and percent elongation in 2 inches. The 2-inch gage length shall be equally spaced about the hole perforations in the test specimen.

2.2 Bend Tests

All bend tests shall be conducted in a suitable 105° vee block and with a bend radius equal to ten times the test specimen thickness. Bend test results shall be visually observed and recorded.

TITLE Specification for Testing Simulated Porosity in 6Al-4V Titanium Alloy Welds

ISSUED

WRITTEN BY L. R. Stoecker REVISED

3.0 TEST SPECIMEN REQUIREMENTS

3.1 Welded Blank

A suitable welded blank shall be prepared by Boulder Division personnel utilizing the present welding equipment and technique per B. S. 2714. This blank shall be X-rayed per B. S. 2712 and leak checked per B. S. 6183 prior to shipment to Wichita.

3.2 Preliminary Test Specimen Preparation

All test specimens (tensile and bend) will be 1" x 6" see Figure 1. Any individual test coupon that has any detectable (by X ray, electronic or optical means) porosity, inclusions, cracks or surface irregularities shall not be used.

3.3 Final Test Specimen Preparation

All test specimens will be prepared in accordance with Figure 1. Prior to welding the blank as noted in Section 3.1, a reference line located 1.0000" from the edge of joint to be welded will be made. All dimensions for the hole centerlines are made from this line and are measured perpendicular to the theoretical centerline of the weld joint. Care should be exercised in locating and drilling the noted holes.

3.4 Test Specimen Identification

All test specimens shall be suitably identified in the following manner:

First number denotes tensile or bend specimen (B or t).
Second number denotes number of holes in specimen.
Third number denotes diameter of hole in ten thousandths.
Fourth number denotes distance that holes are located from reference line in hundredths.

TITLE Specification for Testing Simulated Porosity in 6Al-4V Titanium Alloy Welds

ISSUED

WRITTEN BY L. R. Stoecker REVISED

Example: B-3-156-97 is the bend test specimen with three .0156-inch diameter holes located .9700" from the reference line.

3.5 Test Specimen Inspection

All finished test specimens shall be X rayed or optically inspected to determine exact hole sizes and locations. All information shall be recorded and returned to Boulder Engineering.

TITLE Specification for Testing Simulated Porosity in 6Al-4V Titanium Alloy Welds

ISSUED

WRITTEN BY L. R. Stoecker REVISED

FIGURE 1
TEST SPECIMEN CONFIGURATION

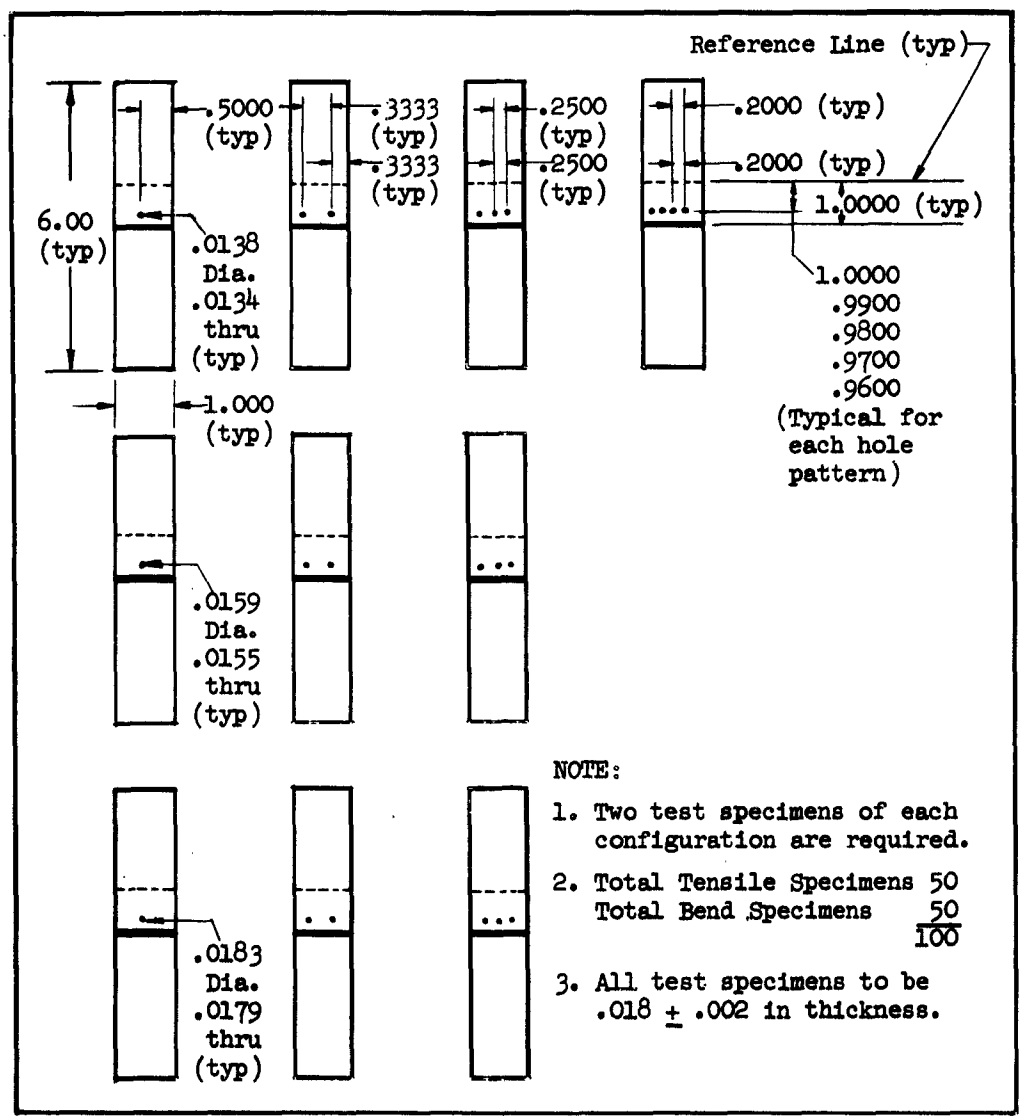

LIST OF REFERENCES

1. Engineering Report No. 6168, Establishing Proven Design Criteria for Cryogenic Boost Tanks, Quarterly Progress Report, Beechcraft Research and Development, Inc., December 1958 (SECRET).

2. WADC TR 59-101, Establishing Proven Design Criteria for Cryogenic Boost Tanks, Quarterly Progress Report, Beechcraft Research and Development, Inc., March, 1959, (SECRET).

3. WADC TN 59-177, Establishing Proven Design Criteria for Cryogenic Boost Tanks, Quarterly Progress Report, Beechcraft Research and Development, Inc., June 1959 (SECRET).

4. FTRDI MR59-1, Establishing Proven Design Criteria for Cryogenic Boost Tanks, Quarterly Progress Report, Beechcraft Research and Development, Inc., September, 1959 (SECRET).

5. FTRDI MR59-2, Establishing Proven Design Criteria for Cryogenic Boost Tanks, Quarterly Progress Report, Beechcraft Research and Development, Inc., December, 1959 (SECRET).

6. FTRDI MR60-1, Establishing Proven Design Criteria for Cryogenic Boost Tanks, Quarterly Progress Report, Beechcraft Research and Development, Inc., March, 1960 (SECRET).

7. FTRDI MR60-2, Establishing Proven Design Criteria for Cryogenic Boost Tanks, Quarterly Progress Report, Beechcraft Research and Development, Inc., June, 1960 (SECRET).

8. WADC TR58-273, Research Study for Rocket Vehicle Tank Systems Using Cryogenic Propellants, Beechcraft Research and Development, Inc., June, 1958 (SECRET).

9. R-58AGT823 "Gas Atmosphere Effects on Materials," Interim Progress Report No. 2, General Electric Co., November 15, 1958.

10. McClintock, R. M. and Van Gundy, D. A., Adhesives at Low Temperatures, NBS Cryogenic Laboratory, Lab Note 545, June, 1954.

11. WADC TR 58-530, Rocket Vehicle Tankage Research for a Cryogenic Propellant, Beechcraft Research and Development, Inc., September 1958 (SECRET).

12. Wilkes, G. B., "Thermal Conductivity, Expansion, and Specific Heat of Insulators at Extremely Low Temperatures," Ref. Eng., July, 1956.

13. Vershoor, J. D., "Thermal Conductivity of Commercial Insulations at Low Temperature," Refrigerating Eng., September, 1954.

14. Proceedings of the 1958 Cryogenic Engineering Conference, "The Performance of Glass Fiber Insulation Under High Vacuum," R. M. Christianson and M. Hollingsworth.

15. Proceedings of the 1959 Cryogenic Engineering Conference, "Low Temperature Insulation Systems," R. M. Christianson, M. Hollingsworth, H. N. March, Jr.

16. Larkin, B. K., "A Study of the Rate of Thermal Radiation Through Porous Insulating Materials," Ph.D. Thesis, University of Michigan, Ann Arbor, Michigan, 1957.

17. Scott, R. B., "Cryogenic Engineering," D. Van Nostrand, 1959.

18. Hunter, B. J., et. al., "Metal Powder Additives in Evacuated Powder Insulation," Proceedings of the 1959 Cryogenic Engineering Conference.

19. Paper 4.02 Proceedings of the 1954 Cryogenic Engineering Conference.

20. Fulk, M. M., "Evacuated Powder Insulation for Low Temperatures." Progress in Cryogenics -1, London: Reywood and Company, Ltd., 1959.

21. McClintock, R. M. and Piza, J. J., Epoxy Resins for Cryogenic Structural Adhesives, NBS Cryogenic Laboratory Report No. 5093, June, 1957.

22. WADC TR 58-386, The Mechanical Properties of Certain Aircraft Structural Materials at Very Low Temperatures, Battelle Memorial Institute, November, 1958.

23. Compilation of Available Information on Ti 6Al-4V Alloy, Titanium Metallurgical Laboratory Memorandum, Battelle Memorial Institute, February 28, 1958.

24. Special Report on Missile Design Data, First Edition, Rem-Cru Titanium, Inc., June 19, 1957.

25. Cooruccini, R. J., "Properties of Materials at Low Temperatures," Chemical Engineering Progress, June, July, August, 1957.

26. Tyler, W. W., and Wilson, A. C., Jr., Thermal Conductivity, Electrical Resistivity, and Thermoelectrical Power of Titanium Alloy RC-130-B, Knolls Atomic Power Laboratory Report 803, 1952.

27. Shiffman, C. A., The Heat Capacities of the Elements Below Room Temperature, General Electric Research Laboratory, October, 1952.

28. Product Information Book, Min-K Insulation Handbook, Johns Manville, Undated.

DISTRIBUTION LIST

		No. of Copies
1.	Commander Air Research and Development Command ATTN: RDZND Andrews AFB Washington 25, D. C.	1
2.	Headquarters, Directorate Project CENTAUR Air Force Ballistic Missile Division ATTN: WDZC, Maj. J. R. Brill Air Force Unit Post Office Los Angeles 45, California	3
3.	Pesco Products Division of Borg Warner Corporation ATTN: Mr. John DeSteffano 24700 North Miles Road Bedford, Ohio	3
4.	Commandant Air Command and Staff College ATTN: Director, Weapons Course Maxwell AFB, Alabama	1
5.	Commander Air Force Ballistic Missile Division Air Research and Development Command 5760 Arbor Vitae Avenue Inglewood, California	1
6.	Commander Air Force Special Weapons Center ATTN: Dr. Tester, SWOI Kirtland AFB, New Mexico	1
7.	Commander Air Technical Intelligence Center ATTN: AFOIN-4E3, A. Voedisch Wright Patterson AFB, Ohio	1
8.	U. S. Atomic Energy Commission Albuquerque Operations Office ATTN: Asst. Mgr. for Advance Planning P. O. Box 5400 Albuquerque, New Mexico	1

DISTRIBUTION LIST
(Continued)

		No. of Copies
9.	Assistant Secretary of Defense, R & D ATTN: Weapons System Evaluation Group Dr. William F. Offutt Pentagon Building Washington 25, D. C.	1
10.	National Aeronautics and Space Administration Lewis Flight Propulsion Laboratory Cleveland Airport Cleveland, Ohio	1
11.	Air Force Plant Representative Douglas Aircraft Company, Inc. ATTN: Mr. Charles S. Glasgow, Chief Engineer Long Beach Division Long Beach, California	2
12.	Assistant Air Force Plant Representative Rocketdyne Division, North American Aviation ATTN: Mr. George P. Sutton 6633 Canoga Avenue Canoga Park, California	3
13.	Assistant Air Force Plant Representative North American Aviation, Inc. Missile Development Division ATTN: Mr. William S. Reid, Jr. 12214 Lakewood Boulevard Downey, California	3
14.	ARDC-ANP Liaison Office Convair Division, General Dynamics Corporation Government Aircraft Plant No. 4 ATTN: Messrs. Keith G. Brown and Richard E. Adams P. O. Box 371 Fort Worth, Texas	3
15.	Commander Field Command, AFSWP ATTN: Capt. Edwin R. Turner, SWTG Technical Library Albuquerque, New Mexico	1

DISTRIBUTION LIST
(Continued)

		No. of Copies
16.	Bureau of Aeronautics Representative Aerojet General Corporation P. O. Box 296 Azusa, California	3
17.	Commanding Officer Jet Propulsion Laboratory ATTN: Messrs. W. H. Pickering/I. E. Newlan Pasadena, California	1
18.	Office of Naval Research ATTN: E. E. Sullivan Department of the Navy - Code 735 Washington 25, D. C.	1
19.	Air Force Plant Representative Boeing Airplane Company ATTN: Mr. John J. Zipp, Jr. Oklahoma City Air Materiel Area Seattle 24, Washington	3
20.	Air Force Plant Representative Convair Division, General Dynamics Corporation (Astronautics) ATTN: Mr. Louis Canter P. O. Box 1950 3165 Pacific Highway San Diego 12, California	3
21.	Assistant Air Force Plant Representative Missile Systems Division ATTN: Mr. Frank Clark Hoyt Lockheed Aircraft Corporation Sunnyvale, California	3
22.	Air Force Plant Representative The Martin Marietta Corporation ATTN: Mr. George E. Halpern, Chief, Libraries Baltimore 3, Maryland	3
23.	Commander Wright Air Development Center ATTN: WCLPPIT Wright-Patterson AFB, Ohio	1

DISTRIBUTION LIST
(Continued)

		No. of Copies
24.	AiResearch Manufacturing Company Division Garrett Corporation 9851 Sepulveda Boulevard Los Angeles 45, California	3
25.	Chandler-Evans Corporation Charter Oak Boulevard West Hartford 1, Connecticut	2
26.	National Bureau of Standards Boulder, Colorado	1
27.	The Glenn L. Martin Company Missile Division Denver, Colorado	3
28.	Boeing Airplane Company ATTN: Mr. C. M. Long Wichita, Kansas	1
29.	Arthur D. Little, Inc. 30 Memorial Drive Acorn Park Cambridge 40, Massachusetts	1
30.	National Aeronautics and Space Administration 1520 H Street Northwest Washington 25, D. C.	6
31.	Commander Air Force Flight Test Center ATTN: FTRDI Edwards AFB, California	7
32.	Air Force Plant Representative Douglas Aircraft Company 3000 Ocean Park Boulevard Santa Monica, California	1
33.	Mr. E. W. Schwartz, Design Specialist AeroPhysics Mail Zone 595-10 Convair Astronautics San Diego, California	1

DISTRIBUTION LIST
(Continued)

		No. of Copies
34.	Air Force Ballistic Missile Division Headquarters, Air Research and Development Command Los Angeles 45, California	1
35.	Headquarters Armed Services Technical Information Agency Arlington Hall Station Arlington 12, Virginia	27
36.	The Marquardt Corporation ATTN: Mary Burdett 16555 Saticoy Street Van Nuys, California	1
37.	Liquid Propellant Information Agency Applied Physics Laboratory The Johns Hopkins University Silver Spring, Maryland	3
38.	Arnold Engineering Development Center Air Force Systems Command ATTN: AEOIM United States Air Force Arnold Air Force Station, Tennessee	1
39.	George C. Marshall Space Flight Center ATTN: Mr. W. Y. Jordan, Jr. M-S & M-FE Huntsville, Alabama	1
40.	Office of the Chief of Staff, USAF Scientific Advisory Board Energy Conversion Committee Washington 25, D. C.	1